Prepared in cooperation with the Wisconsin Department of Natural Resources

A Model for Evaluating Stream Temperature Response to Climate Change in Wisconsin

Present-day stream temperatures (estimated)

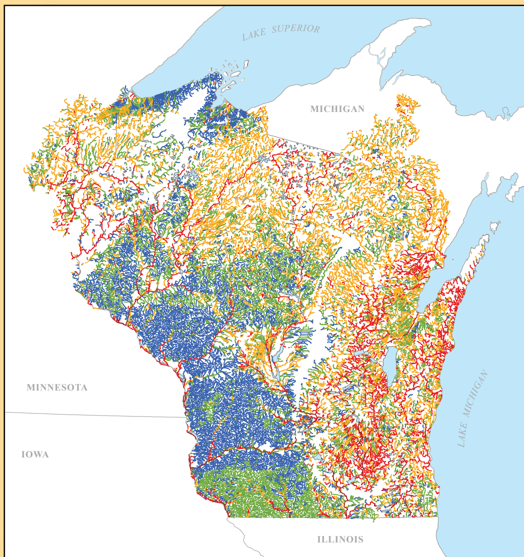

Late 21st century stream temperatures (projected)

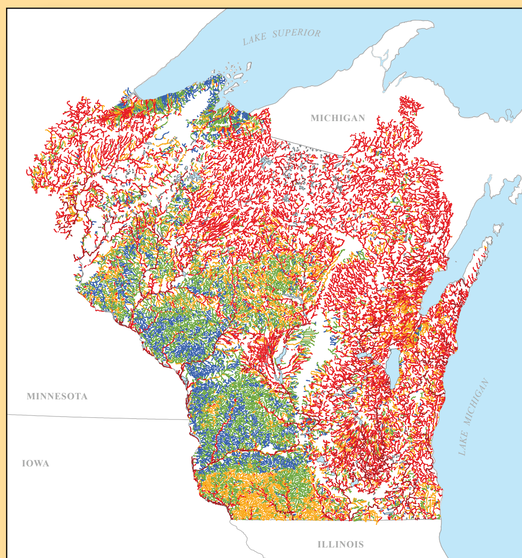

Thermal class (July mean)

- Cold
- Cold transition
- Warm transition
- Warm
- Very warm

Scientific Investigations Report 2014–5186

U.S. Department of the Interior
U.S. Geological Survey

A Model for Evaluating Stream Temperature Response to Climate Change in Wisconsin

By Jana S. Stewart, Stephen M. Westenbroek, Matthew G. Mitro, John D. Lyons, Leah E. Kammel, and Cheryl A. Buchwald

Prepared in cooperation with the Wisconsin Department of Natural Resources

Scientific Investigations Report 2014–5186

U.S. Department of the Interior
U.S. Geological Survey

U.S. Department of the Interior
SALLY JEWELL, Secretary

U.S. Geological Survey
Suzette M. Kimball, Acting Director

U.S. Geological Survey, Reston, Virginia: 2015

For more information on the USGS—the Federal source for science about the Earth, its natural and living resources, natural hazards, and the environment, visit http://www.usgs.gov or call 1–888–ASK–USGS.

For an overview of USGS information products, including maps, imagery, and publications, visit http://www.usgs.gov/pubprod

To order this and other USGS information products, visit http://store.usgs.gov

Suggested citation:
Stewart, J.S., Westenbroek, S.M., Mitro, M.G., Lyons, J.D., Kammel, L.E., and Buchwald, C.A., 2015, A model for evaluating stream temperature response to climate change in Wisconsin: U.S. Geological Survey Scientific Investigations Report 2014–5186, 64 p., *http://dx.doi.org/10.3133/sir20145186*.

ISSN 2328-0328 (online)

Contents

Figures

Tables

Conversion Factors and Datums

SI to Inch/Pound

Multiply	By	To obtain
	Length	
millimeter (mm)	0.03937	inch (in.)
meter (m)	3.281	foot (ft)
kilometer (km)	0.6214	mile (mi)
	Area	
square kilometer (km^2)	0.3861	square mile (mi^2)
	Flow rate	
inch per year (in/yr)	25.4	millimeter per year (mm/yr)

Temperature in degrees Celsius (°C) may be converted to degrees Fahrenheit (°F) as follows:

°F=(1.8×°C)+32

Vertical coordinate information is referenced to National Geodetic Vertical Datum of 1988 (NGVD 88).

Horizontal coordinate information is referenced to either the North American Datum of 1927 (NAD 27) or the North American Datum of 1983 (NAD 83).

Abbreviations used in this report

ANN	artificial neural network
ANNv1	artificial neural network version 1 stream temperature model (Stewart and others, 2006)
APWL	accumulated potential water loss
AWC	available water-holding capacity
CGCM	General Circulation Model: CGCM3.1 (T63); Canadian Centre for Climate Modelling and Analysis, Canada
CNRM	General Circulation Model: CNRM-CM3; Météo-France / Centre National de Recherches Météorologiques, France
CRP	Conservation Reserve Program
CSIRO	General Circulation Model: CSIRO-Mk3.5; CSIRO Atmospheric Research, Australia
DSI	Data Series Index
ECHO	General Circulation Model: ECHO-G; Meteorological Institute of the University of Bonn, Meteorological Research Institute of KMA, and Model and Data group, Germany/Korea
FGOALS	General Circulation Model: FGOALS-g1.0; LASG / Institute of Atmospheric Physics, China
GCM	General Circulation Model
GDD	growing degree-day
GFDL	General Circulation Model: GFDL-CM2.0; U.S. Dept. of Commerce / NOAA / Geophysical Fluid Dynamics Laboratory, USA
GIS	geographic information system
GISS	General Circulation Model: GISS-AOM; NASA / Goddard Institute for Space Studies, USA
GUI	graphical user interface
HSG	hydrologic soils group
INGV	General Circulation Model: INGV-ECHAM4; Instituto Nazionale di Geofisica e Vulcanologia, Italy
IPCC	Intergovernmental Panel on Climate Change
IPSL	General Circulation Model: IPSL-CM4; Institut Pierre Simon Laplace, France
MIROC	General Circulation Model: MIROC3.2(hires); Center for Climate System Research (The University of Tokyo), National Institute for Environmental Studies, and Frontier Research Center for Global Change (JAMSTEC), Japan
MSE	mean square error
NCDC	National Climatic Data Center

NED	National Elevation Data
NHD	National Hydrography Dataset
NLCD	National Land Cover Database
PDF	probability density function
PEST	parameter estimation software
PME	percent model error
r	Pearson's correlation coefficient
R^2	coefficient of determination
RMSE	root mean square error
SSURGO	Soil Survey Geographic Database
SWB	soil-water-balance
SWB-ANNv1	Integrated Soil-Water-Balance and Artificial Neural Network version 1 Model
USGS	U.S. Geological Survey
UWCCR	University of Wisconsin Center for Climatic Research
WDNR	Wisconsin Department of Natural Resources
WICCI	Wisconsin Initiative on Climate Change Impacts

Acknowledgments

Ed Roehl (Advanced Data Mining, Inc.), Paul Conrads and Judith Thomas (U.S. Geological Survey (USGS)), and Alex Martin and Christopher Smith (Wisconsin Department of Natural Resources (WDNR)) are acknowledged for their assistance in developing and reviewing methods, and deriving and managing geographic information system data. Funding for this study was provided in part by the USGS National GAP Analysis Program, Great Lakes Aquatic GAP project, and the Federal Aid in Sportfish Restoration, Project F-95-P, studies SSMP and SSCN.

A Model for Evaluating Stream Temperature Response to Climate Change in Wisconsin

By Jana S. Stewart,[1] Stephen M. Westenbroek,[1] Matthew G. Mitro,[2] John D. Lyons,[2] Leah E. Kammel,[1] and Cheryl A. Buchwald[1]

Abstract

Expected climatic changes in air temperature and precipitation patterns across the State of Wisconsin may alter future stream temperature and flow regimes. As a consequence of flow and temperature changes, the composition and distribution of fish species assemblages are expected to change. In an effort to gain a better understanding of how climatic changes may affect stream temperature, an approach was developed to predict and project daily summertime stream temperature under current and future climate conditions for 94,341 stream kilometers across Wisconsin. The approach uses a combination of static landscape characteristics and dynamic time-series climatic variables as input for an Artificial Neural Network (ANN) Model integrated with a Soil-Water-Balance (SWB) Model. Future climate scenarios are based on output from downscaled General Circulation Models (GCMs). The SWB model provided a means to estimate the temporal variability in groundwater recharge and provided a mechanism to evaluate the effect of changing air temperature and precipitation on groundwater recharge and soil moisture. The Integrated Soil-Water-Balance and Artificial Neural Network version 1 (SWB-ANNv1) Model was used to simulate daily summertime stream temperature under current (1990–2008) climate and explained 76 percent of the variation in the daily mean based on validation at 67 independent sites. Results were summarized as July mean water temperature, and individual stream segments were classified by thermal class (cold, cold transition, warm transition, and warm) for comparison of current (1990–2008) with future climate conditions.

Integrating the SWB Model with the ANN Model provided a mechanism by which downscaled global or regional climate model results could be used to estimate the potential effects of climate change on future stream temperature on a daily time step. To address future climate scenarios, statistically downscaled air temperature and precipitation projections from 10 GCMs and 2 time periods were used with the SWB-ANNv1 Model to project future stream temperature. Projections of future stream temperatures at mid- (2046–65) and late- (2081–2100) 21st century showed the July mean water temperature increasing for all stream segments with about 80 percent of stream kilometers increasing by 1 to 2 degrees Celsius (°C) by mid-century and about 99 percent increasing by 1 to 3 °C by late-century. Projected changes in stream temperatures also affected changes in thermal classes with a loss in the total amount of cold-water, cold-transition, and warm-transition thermal habitat and a gain in warm-water and very warm thermal habitat for both mid- and late-21st century time periods. The greatest losses occurred for cold-water streams and the greatest gains for warm-water streams, with a contraction of cold-water streams in the Driftless Area of western and southern Wisconsin and an expansion of warm-water streams across northern Wisconsin. Results of this study suggest that such changes will affect the composition of fish assemblages, with a loss of suitable habitat for cold-water fishes and gain in suitable habitat for warm-water fishes. In the end, these projected changes in thermal habitat attributable to climate may result in a net loss of fisheries, because many warm-water species may be unable to colonize habitats formerly occupied by cold-water species because of other habitat limitations (e.g., stream size, gradient). Although projected stream temperatures may vary greatly, depending on the emissions scenario and models used, the results presented in this report represent one possibility. The relative change in stream temperature can provide useful information for planning for potential climate impacts to aquatic ecosystems. Model results

[1] U.S. Geological Survey.

[2] Wisconsin Department of Natural Resources.

can be used to help identify vulnerabilities of streams to climate change, guide stream surveys and thermal classifications, prioritize the allocation of scarce financial resources, identify approaches to climate adaptation to best protect and enhance resiliency in stream thermal habitat, and provide information to make quantitative assessments of statewide stream resources.

Introduction

Water temperature is an important determinant of where fish and other aquatic organisms live in streams. Most fish are ectotherms, which exchange heat with and are generally the same temperature as their surrounding aquatic environment. The thermal environment in which a given species of fish exists can be defined by lower and upper lethal limits, and within these bounds are optimal temperatures for feeding, growth, and reproduction. Knowledge of how water temperature varies temporally and spatially within and among streams is critical to understanding how fish species are distributed in streams.

In temperate regions such as Wisconsin, stream fishes typically encounter water temperatures in the range of 0–30 degrees Celsius (°C). At any given time of year, water temperatures may vary within and among streams. Useful metrics for classifying streams can be derived from summertime water temperatures. Lyons and others (2009) classified Wisconsin streams into cold-water, cold-transition, warm-transition, and warm-water thermal classes based on the presence (or absence) of fish species, species abundance, and summertime water temperature metrics (June–August mean, July mean, and maximum daily mean) (table 1).

Cold-water and cold-transition streams can support high abundances of cold-water fishes such as brook trout Salvelinus fontinalis and brown trout Salmo trutta. Cold-water fishes are less abundant in warm-transition streams and absent from warm-water streams during summertime but may occur in warm-water streams during colder seasons. Warm-water and warm-transition streams can support high abundances of warm-water fishes such as fathead minnows *Pimephales notatus* and smallmouth bass *Micropterus dolomieu*. Warm-water fishes are less abundant in cold-transition streams and absent from cold-water streams. Summertime water temperature is therefore an important factor in explaining fish distribution patterns in streams of the Laurentian Great Lakes region (Wehrly and others, 2003; Chu and others, 2008; Steen and others, 2008; Lyons and others, 2009, 2010). Understanding the distribution of stream temperatures across all streams in a region will help in understanding how fish species are distributed.

Water temperature in streams is affected by many factors operating at multiple spatial and temporal scales, often with complex interactions. Air temperature, for example, is a significant climatic determinant of water temperature in streams in Wisconsin and other temperate regions (Magnuson and others, 1979; Stewart and others, 2006; Westenbroek, 2010b). However, stream temperatures in Wisconsin are highly heterogeneous as compared to air temperatures across the landscape. Streams or even stream reaches in close proximity to one another and under similar climate conditions may exhibit different temperature characteristics because of local variation in geology and groundwater input. Wehrly and others (1998, 2006) have developed models to identify landscape effects on stream temperature.

Given the important role that air temperature plays in the list of factors that determine stream temperature, resource managers are concerned that changes in climate will impact stream temperatures and fish distribution. Wisconsin has on average become warmer and wetter over the past 60 years, and this warming trend is predicted to continue and increase, with the statewide average air temperature increasing by up to 3–4 °C by the year 2050 (WICCI, 2011). These increases in air temperature along with changes in the timing and amount of precipitation are expected to alter thermal and hydrologic regimes of Upper Midwestern streams over the coming decades (Magnuson and others, 1997; Mosheni and others, 1999), affecting the distribution of fish and other aquatic species (Mosheni and others, 2003; Lyons and others, 2009, 2010). Current and future management of statewide stream resources would greatly benefit from an improved understanding of the current distribution of stream thermal habitat and the fish communities that live there.

Table 1. Water temperature criteria for classifying Wisconsin streams into thermal classes and subclasses (Lyons and others, 2009).

[deg C, degrees Celsius; <, less than; >, greater than]

Thermal class	Subclass	July mean (deg C)	June-August mean (deg C)	Maximum daily mean (deg C)
Cold water		< 17.5	< 17	< 20.7
Cold transition		17.5 - 19.5	17.0 - 18.7	20.7 - 22.6
Warm transition		19.5 - 21	18.7 - 20.5	22.6 - 24.6
Warm water		> 21	> 20.5	> 24.6
	very warm*	> 24		

*Very warm thermal subclass was added for purpose of estimating climate-change effects on warm-water streams.

One limitation to stream and fisheries resource management in Wisconsin and elsewhere is the relatively small number of streams that can be physically sampled in a given year, whether sampling involves deploying data loggers to measure continuous stream temperature data or surveying fish populations. Modeling is a tool resource managers may use to make inferences from sampled stream sites to unsampled stream sites to help address those limitations.

To help gain a better understanding of statewide stream resources, an Artificial Neural Network (ANN) model was developed for Wisconsin using water temperature data collected at 254 stream sites over the summertime period for 1990–2002 (Stewart and others, 2006; Westenbroek and others, 2010b). The model was applied to stream segments statewide to predict daily summertime stream temperature and classify streams into summer thermal classes (Lyons and others, 2009) and will be referred to as Artificial Neural Network version 1 stream temperature model (ANNv1) throughout this report. ANN models also have been used to successfully predict water temperature in other regions of North America (Chenard and Caissie, 2008; McKenna and others, 2010; Risley and others, 2003).

Lyons and others (2010) used the ANNv1 predictions to predict and project current and future distributions of 50 fish species in Wisconsin streams. In order to simulate stream temperature under three future climate-warming scenarios, Lyons and others (2010) adjusted July mean water temperature by 0.8 °C (low), 2.4 °C (medium), and 4 °C (high) to represent air temperature increases of low = 1 °C, medium = 3 °C, and high = 5 °C, based on Pilgrim and others (1998). A key limitation to this effort was the oversimplification of the relation between air and water temperature as a single statewide ratio and lack of any connection between precipitation, groundwater, stream recharge, and water temperature.

As Lyons and others (2010) demonstrated, stream temperature models can provide a means to make inferences to the potential impacts climate change may have on the stream environment and fish populations therein. However, new modeling efforts are required to improve how site-specific stream environmental landscape characteristics can be combined with continuous climate data to make projections on how stream temperature may respond to changes in climatic variables under future conditions. Resource managers tasked with developing adaptation strategies to protect streams and fisheries opportunities can use such models to help prioritize the allocation of scarce financial resources and make quantitative assessments of statewide stream resources.

Purpose and Scope

The purpose of this study was to develop models for predicting stream temperatures in all Wisconsin streams and to evaluate how stream temperatures may respond to climate change. This report describes the development of an Integrated Soil-Water-Balance and Artificial Neural Network version 1 (SWB-ANNv1) Model to predict stream temperature from continuous climate time series and watershed-landscape characteristics under current climate conditions and project future stream temperature through integration with results of GCMs. The development of the SWB-ANNv1 model builds upon ANNv1 (Stewart and others, 2006), and the integration of the Soil-Water-Balance (SWB) model is an enhancement to this earlier modeling effort (Westenbroek and others, 2010b). The integration of SWB with the ANN provides a means to link changing climate patterns and precipitation amounts over time to stream temperature and potential groundwater recharge. Stream temperature is an important factor in determining the ecological status of temperate region streams in terms of which fish species can and cannot live and persist in those streams. The results of this study can be used subsequently to update stream fish models for predicting or projecting presence and absence of 50 fish species in Wisconsin streams under current and future climate scenarios (Lyons and others, 2010).

This study also is relevant to the mission of the U.S. Geological Survey (USGS) and its core science strategies with priorities to identify climate change impacts on fish and wildlife species. The resulting research and products can help provide the scientific foundation by which policymakers, resource managers, and the public make informed decisions about the management of natural resources on which they and others depend (Burkett and others, 2013).

Study Area

The study area includes 94,341 km of streams (n = 38,423 segments) across the entire State of Wisconsin (1:100,000 scale U.S. National Hydrography data) and for two bordering watersheds: the Menominee River Basin (Upper Peninsula of Michigan) and the St. Croix River Basin (Minnesota) (fig. 1). Wisconsin includes rivers that drain to the Mississippi River Basin to the south and west, and the U.S. Great Lakes Basin, to the north (Lake Superior) and east (Lake Michigan). The proximity to the Great Lakes has a strong influence on Wisconsin's climate and plays a major role in seasonal climate variations. The landscape is dominated by forested lands in the north, agricultural lands in the central and southeast, and major urban centers in the southeast portion of the State. The many rivers and lakes and other glacial landforms are common features of Wisconsin's landscape, as glaciers once blanketed all but portions of western and southwestern Wisconsin. The unglaciated southwestern part of the State is commonly referred to as the Driftless Area and is characterized by rugged topography and groundwater-dominated streams that support thriving cold-water fisheries for brook trout and brown trout. Cold-water streams also exist as part of the glaciated landscape in other parts of the State; however, warmer thermal classes of streams tend to be more prevalent in those areas (Trout Unlimited, 2005; Lyons and others, 2009).

Figure 1. Location of study area in Wisconsin and portions of Michigan and Minnesota.

Approach

An approach was developed to predict stream temperature under current climate conditions and to project how stream temperature may change under future climate conditions. The approach uses a combination of static watershed landscape characteristics and dynamic time-series climatic variables as input for the SWB-ANNv1 model. Future climate scenarios are based on output of downscaled GCMs. The SWB-ANNv1 model was developed in order to simulate summertime mean daily stream temperature as a continuous time series for confluence-to-confluence stream segments using data collected at 371 stream temperature monitoring locations across Wisconsin. The SWB-ANNv1 model was applied across the study area to predict current and project future daily summertime stream temperature for all 94,341 km of stream. The summary variable July mean water temperature was used in this report to classify stream segments into thermal classes and for comparison to assess the effects of projected future climate on stream temperature (Lyons and others, 2009).

This study builds upon ANNv1 developed by Stewart and others (2006) that used water temperature data collected at 254 stream sites over the summertime period for 1990–2002 (Westenbroek and others, 2010b). The ANN model is a nonlinear model that uses neural network algorithms to link dynamic climate signals and static watershed landscape characteristics to predict time series of stream temperature. The static variables provide a link to the spatial variability of stream temperature across the State, associated with the changing landscape, while the dynamic time-series climate variables provide a link to the temporal component of stream temperature, associated with climate patterns. The approach involves time-series clustering, a technique that was initially used to predict hourly stream temperatures in western Oregon (Risley and others, 2003) and by Roehl and others (2006) to generate spatially continuous water-level predictions for a Florida aquifer. Stewart and others (2006) used a slightly modified time-series clustering approach than these other studies for ANNv1 because most of the Wisconsin stream temperature data were temporally discontinuous, having been measured during different summers over a 13-year period (1990–2002). The key climate signals in the ANNv1 model were 6 air temperature time-series variables obtained by clustering air temperature time-series data measured at 156 weather stations across the State into 6 groups. A key limitation to the approach taken in development of ANNv1 was the absence of any link between precipitation and stream temperature.

This limitation was addressed by integrating a deterministic SWB model that uses precipitation and air temperature along with landscape characteristics as inputs to track soil moisture and generate a time-series estimate of potential groundwater recharge at a daily time step (Westenbroek and others, 2010a and b; Dripps and Bradbury, 2007; Hart and others, 2009). In addition to the SWB enhancement, the spatial and temporal extent of stream temperature measurements used in ANNv1 was expanded by including additional monitoring sites and extending the simulation period from the year 2002 to 2008.

Future stream temperature will not only be influenced by changes in air temperature but also by changes in base flow that may be attributable to changes in precipitation. The amount of groundwater-derived base flow can play a key role in determining stream temperature and has been shown to be of critical importance to the viability of cold-water trout fisheries, particularly in the upper Midwest (Gaffield and others, 2005; Zorn and others, 2002; Wehrly and others, 2006). The SWB model provided a means to estimate the temporal variability in groundwater recharge and provided a mechanism to evaluate the influence of changing air temperature and precipitation on groundwater recharge and soil moisture through the integration of GCMs downscaled for Wisconsin. Integrating the SWB model with the ANN model in turn provided a mechanism by which results from downscaled GCMs could be integrated to estimate the potential effects of climate change on stream temperature (fig. 2).

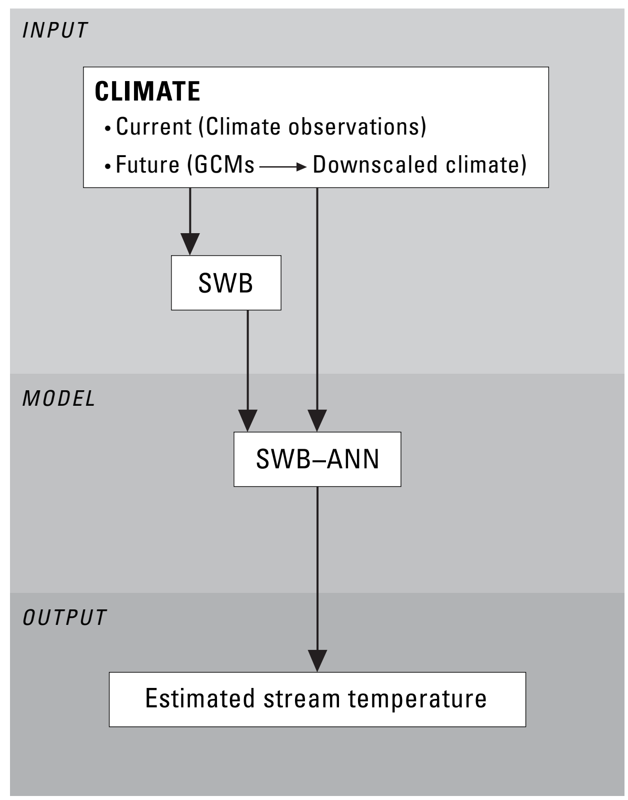

EXPLANATION

GCMs = General Circulation Models

SWB = Soil-Water-Balance Model

ANN = Artificial Neural Network Model

SWB–ANN = Integrated SWB and ANN Model

Figure 2. Conceptual modeling approach for evaluating stream temperature response to climate change in Wisconsin.

To address future climate scenarios, this study used statistically downscaled air temperature and precipitation projections from the University of Wisconsin Center for Climatic Research (UWCCR) for 10 GCMs. The UWCCR used a process known as statistical downscaling to relate the large-scale atmospheric conditions predicted by GCMs to the value of observed climate data at a given point. To allow for simulation of local climate variability and extremes while also simulating the large-scale weather pattern, the UWCCR related the large-scale GCM results to a probability density function of values at each of 170 climate observing stations (Notaro and others, 2011). This procedure is reported to reduce the variance and extremes that often occur when interpolating raw GCM data (Notaro and others, 2011).

Statistical downscaling of daily air temperature and precipitation was available for three time periods—late-20th century-baseline historical hindcast (1961–2000), mid-21st century (2046–65), and late-21st century (2081–2100)—and three different future greenhouse-gas emissions scenarios (B2 scenario (low emissions), A1 scenario (high emissions), and the A1B scenario (moderate to high emissions) (Notaro and others, 2011)). Changes in stream temperature in future years will likely reflect realized changes in greenhouse-gas emissions; future stream temperatures described in this report assume that future carbon emissions develop as envisioned in the A1B emissions scenario. The A1B emissions scenario is a middle-of-the-road greenhouse-gas emissions scenario developed by the Intergovernmental Panel on Climate Change (IPPC) (IPCC, 2007). This scenario assumes continued use of fossil fuels and a continued and steady upward trajectory of carbon emissions over the next few decades, from about 400 parts per million today to about 550 parts per million by mid-century. The three time periods—1961–2000, 2046–65, and 2081–2100—are treated as stationary periods, even though greenhouse-gas emissions are continuing to change through each timespan. This study considers only a single emissions scenario and single statistical realization owing to limited resources and time constraints. Climate data from UWCCR in the form of projected future daily air temperature and precipitation served as input for the SWB-ANNv1 model to estimate the effect of 10 GCMs on stream temperature.

The following sections describe the development of the SWB model and the integration of groundwater-recharge estimates from the SWB model into the ANN model (SWB-ANNv1) to generate daily time-series estimates of stream temperature across Wisconsin. Both estimates were made under current and future climate conditions, using empirical climate observations for current conditions and statistically downscaled air temperature and precipitation projections from 10 GCMs for future conditions. The SWB-ANNv1 model was applied to all stream segments statewide for current and future time periods. Model results are then presented, showing how stream temperature is projected to change across GCMs, future time periods, and thermal classes of streams.

The Soil-Water-Balance Model

The USGS SWB software (Westenbroek and others, 2010a) was used to supply estimates of spatially explicit groundwater-recharge over time for use in the SWB-ANNv1 stream temperature model. The USGS SWB model code estimated potential groundwater recharge for a grid of cells on a daily basis. The model simulated the major components of a water budget, including the processes of interception, runoff, evapotranspiration, snowfall, and snowmelt. Soil moisture is determined by calculating the net gain or loss of water to the soil in a given grid cell, and then by consulting the Thornthwaite-Mather soil moisture-retention tables; the tables allow one to estimate how much moisture may be extracted from a soil given the history of precipitation and evapotranspiration to which it has been exposed (Thornthwaite and Mather, 1957). The difference between the inputs and outputs of water for each cell, including the change in soil moisture storage, was assumed to be potential recharge. More detail about model formulation, parameterization, and calibration of the SWB model may be found in Westenbroek and others (2010a).

Source Data

Application of the SWB model required a tabular or gridded climate dataset, along with four gridded datasets describing landscape characteristics. The following sections describe how these source data were prepared for use with the SWB model.

Climate Observations

An interpolated climate dataset was created to encompass all Wisconsin streams and for streams outside of Wisconsin in two bordering watersheds: the St. Croix (Minnesota) and Menominee (Michigan) River Basins. Data from more than 1,000 meteorological stations were extracted from the Data Series Index (DSI)-3200 daily surface database maintained by the National Climatic Data Center (NCDC) for the time period 1950–2008 (National Oceanic and Atmospheric Administration, 2011). Due to the grid-based nature of SWB, the selected stations extended beyond the study area, covering Wisconsin and parts of Michigan, Minnesota, Illinois, Indiana, and Iowa. Data elements included maximum and minimum daily air temperature, total daily precipitation, daily snowfall, and cumulative snow depth. Air temperature and precipitation data elements were used as SWB input and snow data elements were used in SWB verification. The input for this gridded dataset was nearly identical to that used by Serbin and Kucharik (2009). Because their model domain did not extend beyond Wisconsin, it was necessary for us to include additional meteorological stations and create a similar grid for a slightly larger model domain.

Grids were prepared for each of the five climate variables by means of a custom R script (R Development Core Team, 2011), in which a thin-plate spline—a two-dimensional smoothing technique—was calculated for each set of daily climate data (Fields Development Team, 2006) for the purposes of data interpolation and smoothing. Data were discarded from the analyses if there were duplicate records, if daily values were flagged as “accumulated” or “missing,” or if data values fell outside of realistic data ranges (e.g., a maximum air temperature greater than 49 °C, a minimum air temperature less than −34 °C, or total daily precipitation greater than 508 millimeters (mm)).

In addition, daily precipitation totals were adjusted on the basis of the recorded time of observation. A station at which precipitation values are recorded at 8:00AM is possibly more representative of the precipitation that fell during the 16 hours of the previous calendar day than the 8 hours of the recorded date. Thus, precipitation values were adjusted to account for the number of hours actually represented by the value on the recorded day. For example, 22.9 mm of precipitation recorded at a station with an observation time of 8:00AM would result in 15.2 mm of that precipitation amount reallocated to the previous day, retaining 7.7 mm for the current day. The resulting data were prepared for use in SWB model calibration.

Landscape Characteristics

Landscape-characteristic grids for SWB model input included land cover from the 2001 National Land Cover Database (NLCD), available water-holding capacity (AWC), and hydrologic soils group (HSG) from the Natural Resources Conservation Service Soil Survey Geographic Database (SSURGO), and a flow-direction grid derived from a hydrologically corrected version of the National Elevation Data (NED) (U.S. Geological Survey, 2003, 2004a; U.S. Department of Agriculture, 2009).

The source-data grids for the landscape characteristics were obtained at 30 meter (m) resolution; SWB model grid resolutions tested for this project ranged from 400 to 1,600 m. Generalization of the source-data grids to the SWB grids was performed as follows: for land cover, flow direction, and HSG grids, an SWB grid cell was assigned the value contained in the majority of the underlying input grid cells; for the AWC grid, an SWB grid cell was assigned a value equal to the simple mean of underlying grid cells.

Model Calibration for the Soil-Water-Balance Model

An initial SWB model for Wisconsin was created by combining the four landscape characteristics grids and the climate grids with a lookup table, which was populated with textbook values for the runoff curve number, rooting depth, and snow parameter values (Cronshey and others, 1986) for each combination of HSG and land-cover type.

The SWB model was calibrated by use of parameter estimation software (PEST) (Doherty, 2009) in two steps. The first calibration step optimized the SWB model snow parameters to maximize model agreement with first-order climate station snowfall observations and included rain and snowfall correction factors and the assumed temperatures at which precipitation falls as entirely rain or snow. The second calibration step optimized SWB model runoff curve number, maximum infiltration rates, and rooting depth parameters to maximize model agreement with independently calculated groundwater-recharge values for Wisconsin. The relation between each of these data types and the SWB code is shown in figure 3.

The estimates of recharge used in the calibration process were generated by Gebert and others (2007) by performing base-flow separation analysis on stream discharge records for the period 1970–99. For the calibration work, we chose a subset (n = 44 gaging stations) of the basin recharge estimates that were judged to have the least amount of difference between groundwater and surface-water divide boundaries. Figure 4 shows the ratio of the SWB model predicted recharge to the recharge calculated by Gebert and others, 2007, and figure 5 shows SWB model output (recharge, inches per year) generated with calibrated snow, runoff, and soil depth parameters.

Model simulations were run at three resolutions (400, 800, and 1,600 m) for the period 1989–2000 to determine optimal cell size. The finer resolution simulations did not appreciably improve predictions; therefore, the 1,600 m cell size was selected for SWB model simulation. The SWB simulations were then run for the 1,600 m cell size for the period 1990–2008 to match up with the period of stream temperature observations and SWB-ANNv1 model simulation.

The Integrated Soil-Water-Balance and Artificial Neural Network version 1 Stream Temperature Model

The SWB-ANNv1 model (fig. 6) was built upon the ANNv1 stream temperature model developed by Stewart and others (2006) for Wisconsin as described in the Approach section of this report. The spatial and temporal extent of the ANNv1 model was expanded in this study by including additional stream measurement sites (from 254 in ANNv1 to 371 sites in this study) and extending the simulation period from 2002 to 2008. The approach and methods used in development of ANNv1 and this study were nearly identical with the following exception: an SWB component, described in this report, was added as an enhancement to incorporate groundwater-recharge estimates under current conditions and to provide a link to global climate models as a means to simulate future stream temperature conditions under different climate

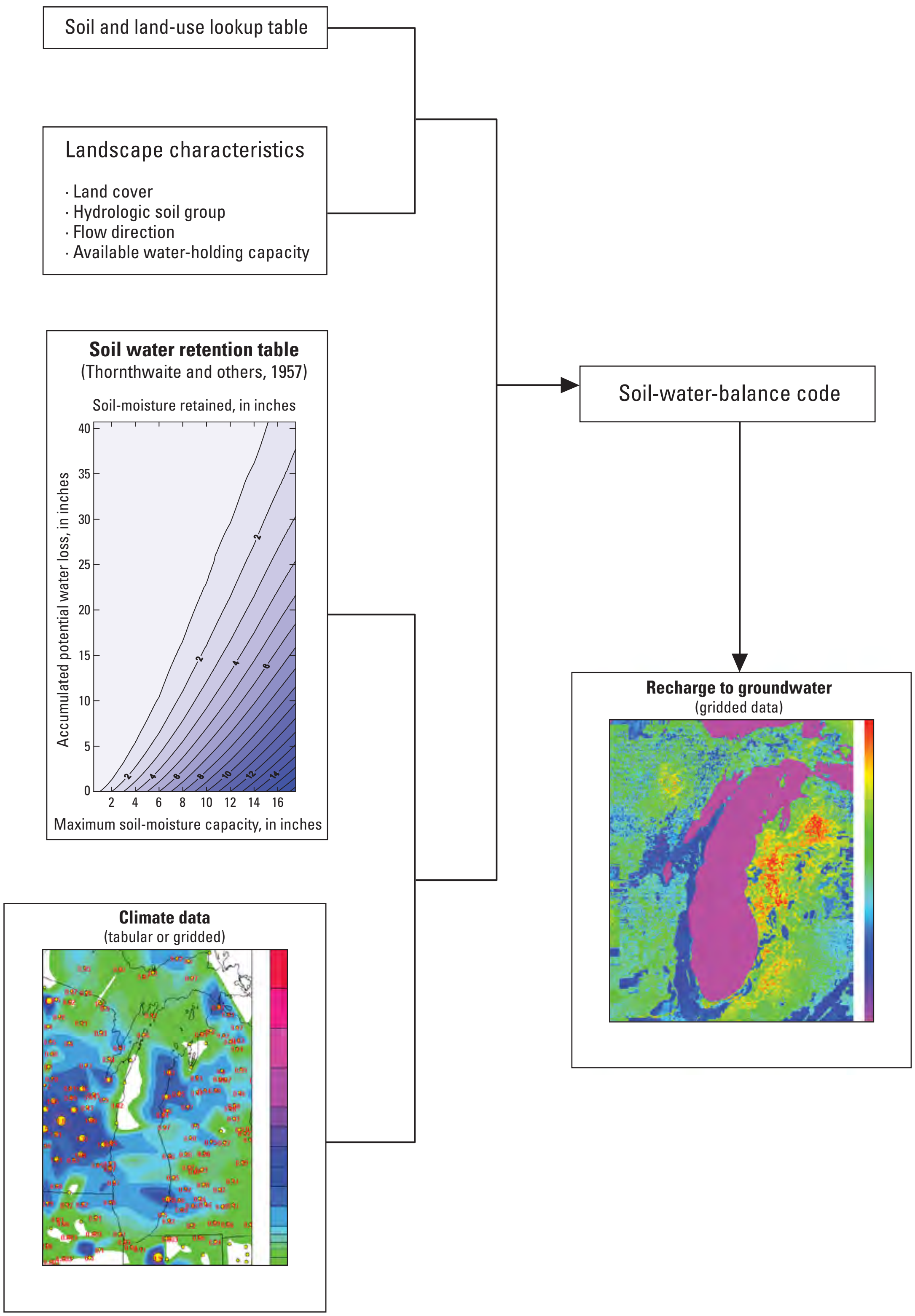

Figure 3. Approach and components of the Soil-Water-Balance Model (Westenbroek and others, 2010a).

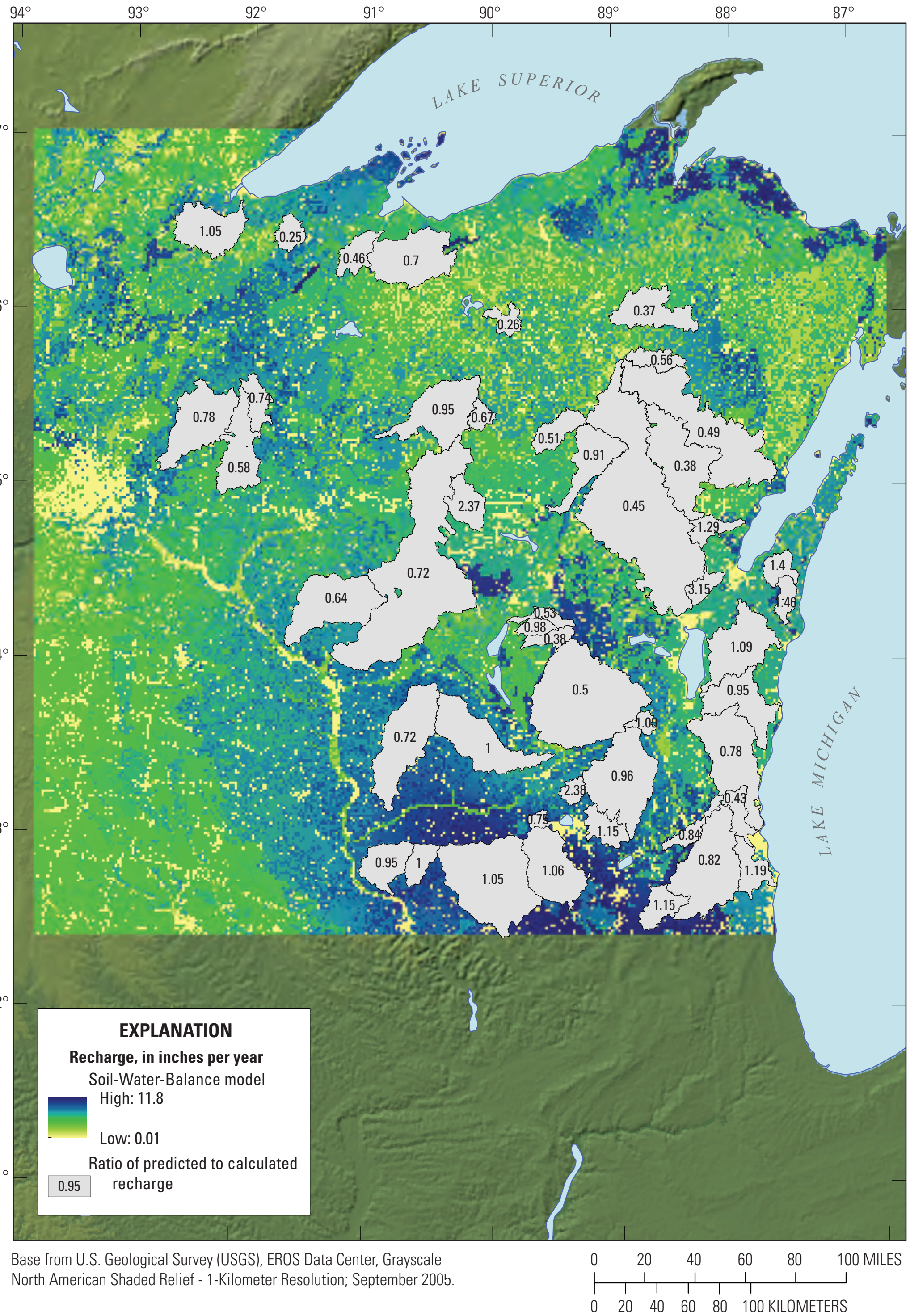

Figure 4. Ratio of Soil-Water-Balance predicted recharge to recharge calculated based on measured streamflow records (Gebert and others, 2007).

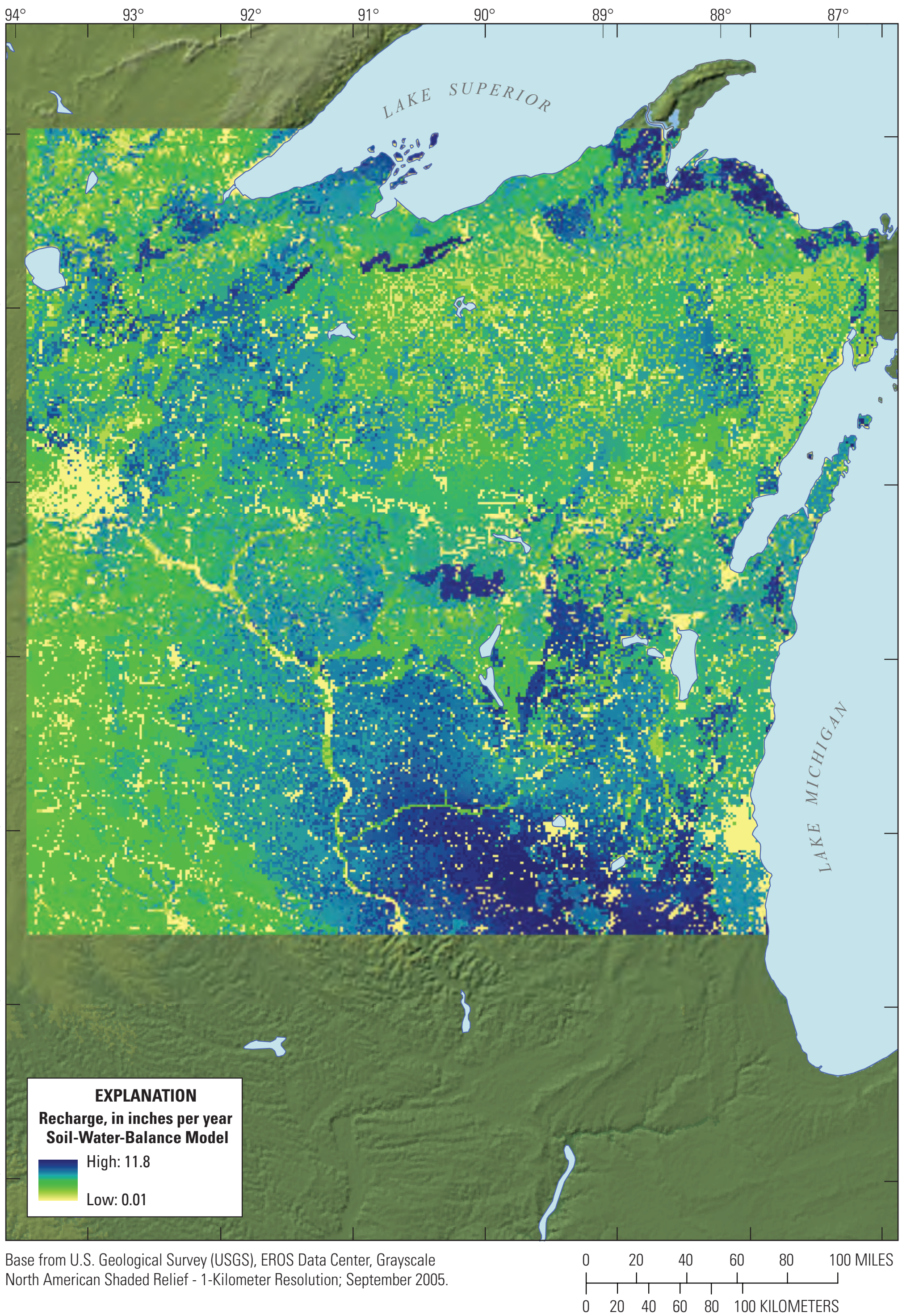

Figure 5. Results of the Soil-Water-Balance Model for Wisconsin, 1970–2000.

scenarios (Roehl and others, 2006; Stewart and others, 2006, Westenbroek and others, 2010a and b). The output from SWB in the form of accumulated potential groundwater recharge, served as an additional ANN input variable in this study, in contrast to ANNv1. A detailed schematic of the SWB-ANNv1 model approach is shown in figure 6. The calibrated SWB-ANNv1 model was applied to all stream segments in the study area to estimate stream temperature statewide under current and future climate conditions.

Source Data

Development of the SWB-ANNv1 model utilized five input datasets including (1) empirical stream temperature time-series observations, (2) empirical climate time-series observations, (3) geographic information system (GIS)-derived landscape characteristics, (4) SWB estimates of groundwater recharge, and (5) climate time-series projections from downscaled GCMs. The following sections describe how these source data were prepared for development of the SWB-ANNv1 model.

Stream Temperature Observations

Water temperature was measured each half hour from June 1 to August 31 at 371 stream sites for 1990–2008 by the Wisconsin Department of Natural Resources (WDNR) and the USGS. The data were discontinuous in that some stream sites were sampled over a single summer and others were sampled multiple summers over the 19-year period. The SWB-ANNv1 stream temperature model was developed using 243 of the 254 stream sites used in ANNv1, 11 of the ANNv1 sites were dropped in this study after they were determined to be outliers during model calibration, an additional 128 sites were added, and the time period was extended from 2002 to 2008. Most streams were wadeable (drainage area < 1,600 square kilometers (km^2)), with the exception of 11 sites with drainage areas ranging from 1,784 to 15,923 km^2. Stream sites were fairly evenly distributed across the full range of stream thermal classes with 25 percent cold, 18 percent cold-transition, 20 percent warm-transition, and 37 percent warm-water sites (Lyons and others, 2009). Time series of mean daily water temperature were calculated for each site and served as the response variable (fig. 7; appendix 1).

Sites were selected that had at least 62 out of 92 days of measurements during a single summertime (June–August) period. Temperature measurements outside of three standard deviations from the mean for the entire period of measurement at a given site were considered outliers and were deleted (Wagner and others, 2011). Most water temperature sites (243 of 371) had only a single summer of data; the remaining 128 sites had from 2 to 17 summers of water temperature measurements for a total of 67,356 discrete daily stream temperature measurement data points.

Climate Observations from Empirical Data

Climatic data were acquired from the NCDC for weather stations across the study area (National Oceanic and Atmospheric Administration, 2011). Climate stations with data collected during 1990–2008 and with the most complete record during the summertime (June–August) period were identified. Daily time series were compiled and consisted of data from 7 weather stations for air pressure, 160 stations for air temperature, 13 stations for dew point, 160 stations for precipitation, and 13 stations for solar radiation. Mean daily values were calculated for all variables with the exception of precipitation, in which case total daily precipitation was calculated.

With as many as 160 air temperature and precipitation climate stations, it was necessary to simplify the dataset to a more manageable number of climate variables for model development (Roehl and others, 2006; Stewart and others, 2006; Westenbroek and others, 2010b). “Time-series clustering” is a data-mining technique that can optimally segment a large collection of time-series signals into a smaller number of dynamically similar “groups.” A cross-correlation of Pearson coefficients (r) was calculated for each of the climate time-series variables (e.g., air temperature, precipitation), with individual climate stations each representing a separate time series; then the k-means clustering technique was applied to the cross-correlation matrix to determine the ideal number of clusters or groups for each climate variable. The k-means clustering technique provided in the Data Miner Software Kit of Weiss and Indurkhya (1997) was implemented, which is based on the algorithm of Hartigan and Wong (1979). For k number of groups, the k-means algorithm optimizes which members of the overall group should be in groups 1 through k. The optimal partitioning of groups is determined by using the root mean square error (RMSE) as a measure of the difference in distance between each member and the mean of the group such that movement of any point from one group to another will not decrease the RMSE for either group. The k-means clustering technique was repeated for a range of group sizes (k values), and a mean RMSE for all groups was computed and plotted for each k value. The optimal number of groups was selected at the inflection point between a sharp vertical decline in mean RMSE and a horizontal plateau, or in some cases where a more gradual reduction in RMSE occurred with increasing number of groups. The mean time series for each climate variable group was determined by calculating the mean daily value of all climate station members within a group.

The resulting time series were decorrelated by calculating an average time series for each group (average of all climate station members), assigning one group to be a reference time series (i.e., the group with the largest number of members), and calculating differences from the averages on a daily time step for the other groups. This greatly reduced the number of time-series variables (e.g., air temperature from 160 stations to 6 time-series groups) while preserving a semblance of spatial and temporal variability. All climate variable time-series groups with the exception of air temperature were subsequently

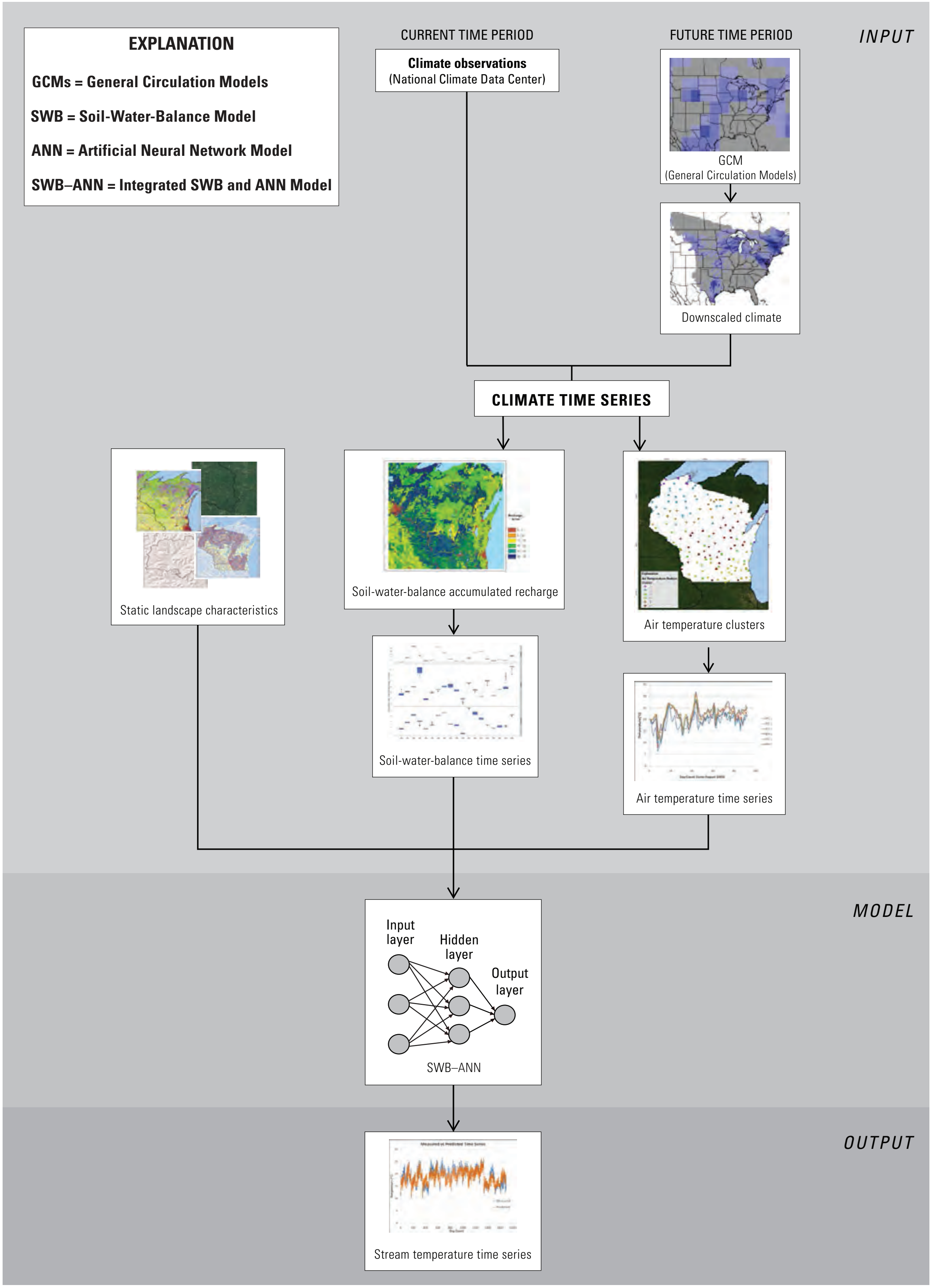

Figure 6. Approach and components of an Artificial Neural Network stream temperature Model integrated with a Soil-Water-Balance Model and General Circulation Models.

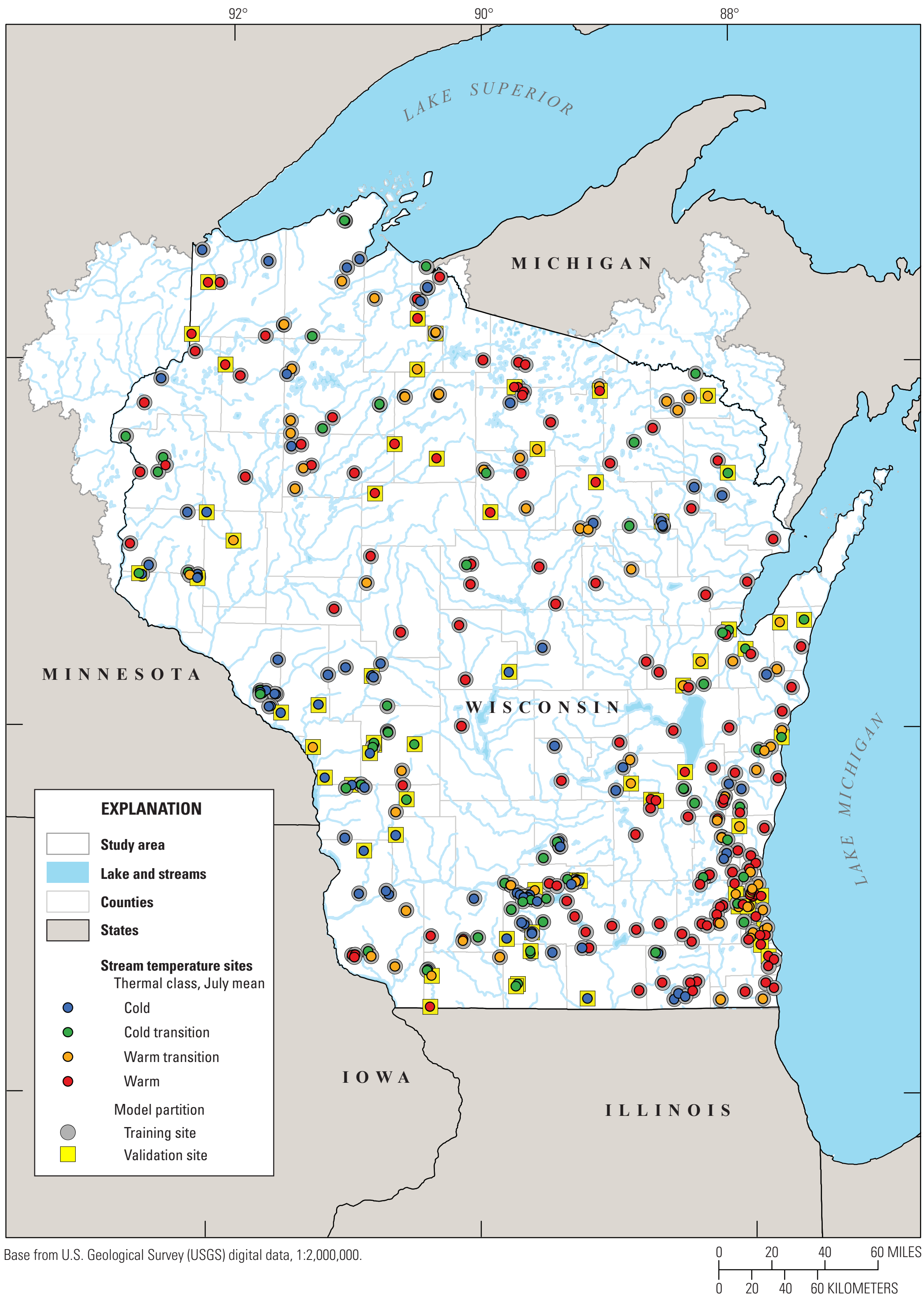

Figure 7. Location of 371 stream temperature monitoring sites used for training and validation of the Integrated Soil-Water-Balance and Artificial Neural Network version 1 (SWB-ANNv1) stream temperature model.

dropped after they did not help to improve model performance during ANNv1 model calibration. The six remaining air temperature time-series groups served as variables for model training for both ANNv1 and the SWB-ANNv1 model (figs. 8 and 9; appendix 2).

Landscape Characteristics

The 1:100,000 scale National Hydrography Dataset (NHD) served as the framework to which all of the landscape characteristics were attributed (U.S. Geological Survey, 2004b). Watershed boundaries were delineated using the 30-m NED for every confluence to confluence stream reach; static landscape variables were derived using a GIS for the entire upstream contributing area, 60-m riparian buffer, and the stream network (U.S. Geological Survey, 2004a). The landscape variables included drainage area, land cover, geology, Darcy groundwater potential (Baker and others, 2003a and b), annual streamflow exceedance, topography, geographic location, and network position as described in Brenden and others (2006). Pearson's correlation coefficient ($r \geq 0.75$) was used to identify and cull highly correlated variables to reduce dimensionality of the dataset; for highly correlated pairs, we chose the variable more strongly correlated with water temperature, resulting in 20 static landscape variables for model development.

Because the stream temperature time series were discontinuous among years, clustering and classification were used to identify the best landscape variables to explain the interannual variability in stream temperature and further reduce the list of variables for use in model training (Risley and others, 2003; Roehl and others, 2006). This approach helped determine the variables that best discriminated stream temperature sites across multiple summers and also sites with similar thermal characteristics (Stewart and others, 2006; Brenden and others, 2006).

Clustering and classification involved three steps: (1) stream temperature time series were clustered to group measurement sites with similar patterns into time-series groups, (2) classification models were developed to determine the smallest set of landscape variables that best discriminated each group within a single summer, and (3) a scoring procedure was developed to determine those landscape variables that best discriminated site groups across multiple summers. This process reduced the list of candidate static landscape variables to 10 (Westenbroek and others, 2010b; Brenden and others, 2006). All 10 variables were used in calibration of ANNv1 but 2 variables were dropped for calibration of SWB-ANNv1 resulting in 8 variables, because they were either spatial scale dependent (e.g., downstream link; Shreve, 1967) or they did not seem to improve model performance (e.g., percent fines; table 2).

Groundwater-Recharge Projections from the Soil-Water-Balance Model

The SWB model tracked and output a variety of variables of potential use in stream temperature prediction including growing degree-day (GDD), accumulated potential water loss (APWL), running sum of unmet potential evapotranspiration, soil moisture, and potential recharge. All of these variables except potential recharge had "lag-time" associated with them,

Table 2. Static landscape variables used as model predictors of stream temperature in Wisconsin (Brenden and others, 2006).

[Spatial unit defines the spatial scale over which the values apply; WT, total upstream watershed; CH, local channel; RT, total upstream 60 meter riparian buffer; USGS, U.S. Geological Survey]

Static variable (code, units)	Spatial unit	Mean	Minimum	Maximum	Standard deviation	Source
Drainage area (AREAKM, square kilometers)	WT	310.2	0.7	15,923.40	1,460.30	Computed from (USGS, 2004a)
Sinuousity (SINUOUS, unitless)	CH	1.3	1.0	4.2	0.3	Computed from (USGS, 2004b)
Urban - land cover (URBWT, percent)	WT	12.6	0.0	100.0	19.9	(USGS, 2003)
Agriculture - land cover (AGWT, percent)	WT	42.9	0.0	95.3	30.2	(USGS, 2003)
Open water - land cover (WATWT, percent)	WT	1.5	0.0	29.7	3.8	(USGS, 2003)
Wetland - land cover (WETWT, percent)	WT	7.6	0.0	53.3	10.4	(USGS, 2003)
Darcy - groundwater delivery (DARWT, meters day-1)	WT	-87.5	-749.0	5.2	98.6	(Baker and others, 2003a)
Darcy - groundwater delivery (DARRT, meters day-1)	RT	77.6	-43.7	474.2	88.2	(Baker and others, 2003a)

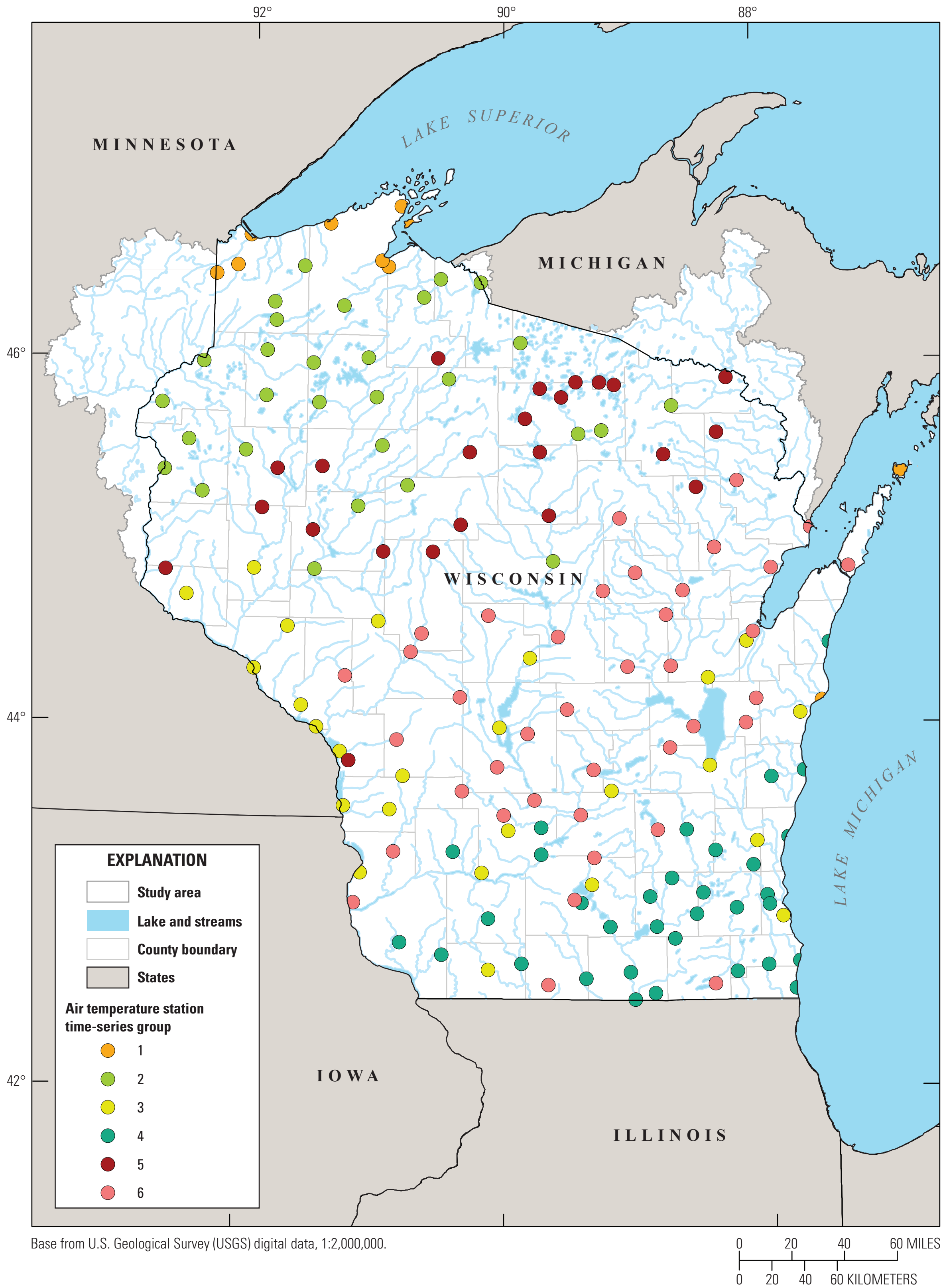

Figure 8. Location of 160 air temperature climate stations used for time-series clustering and for training of the Integrated Soil-Water-Balance and Artificial Neural Network version 1 (SWB-ANNv1) stream temperature model. Six air temperature station time-series groups are indicated by color.

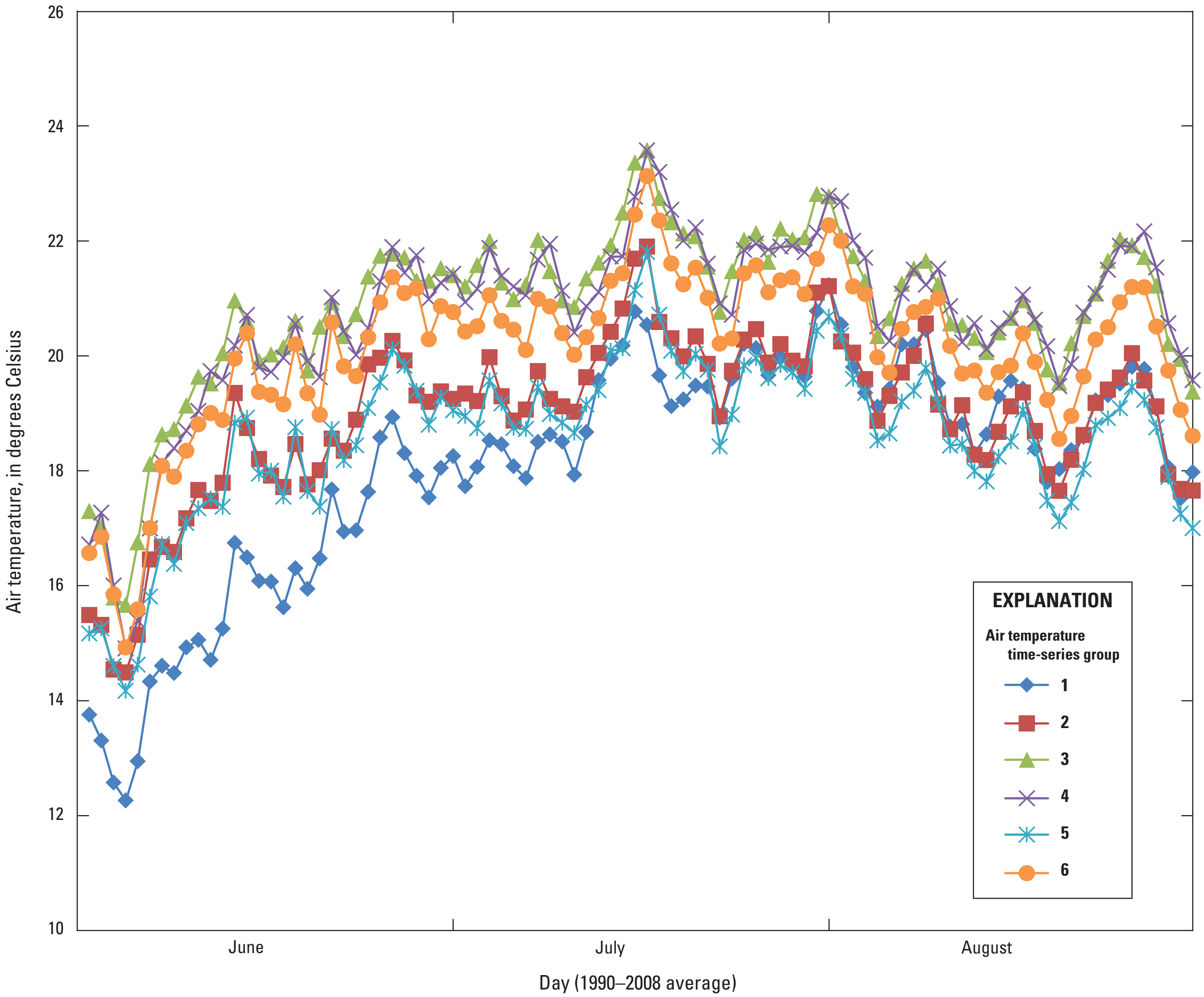

Figure 9. Average daily air temperature for six air temperature time-series groups averaged over 19 years (1990–2008) for the summertime (June–August) period.

such that the value on a given day was highly correlated to the value on the preceding day. The accumulation of potential recharge is useful in that it serves as perhaps a better indicator of general groundwater availability during the course of a summer season. In order to provide a more stable indicator of general groundwater availability, a running sum of the daily potential recharge was calculated (beginning on January 1st of each year) as well as mean annual recharge for each cell in the SWB model for the period 1990–2008. The summed potential recharge grid was used in SWB-ANNv1 model calibration because it addressed both the spatial and temporal components of recharge, unlike mean annual recharge where recharge values were averaged over the entire year. Time series of potential recharge were generated for every grid cell in the SWB model domain.

In order to take advantage of the dynamic nature of the SWB model and reduce the number of daily time series of potential recharge to a more manageable number, the model domain was divided into 16 different relatively homogenous spatial landscape units based on a combined hill-climbing/iterative minimum distance method (Rubin, 1967; Forgy, 1965). The landscape units were derived using a GIS and represented a combination of landscape characteristics likely to affect groundwater recharge and included quaternary geology, HSG, land cover, and NED (Fullerton and others, 2003; U.S. Department of Agriculture, 2009; U.S. Geological Survey, 2003 and 2004a).

An average time series of mean daily accumulated potential recharge was extracted from the SWB model for each of the 16 spatial landscape units. Accumulated potential recharge starting with January 1st were summed for all days leading up to June 1st, to match up with the beginning of the SWB-ANNv1 model calibration period; values for subsequent days were added to the total on a daily time step for the summertime (June–August) period.

One of the 16 SWB time series was dropped from further analysis because it represented the land-cover class of water. The remaining 15 SWB time series were tested for cross-correlation using Pearson's correlation coefficient to determine if some of the SWB time-series signals were similar to one another ($r \geq 0.85$); highly correlated time series and time series with poor spatial representation across the landscape were dropped, leaving 3 SWB model accumulated daily potential recharge time-series groups for use in the SWB-ANNv1 model calibration. These 3 time series of accumulated daily potential recharge are referred to as Soil-Water-Balance groups 2, 6, and 12 in figure 10.

Climate Projections from General Circulation Models

Downscaled climate data were acquired from UWCCR for the A1B scenario and 10 GCMs for 3 time periods (late 20th century-baseline (1961–2000), mid-21st century (2046–65), and late-21st century (2081–2100)) as daily grids with a 0.1 × 0.1 degree resolution (or about 8 × 8 km). Air temperature and precipitation were extracted from the daily grids and used as input to the SWB-ANNv1 model to simulate future summertime mean daily stream temperatures for all 30 GCM-time period combinations (10 GCMs × 3 time periods) for all stream segments in the study area.

In order to make use of the downscaled GCM data in the SWB-ANNv1 model, the downscaled results were distributed to each grid cell within the study area using a smoothing procedure. The R package "fields" (Fields Development Team,

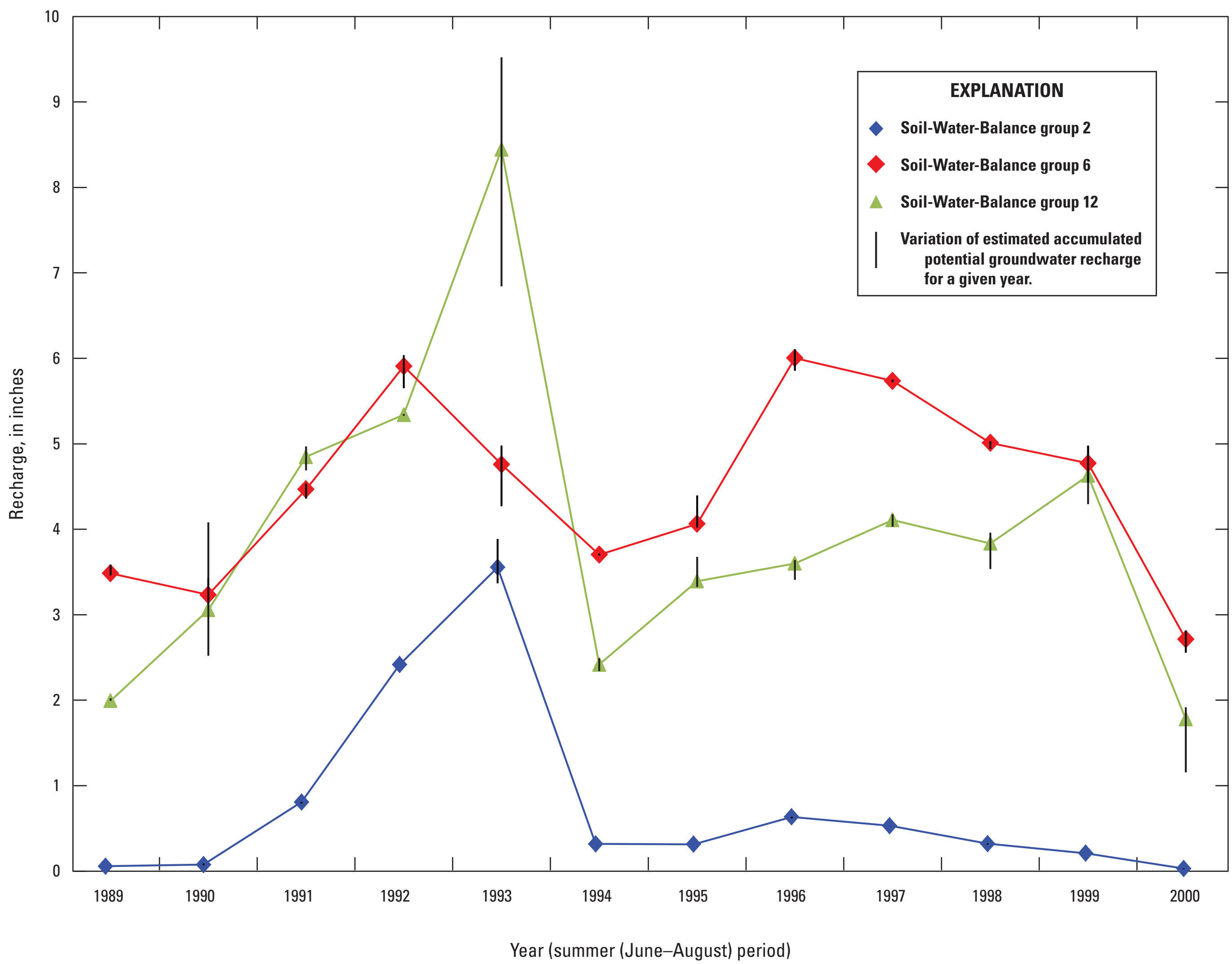

Figure 10. Soil-Water-Balance time series of accumulated potential groundwater recharge used for input to the Integrated Soil-Water-Balance and Artificial Neural Network version 1 (SWB-ANNv1) stream temperature model.

2006) was used to apply a kernel smoothing algorithm to the GCM output to produce a set of grids with the same projection and resolution as the SWB model domain (1,600 m × 1,600 m grid cell size).

Projections of air temperature were generated for each of the 6 air temperature time-series groups for the 30 GCM-time period combinations. Air temperature time series were extracted from each of the GCMs for grid cells that matched the location of the 160 climate stations used in SWB-ANNv1 model calibration. Daily averages were then generated for each of the six air temperature time-series groups, followed by decorrelation of group averages on a daily time step. This resulted in 30 time series (3 time periods × 10 GCMs) for each of the 6 air temperature groups. The results were assembled into 30 data files of projected daily air temperature; each data file included values for all 6 groups for a specific time period and GCM.

Future projections of accumulated daily potential recharge were derived for each SWB time series by running the SWB model with air temperature and precipitation estimates from the 10 GCMs (table 3) and 3 time periods (1961–2000, 2046–65, and 2081–2100). Accumulated daily potential recharge time series were then extracted for the 3 SWB groups required for SWB-ANNv1 model input, resulting in 30 time series (3 time periods × 10 GCMs). The results were assembled into 30 SWB data files of daily accumulated potential recharge; each data file included values for all 3 SWB time series for a specific time period and GCM.

Model Development and Application for the Integrated Soil-Water-Balance and Artificial Neural Network version 1 Stream Temperature Model

Modeling highly dynamic hydrologic systems on a statewide scale is challenging because the systems vary discontinuously both spatially and temporally. Stream temperature models come in many different varieties, but may be lumped into two groups: deterministic and statistical (Benyahya and others, 2007). Deterministic stream temperature models generally calculate a segment-by-segment energy balance and require detailed data on physical characteristics of the stream (Allen, 2008; Cox and Bolte, 2007), data that are largely unavailable statewide. Statistical models, such as ANNs, are attractive in that they generally require much less site-specific data to implement; however, building representative empirical models requires sufficient data to capture diverse causes and effects. We chose to use ANN models because they are able to handle non-linear relations, interactions among predictors, and discontinuous time-series climate data, and are relatively quick to develop while still having high predictive power (Conrads and others, 2013; McKenna and others, 2010; Risley and others, 2003; Roehl and others, 2006; Stewart and others, 2006; Westenbroek and others, 2010b).

Artificial Neural Networks

ANN models are empirical; they are developed directly from data. These models are a multivariate, nonlinear curve fitting technique with a flexible mathematical structure capable of describing complex nonlinear relations between input and output datasets. The structure of ANN models is loosely based on the biological nervous system and contains interconnected units that are analogous to neurons (Hinton, 1992). The neurons perform a simple “transfer function” whereby the input layer neurons are connected to all hidden layer neurons and all hidden layer neurons are connected to all output layer neurons. Each connection has a weight associated with it; the output of a neuron is the simple combination of the values it receives through its input connections, the associated weights, and the neuron’s transfer function (fig. 11). An ANN model is “trained” by iteratively adjusting its weights to minimize the error by which it maps inputs to outputs for a dataset composed of input/output vector pairs. Prediction accuracy can be measured by metrics such as the coefficient of determination (R^2) and RMSE, both during and after training.

In developing ANN models, it is customary to split datasets into “training” and “validation” datasets. Training datasets are used for model development, and validation datasets are used for model testing to provide an independent evaluation of model performance. For a large dataset with broad representation over the range of historical behaviors, a small percentage of the dataset (10–25 percent) may be selected for the training dataset; for a limited dataset, a larger percentage (75–100 percent) may be used in the training dataset. To prevent overfitting, the ANN models can be conservatively trained using a method referred to as “stop training.” Stop training allows the modeler to stop the training process before the ANN model has fit the data to the maximum extent possible. Adjustments to architectural and training parameters also allow the modeler to control the geometric complexity of the surface that the ANN model fits to the data. The data-mining software used for this application writes R^2 and RMSE to the graphical user interface (GUI) during training, and an inflection in the rate of change in these parameters indicates a transition from a generally linear, multivariate surface fit to a progressively nonlinear fit. This inflection point was used to trigger stop training. In general, a high-quality predictive model can be obtained when the data ranges are well distributed throughout the state space of variables describing the physical system of interest, the input variables selected by the modeler share mutual information about the output variables, and the functional form “prescribed” or “synthesized” by the model to “map” (correlate) input variables to output variables is a good one.

Training and Validation

A single SWB-ANNv1 model was developed to simulate daily summertime stream temperature (June 1 to August 31)

Table 3. List of 10 General Circulation Models used in this study, run with the A1B emissions scenario, including their originating group, country, model identification, and model code (Notaro and others, 2011).

Originating group(s)	Country	Model identification	Model code
Canadian Centre for Climate Modelling and Analysis	Canada	CGCM3.1 (T63)	CGCM
Météo-France / Centre National de Recherches Météorologiques	France	CNRM-CM3	CNRM
Commonwealth Scientific and Industrial Research Organisation (CSIRO) Atmospheric Research	Australia	CSIRO-Mk3.5	CSIRO
Meteorological Institute of the University of Bonn, Meteorological Research Institute of the Korea Meteorological Administration (KMA), and Model and Data Group	Germany / Korea	ECHO-G	ECHO
National Key Laboratory of Numerical Modeling for Atmospheric Sciences and Geophysical Fluid Dynamics / Institute of Atmospheric Physics (LASG / IAP)	China	FGOALS-g1.0	FGOALS
U.S. Department of Commerce / National Oceanic and Atmospheric Administration / Geophysical Fluid Dynamics Laboratory	USA	GFDL-CM2.0	GFDL
National Aeronautics and Space Administration / Goddard Institute for Space Studies	USA	GISS-AOM	GISS
Instituto Nazionale di Geofisica e Vulcanologia	Italy	INGV-ECHAM4	INGV
Institut Pierre Simon Laplace	France	IPSL-CM4	IPSL
Center for Climate System Research (The University of Tokyo), National Institute for Environmental Studies, and Frontier Research Center for Global Change (JAMSTEC)	Japan	MIROC3.2 (HiRes)	MIROC

for 1990–2008. The model was developed using the iQuest® (ADMi, 2011) data-mining software (Version 2.03C DM Rev31). Model input comprised static landscape variables and dynamic climate and SWB time series. The data matrix for SWB-ANNv1 model simulation was organized with each row representing a site on a particular day and the columns representing input and output variables. The data were stacked or concatenated by site, and time-series signals (air temperature, SWB, and stream temperature) were matched by calendar day. The SWB-ANNv1 model built upon the approach and results of the ANNv1 by using the same methodology and data sources; however, it expanded the spatial and temporal extent of stream temperature sites and observations and added the SWB component as an enhancement and a link to future climate projections.

The SWB-ANNv1 model was trained with 90 percent of the available data (n = 304 sites; 60,618 measurement days); the remaining 10 percent were reserved for model validation (n= 67 sites; 6,738 measurement days) (fig. 7). Independent training data included sites with the highest information content that represent the breadth of behavior in the data; data with redundant or similar information were reserved for the independent validation dataset. Both training and validation sets included sites covering the range of thermal conditions, from cold-water to warm-water sites (Lyons and others, 2009). Sites with multiple years of measurements were assigned to the training set, whereas sites with a single summer of data were set aside for model validation. A number of candidate models were trained and evaluated for their statistical accuracy using measures of R^2 and RMSE.

The model development process involved training the SWB-ANNv1 model iteratively by starting with a candidate pool of static and dynamic input variables followed by adjusting learning rates, the number of hidden layer neurons, and model weights to maximize the R^2 and minimize the mean square error (MSE) across training and validation sets. In

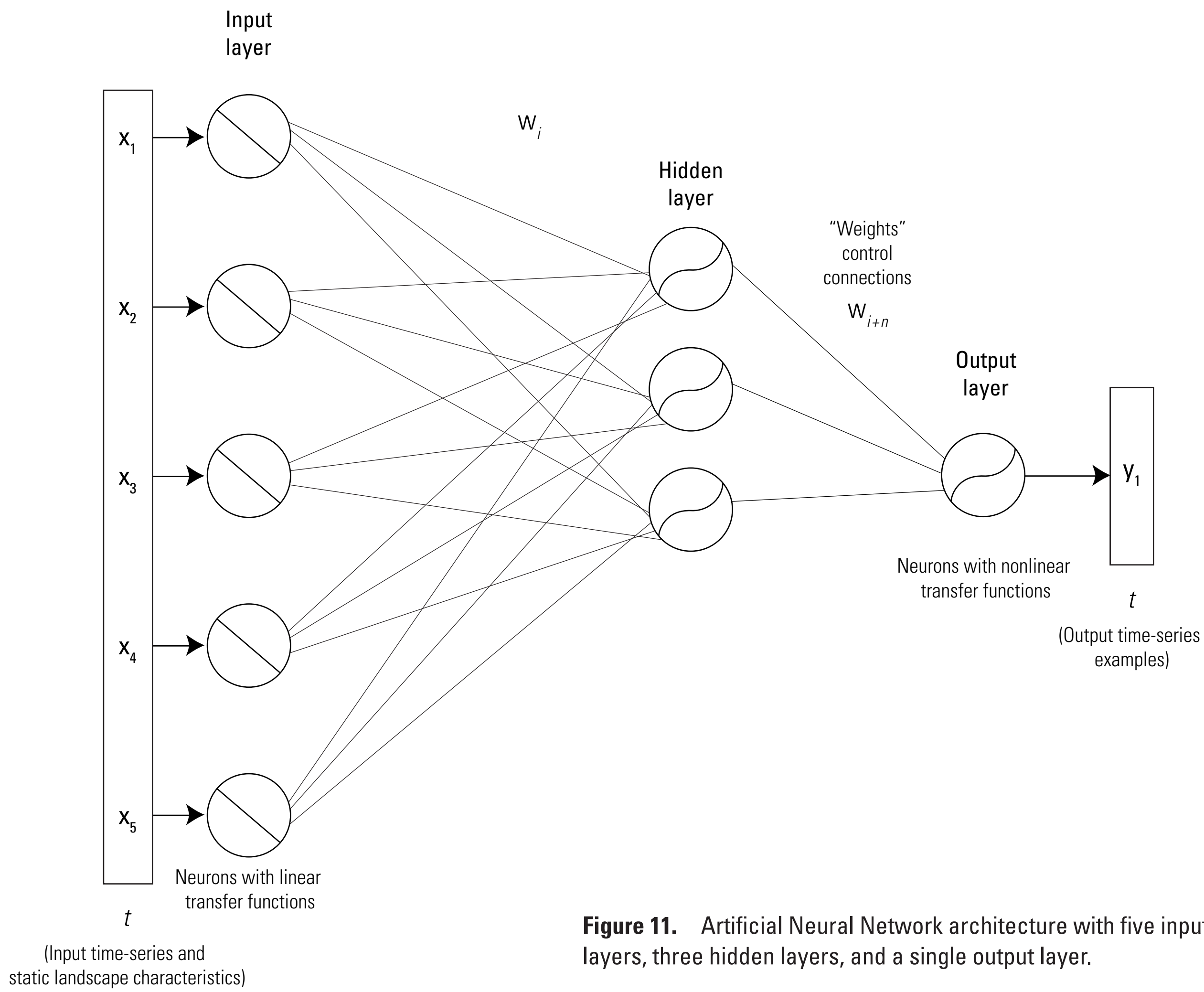

Figure 11. Artificial Neural Network architecture with five input layers, three hidden layers, and a single output layer.

addition to the use of "stop training" to prevent overfitting, we also slowed the training rates by a factor of 10 (e.g., .075 to .0075) when the training and (or) testing R^2 values began to stabilize. We limited the number of hidden layer neurons to a maximum value of 3. Each time training rates were adjusted, model performance (R^2) and input-output sensitivities were used to evaluate the stability of the model input variables and to remove those static variables with the least amount of influence on the output variable. The model was trained using standard back-error propagation (Rumelhart and others, 1986) by which the neural network software calculated an output value, compared it to the actual measured target value, determined the error, and readjusted model weights to reduce the error. This iterative process continued until the error was minimized, at which time no learning was taking place. This approach to model development is a common and widely used method for determining error weights and training a neural network.

The ability of the model to predict daily mean stream temperature was evaluated using four "goodness-of-fit" statistics for the 67 model validation sites and plots of measured and predicted stream temperatures. The importance of individual variables was evaluated using model sensitivity reports. The computed statistics included R^2, MSE, RMSE, and percent model error (PME). The R^2 indicated how much of the overall variability in the data was explained by the model and how well it captured the overall trend in the data; the MSE and RMSE provided a measure of prediction accuracy (i.e., whether the model underpredicted or overpredicted and the magnitude of that discrepancy); and the PME statistic divided the RMSE by the range of the measured data to determine the percent of error over the full range of modeled data. We also evaluated PME for each of four stream thermal classes (cold, cold transition, warm transition, and warm) defined by Lyons and others (2009). Each site was first assigned to a thermal class based on calculated average July mean, all site days were then grouped by thermal class and model partition (training and validation). PME was then calculated for all daily predictions within each thermal class and model partition group.

Model Predictions and Projections for Current and Future Climate Conditions

The calibrated SWB-ANNv1 model was applied to all stream segments (n = 38,243) in the study area using the dynamic (air temperature and SWB) and static (landscape characteristics) input variables to predict mean daily water temperature for each summertime date (June 1–August 31) for 1990–2008 for a total of 1,748 daily water temperature predictions for each stream segment (92 days per year for 19 years). The process was expedited by means of a custom R script (R Development Core Team, 2011). The daily predictions were summarized to generate a number of water temperature variables shown to be important for explaining fish distribution patterns in streams of the Laurentian Great Lakes region (Lyons and others, 2009, 2010). Water temperature variables included July mean, summertime (June–August) mean, summertime maximum daily mean, maximum of the 19 yearly July means, maximum of the 19 yearly summertime maximum daily means, and number of days when stream temperature exceeded a maximum threshold. These summary variables were generated for use in fish species occurrence models and for use in estimating the effects of projected future climate scenarios on stream temperature (Lyons and others, 2010). The summary variable July mean water temperature was used in subsequent analyses in this report to classify stream segments into thermal classes and for comparison to assess the effects of projected future climate on stream temperature. We used the cold, cold transition, warm transition, and warm-water thermal classes identified by Lyons and others (2009), then further subdivided the warm-water thermal class into warm and very warm in order to capture projected impacts of climate change on warm-water streams (table 1).

We used the model calibration period 1990–2008 to represent what we considered “current” conditions along with climate observations extracted from the DSI-3200 daily surface database maintained by the NCDC (National Oceanic and Atmospheric Administration, 2011).

Future stream temperature estimates were made for three time periods (late 20th century (1961–2000), mid-21st century (2046–65), and late 21st-century (2081–2100)) using climate projections from 10 GCMs. This required running the SWB-ANNv1 model 30 times, each time replacing the air temperature and SWB time series with the appropriate data to represent the time period and GCM. The daily estimates were summarized to generate the average July mean stream temperature for each stream segment for the 30 GCM-time period combinations.

Stream temperature projections derived from the 10 GCMs for future time periods (2046–65 and 2081–2100) were referenced to late 20th century baseline (1961–2000) GCM-based projections, representing the “current” time period (WICCI, 2011). In contrast, the statewide stream temperature estimates representing “current” (1990–2008) conditions were based on actual daily air temperature observations. In order to evaluate change in stream temperature from current to future time periods, it was necessary to adjust the future stream temperature projections for 2046–65 and 2081–2100 so they could be referenced to observed current conditions (1990–2008) rather than modeled GCM-based “current” conditions for the 20th century baseline (1961–2000). Model projections of stream temperature under future conditions based on projections from GCMs may be biased. Climate models capture general global trends reasonably well, but significant local biases in air temperature and precipitation may be present in any given model (Haerter and others, 2011). A bias correction factor was applied to bring GCM-based projections of stream temperatures in line with stream temperatures projected from observed climate data for 1990–2008.

The bias correction factor represented the difference in degrees Celsius between GCM-based “current” and the “observation” based “current” July mean stream temperature. The GCM-modeled time period 1961–2000 baseline for current climate conditions and the 1990–2008 time period of stream temperature observations overlapped for the years 1990–2000. Therefore, 1990–2000 served as the baseline for calculation of the bias correction factor.

Bias correction factors were calculated separately for each combination of stream segment and GCM. Bias correction factors were calculated and applied as follows:

1. July mean stream temperature was calculated for stream temperature model outputs run with either the GCM-generated dynamic air temperature data for 1990–2000 or the observed air and stream temperature data for 1990–2000.

2. Bias correction factors were calculated as the GCM-derived July mean stream temperature minus the July mean stream temperature derived from observed air temperature data.

3. Bias correction factors were subtracted from projected stream temperatures derived from models using GCM projections of air temperatures for 2046–65 and 2081–2100.

As an example, if projections of July mean stream temperatures based on models using GCM-generated air temperature input data were 2 °C higher than July mean stream temperatures based on observed air and stream temperature data, then the bias correction factor would be +2 °C. Therefore, projected stream temperatures based on GCMs for future time periods (mid- and late-21st century) would be corrected by subtracting 2 °C.

After correcting the GCM-derived July mean stream temperature for each stream segment using the bias correction factor, the resulting stream temperatures were classified into 1 of 5 thermal classes (table 1) for each of the 10 runs of the SWB-ANNv1 model for both time periods. Results were summarized statewide by GCM and time period using the two metrics, July mean stream temperature and July mean thermal class. A “GCM average” July mean stream temperature was calculated for each stream segment by averaging the values of the bias-corrected GCM-derived July mean stream temperatures that resulted from the 10 SWB-ANNv1 model runs using the GCM-climate source data. The July mean thermal class was then determined for each July mean “GCM average” value. Both the “GCM average” and individual results from running the SWB-ANNv1 model using each of the 10 GCM datasets as climate input were used for comparison of current and future stream temperature projections. In subsequent sections of this report, individual results from the 10 SWB-ANNv1 model runs with GCM climate source data will be referred to by the GCM model code (table 3), and the average of those results will be referred to as the GCM average.

Results and Discussion

Model Performance

The best model predictors of daily stream temperature were the six decorrelated air temperature time series, three SWB time series of accumulated potential groundwater recharge and eight static landscape variables. The sensitivity of the variables in the final model indicated that the daily stream temperature was most sensitive to two of the static variables, Darcy (network watershed; a measure of groundwater delivery) and drainage area, followed by one of the dynamic air temperature time-series groups and the static variable open water (table 4).

The R^2 for the training and validation data were 0.71 and 0.76 for the SWB-ANNv1 model compared to 0.60 and 0.67 for ANNv1, a nine percentage point improvement (Stewart and others, 2006; Westenbroek and others, 2010a). Evaluations of daily predictions for the SWB-ANNv1 model resulted in an RMSE of 1.9 and 1.5 for training and validation data, respectively, and a PME of 8.8 percent for both training and validation data, respectively (table 5), which also are improvements over ANNv1. Nearly one-half (49.2 percent) of summertime (June–August) mean stream temperature predictions using model validation sites were within 1 °C of observed values, 80.5 percent were within 2 °C, and 95.1 percent were within 3 °C (table 6). Nearly one-half (47.4 percent) of July mean predictions also were within 1 °C of observed values, 77.2 percent were within 2 °C, and 93.3 percent were within 3 °C (table 6) for model-validation sites.

The range of measured values for model-validation sites was smallest for cold-water (about 11 °C) and largest for the warm-water sites (about 17 °C). This pattern also was observed for the training sites. Percent model error (which is a function of the range of measured values) by thermal class ranged from about 10 percent for warm water to about 14 percent for cold water, for both validation and training sites (table 7). The PME also was summarized for two validation sites representing the 25th and 75th percentiles for each of the four thermal classes (cold, cold transition, warm transition, and warm) (table 8). The PME interquartile range was about 14 to 28 percent for the cold-water sites, about 10 to 17 percent for cold-transition sites, about 12 to 18 percent for warm-transition sites, and about 12 to 17 percent for warm-water sites.

Table 4. Variables used to calibrate the Integrated Soil-Water-Balance and Artificial Neural Network version 1 (SWB-ANNv1) Model and the average absolute sensitivity.

[Spatial unit defines the spatial scale over which the values apply; WT, total upstream watershed; na, not applicable; RT, total upstream 60 meter riparian buffer; CH, local channel]

Variable (code, units)	Spatial unit	Variable type	Average absolute sensitivity
Groundwater delivery - Darcy (DARWT, meters day-1)	WT	static	0.210
Drainage area (AREAKM, square kilometers)	WT	static	0.161
Air temperature cluster 6 (AT6, degrees Celsius)	na	dynamic	0.157
Open water (WATWT, percent)	WT	static	0.143
Wetland (WETWT, percent)	WT	static	0.071
Agricultural land cover (AGWT, percent)	WT	static	0.046
Urban land cover (URBWT, percent)	WT	static	0.038
Groundwater delivery - Darcy (DARRT, meters day-1)	RT	static	0.034
Air temperature cluster 3 (AT3, degrees Celsius)	na	dynamic	0.032
Sinuousity (SINUOUS, unitless)	CH	static	0.021
Air temperature cluster 1 (AT1, degrees Celsius)	na	dynamic	0.021
Air temperature cluster 4 (AT4, degrees Celsius)	na	dynamic	0.019
Groundwater recharge - Soil-water-balance cluster 6 (SWB6, inches)	na	dynamic	0.011
Groundwater recharge - Soil-water-balance cluster 1 (SWB1, inches)	na	dynamic	0.010
Air temperature cluster 2 (AT2, degrees Celsius)	na	dynamic	0.010
Air temperature cluster 5 (AT5, degrees Celsius)	na	dynamic	0.009
Groundwater recharge - Soil-water-balance 8 (SWB8, inches)	na	dynamic	0.007

Table 5. Summary of performance statistics for the models used to estimate stream temperature for 254 sites (1990–2002) and 371 sites (1990–2008) in Wisconsin.

[R^2, coefficient of determination; RMSE, root mean square error; deg C, degree Celsius; PME, percent model error = root mean square error of the model predictions divided by the range of measured data; ANNv1, Artificial Neural Network version 1 stream temperature Model (Stewart and others, 2006); SWB-ANNv1, Integrated Soil-Water-Balance and Artificial Neural Network version 1 Model]

Model name	Time period	Model partition	Measured data, in degrees Celsius			Number of sites	Number of observations	R^2	RMSE (deg C)	PME (percent)
			Minimum	Maximum	Range*					
ANNv1	1990–2002	Training	7.4	30.5	23.1	223	25,472	0.60	2.3	9.8
		validation	9.8	28.3	18.5	31	2,799	0.67	2.0	11.0
SWB-ANNv1	1990–2008	Training	7.4	30.8	23.4	304	60,618	0.71	1.9	8.8
		validation	10.1	28.5	18.4	67	6,738	0.76	1.5	8.8

*Difference in maximum and minimum measured values.

Table 6. Summary of residuals (absolute value) for the Integrated Soil-Water-Balance and Artificial Neural Network version 1 (SWB-ANNv1) Model used to estimate stream temperature for 371 sites in Wisconsin (1990–2008).

[percent, percent of measured observations; <, less than; >, greater than]

Degrees Celsius	Summer (June–August) mean				July mean			
	Training		Validation		Training		Validation	
	Number of observations	Percent	Number of observations	Percent	Number of observations	Percent	Number of observations	Percent
< 1 degree	24,009	39.6	3,313	49.2	7,789	37.8	1,107	47.4
> 1 - 2 degrees	18,039	29.8	2,106	31.3	6,131	29.8	696	29.8
> 2 - 3 degrees	10,955	18.1	982	14.6	3,801	18.5	376	16.1
> 3 - 4 degrees	5,191	8.6	283	4.2	1,918	9.3	135	5.8
> 4 - 5 degrees	1,889	3.1	51	0.8	753	3.7	19	0.8
> 5 - 6 degrees	431	0.7	2	0.03	159	0.8	0	0
> 6 - 7 degrees	72	0.1	1	0.01	36	0.2	0	0
> 7 - 8 degrees	19	0.03	0	0	11	0.1	0	0
> 8 - 9 degrees	11	0.02	0	0	2	0.01	0	0
> 9 - 10 degrees	2	0.003	0	0	0	0	0	0
Total	60,618		6,738		20,600		2,333	

Table 7. Percent model error by thermal class for the Integrated Soil-Water-Balance and Artificial Neural Network version 1 (SWB-ANNv1) Model used to estimate stream temperature for 371 sites in Wisconsin (1990–2008).

[PME, percent model error = root mean square error of the model predictions divided by the range of measured data]

Thermal class	Training				Validation			
	Number of observa-tions	Percent of observa-tions	Range of measured values*	PME (percent)	Number of observa-tions	Percent of observa-tions	Range of measured values	PME (percent)
Cold water	13,640	22.5	15.8	13.7	1,976	29.3	10.5	14.5
Cold transition	11,447	18.9	18.4	10.5	1,275	18.9	12.2	10.6
Warm transition	9,039	14.9	16.5	10.4	1,733	25.7	13.5	11.5
Warm water	26,492	43.7	20.2	9.5	1,754	26.0	16.7	10.0

*Difference in maximum and minimum measured values.

Table 8. Statistical measure of prediction accuracy for eight validation sites representing the 25th and 75th percentile for cold, cold-transition, warm-transition, and warm-water sites for the Integrated Soil-Water-Balance and Artificial Neural Network version 1 (SWB-ANNv1) Model (1990–2008).

[R^2, coefficient of determination; MSE, mean square error; deg C, degrees Celsius; RMSE, root mean square error; PME, percent model error = root mean square error of the model predictions divided by the range of measured data]

Site number	Thermal class	Year measured	Inner quartile range (percentile)	Number of observations	R^2	MSE (deg C)	RMSE (deg C)	Range of measured data (deg C)*	PME (percent)
420	Cold water	2008	25th	92	0.66	0.5	0.7	5.0	13.8
426	Cold water	2007	75th	92	0.8	6.0	2.4	8.7	28.2
228	Cold transition	1998	25th	92	0.85	0.7	0.8	8.7	9.5
353	Cold transition	2000	75th	84	0.77	0.8	0.9	5.1	17.3
287	Warm transition	2004	25th	92	0.77	1.3	1.1	9.5	11.9
242	Warm transition	2000	75th	92	0.72	2.7	1.6	8.9	18.4
20	Warm water	1999	25th	78	0.76	1.3	1.1	9.3	12.2
46	Warm water	1999	75th	91	0.74	2.4	1.5	9.3	16.6

*Difference in maximum and minimum measured values.

Predicted stream temperature appeared to track the daily time-series pattern for all eight validation sites representing the 25th and 75th percentiles by thermal class (fig. 12). The measured and predicted daily temperatures for the 25th percentile sites appeared to match closely with no bias. For the 75th percentile sites that are classified as cold-water, cold-transition, or warm-transition, however, predicted values were biased high; temperature values for the cold-water, cold-transition, and warm-transition classes were overpredicted when compared to measured values (fig. 12). Conversely, the 75th percentile values for sites classified as warm water appear to be biased low. The PME statistic provides a measure of the percent error across the range of measured data, where the R^2 provides a measure of prediction accuracy and how well it captured the overall trend in the data. This can be observed in figure 12 where sites with similar R^2 values (i.e., warm-transition sites; site 287, 25th percentile, $R^2 = 0.77$, PME = 11.9; site 242, 75th percentile, $R^2 = 0.72$, PME = 18.4) have very different PME values. For these warm-transition sites, the measured versus predicted graphs follow a similar overall trend for both sites as indicated by the R^2; however, for site 242 (75th percentile) the higher PME (18.4 percent) can be observed by viewing the magnitude of differences between the graph lines across the full range of measured values when compared to the graph for site 287 (25th percentile). A similar pattern was observed for the cold-water, cold-transition and warm-water sites (table 8; fig. 12) when comparing R^2 and PME. The PME was greatest for cold-water sites when compared to other thermal classes (table 7) indicating a higher percent error across the range of measured data.

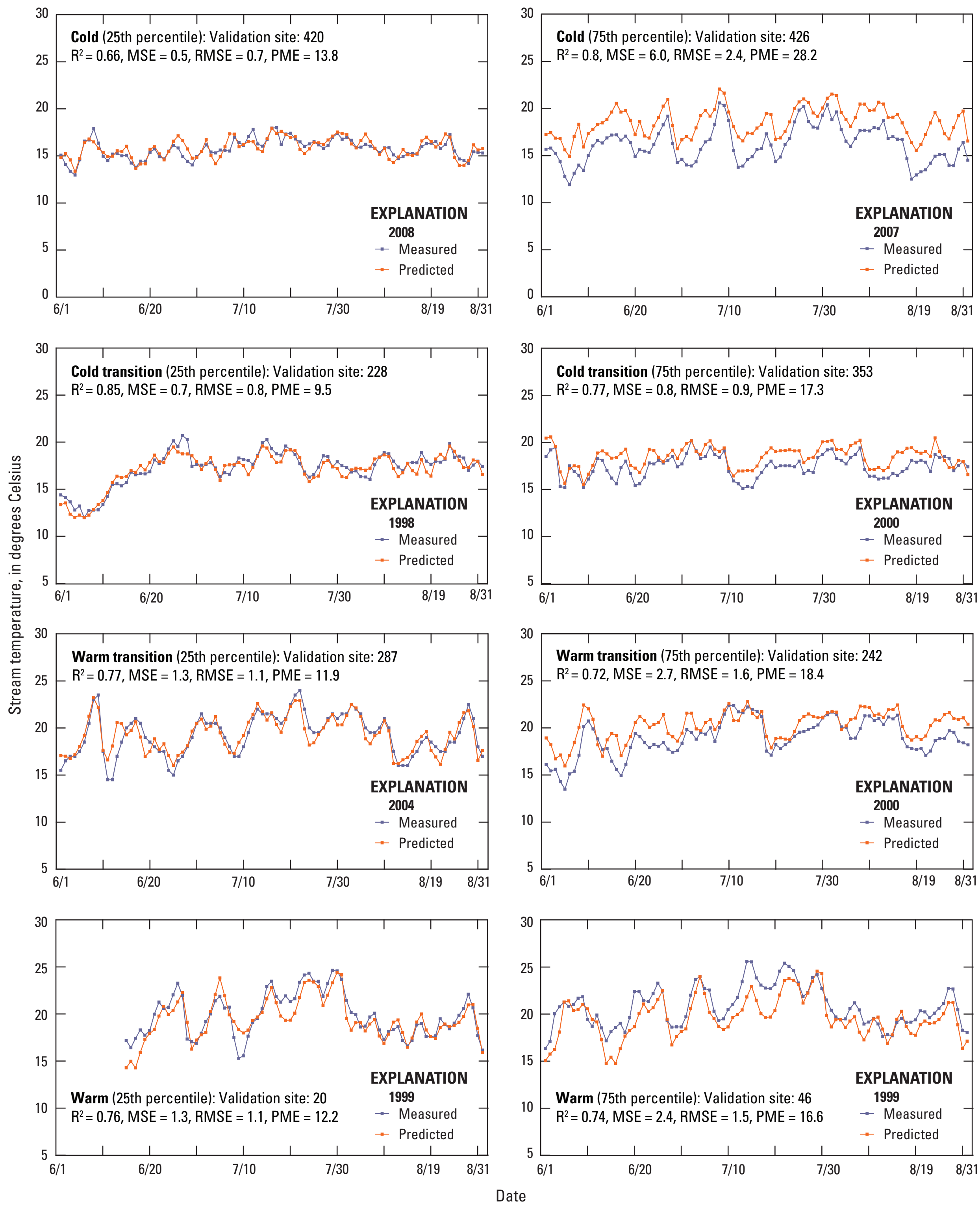

Figure 12. Simulations of stream temperature for eight validation sites, representing 25th and 75th percentiles, based on percent model error for four thermal classes (cold, cold transition, warm transition, and warm) from the integrated Soil-Water-Balance and Artificial Neural Network version 1 (SWB-ANNv1) stream temperature Model.

Model Predictions for Current Conditions

Modeled water temperatures for the current time period (1990–2008), as measured by July mean water temperature, ranged across stream segments from about 9.0 to 32.0 °C with a mean of 18.7 °C and median of 18.8 °C. More than one-half of the stream kilometers in the study area (56.7 percent) were thermally suitable for supporting cold-water fishes such as trout, having thermal classifications of cold (27.1 percent) or cold transition (29.6 percent) (table 9; figs. 13, 14, and 15). The spatial distribution of streams by thermal class indicated a predominance of cold and cold-transition streams in the Driftless Area of western and southern Wisconsin and in the north along Lake Superior (figs. 1, 14, and 15). The remaining stream kilometers were thermally suitable for supporting warm-water fishes such as minnow and sunfishes, having thermal classifications of warm transition (29.6 percent), warm (12.5 percent), and very warm (1.1 percent) (table 9; figs. 13, 14, and 15). The spatial distribution of streams by thermal class indicated a predominance of warm and warm-transition streams in the eastern half of Wisconsin, with warm-transition streams also prominent across northern Wisconsin adjacent to the Upper Peninsula of Michigan (figs. 1, 14, and 15).

For the Wisconsin portion of the study area (excluding the St. Croix River Basin in Minnesota and the Menominee River Basin in Michigan), the SWB-ANNv1 stream temperature model classified streams, based on stream length, as 29.2 percent cold, 30.3 percent cold transition, 27.1 percent warm transition, and 13.4 percent warm. The ANNv1 stream temperature model, in contrast, classified Wisconsin streams as 7.9 percent cold, 45.9 percent cold transition, 28.6 percent warm transition, and 17.6 percent warm (Lyons and others, 2009). Overall, the SWB-ANNv1 model predicted an additional 5.7 percent of stream kilometers as suitable for cold-water fishes, as compared to the ANNv1 model, with about equal proportions of cold and cold transition stream kilometers.

Model Projections for Future Climate Conditions

Future projections of stream temperature were made using climate projections downscaled for Wisconsin from 10 GCMs for the mid-21st century (2046–65) and late-21st century (2081–2100). The projections from the individual GCMs vary widely; therefore, we provide both the GCM average results as well as the results from individual GCMs as a means to show the range of projected values (IPCC, 2007).

Average GCM-based water temperature projections: 2046–65 time period—Projected water temperatures (July mean) for the mid-21st century ranged from about 9.2 to 33.0 °C for all stream segments, similar to the current time period, however the mean (19.9 °C) and median (20.0 °C), were both about 1.0 °C higher when compared to current. Almost two-fifths of the stream kilometers in the study area (38.7 percent) were projected to be thermally suitable for supporting cold-water fishes at mid-century, having thermal classifications of cold (15.5 percent) or cold transition (23.2 percent) (table 9; fig. 13). The remaining 61.3 percent of stream kilometers were thermally suitable for supporting warm-water fishes, having thermal classifications of warm transition (21.3 percent), warm (36.8 percent), and very warm (3.2 percent). These projected mid-21st century changes represent a loss of thermal habitat for cold-water fishes, with a loss of 18 percent of stream kilometers and a concomitant gain of thermal habitat for warm-water fishes.

Average GCM-based water temperature projections: 2081–2100 time period—During the late-21st century projected water temperatures (July mean) ranged from about 9.3 to 31.7 °C, again similar to the current time period, however the mean (20.4 °C) and median (20.5 °C) were both 1.7 °C higher when compared to current. About one-third of the stream kilometers in the study area (33.2 percent) were projected to be thermally suitable for supporting cold-water fishes at late-century, having thermal classifications of cold (11.0 percent) or cold transition (22.2 percent) (table 9; fig. 13). The remaining 66.8 percent of stream kilometers were thermally suitable for supporting warm-water fishes, having thermal classifications of warm transition (18.8 percent), warm (42.4 percent), and very warm (5.8 percent). These projected late-21st century changes represent a loss of thermal habitat for cold-water fishes, with a loss of 23.5 percent of stream kilometers and a concomitant gain of thermal habitat for warm-water fishes.

Individual GCM-based water temperature projections: 2046–65 and 2081–2100 time period—Among SWB-ANNv1 models using climate data from the 10 individual GCMs, the percentage of stream kilometers projected to be suitable for cold-water fishes at mid-century ranged from a high of 46.7 percent (model CGCM climate data) to a low of 25.7 percent (model GFDL climate data) (table 9; fig. 13). By late-century, the percentage of stream kilometers projected to be suitable for cold-water fishes ranged from a high of 48.2 percent (model CSIRO climate data) to a low of 23.5 percent (model MIROC climate data) for stream kilometers suitable for cold-water fishes. In the worst-case scenario for cold-water fishes, a comparison of projections using GCM climate data to predictions under current climate conditions indicates a loss of 30.9 percent of total stream kilometers at mid-century (model GFDL climate data) and a loss of 33.2 percent at late-century (model MIROC climate data) as no longer suitable for supporting cold-water fishes. These projected losses based on data from individual GCMs represent more than a 10 percent reduction in cold-water habitat over the GCM-based average.

Despite the shift from stream kilometers suitable for cold-water fishes (lower percentage) to stream kilometers suitable for warm-water fishes (higher percentage), the gain in stream kilometers occurred only among warm and very warm streams (table 9; fig.13); warm-transition streams also suffered losses. There were about 2.9 times as many warm stream kilometers projected by mid-century and about 3.4 times as many projected by late-century for the GCM average. For very

Table 9. Predictions of stream temperature thermal class (Lyons and others, 2009) and projected change summarized by length and as a percentage of total length (94,341 kilometers) for current (1990–2008) and future (2046–2065 and 2081–2100) climate conditions for 10 General Circulation Models.

[GCM, General Circulation Model; km, kilometer]

GCM code	Thermal class (subclass)	Current time period (1990–2008)		Future (2046–2065)			Future (2081–2100)		
		Length (km)	Length (percent of total)	Length (km)	Length (percent of total)	Length (percent change from current)	Length (km)	Length (percent of total)	Length (percent change from current)
None	Cold	25,597	27.1						
	Cold transition	27,958	29.6						
	Warm transition	27,924	29.6						
	Warm	11,830	12.5						
	Very warm	1,033	1.1						
Average of 10 GCMs	Cold			14,628	15.5	−42.9	10,417	11.0	−59.3
	Cold transition			21,930	23.2	−21.6	20,937	22.2	−25.1
	Warm transition			20,076	21.3	−28.1	17,701	18.8	−36.6
	Warm			34,719	36.8	193.5	39,822	42.2	236.6
	Very warm			2,988	3.2	189.3	5,464	5.8	428.9
CGCM	Cold			19,389	20.6	−24.3	15,238	16.2	−40.5
	Cold transition			24,611	26.1	−12.0	21,909	23.2	−21.6
	Warm transition			27,741	29.4	−0.7	20,261	21.5	−27.4
	Warm			20,717	21.9	75.1	33,992	36.0	187.3
	Very warm			1,883	2.0	82.3	2,940	3.1	184.6
CNRM	Cold			14,748	15.6	−42.4	9,157	9.7	−64.2
	Cold transition			22,249	23.6	−20.4	20,827	22.1	−25.5
	Warm transition			21,990	23.3	−21.3	17,107	18.1	−38.7
	Warm			32,625	34.6	175.8	40,263	42.7	240.3
	Very warm			2,728	2.9	164.1	6,988	7.4	576.5

Table 9. Predictions of stream temperature thermal class (Lyons and others, 2009) and projected change summarized by length and as a percentage of total length (94,341 kilometers) for current (1990–2008) and future (2046–2065 and 2081–2100) climate conditions for 10 General Circulation Models.—Continued

[GCM, General Circulation Model; km, kilometer]

GCM code	Thermal class (subclass)	Current time period (1990–2008)		Future (2046–2065)			Future (2081–2100)		
		Length (km)	Length (percent of total)	Length (km)	Length (percent of total)	Length (percent change from current)	Length (km)	Length (percent of total)	Length (percent change from current)
CSIRO	Cold			18,271	19.4	−28.6	20,543	21.8	−19.7
	Cold transition			23,911	25.3	−14.5	24,918	26.4	−10.9
	Warm transition			26,274	27.9	−5.9	27,553	29.2	−1.3
	Warm			23,808	25.2	101.3	19,590	20.8	65.6
	Very warm			2,076	2.2	101.0	1,738	1.8	68.2
ECHO	Cold			15,597	16.5	−39.1	8,419	8.9	−67.1
	Cold transition			22,002	23.3	−21.3	20,522	21.8	−26.6
	Warm transition			18,848	20.0	−32.5	17,071	18.1	−38.9
	Warm			34,877	37.0	194.8	40,281	42.7	240.5
	Very warm			3,016	3.2	192.0	8,048	8.5	679.1
FGOALS	Cold			17,390	18.4	−32.1	11,582	12.3	−54.8
	Cold transition			23,182	24.6	−17.1	21,501	22.8	−23.1
	Warm transition			19,842	21.0	−28.9	18,244	19.3	−34.7
	Warm			31,258	33.1	164.2	39,027	41.4	229.9
	Very warm			2,669	2.9	158.4	3,987	4.2	286.0
GFDL	Cold			5,120	5.4	−80.0	5,834	6.2	−77.2
	Cold transition			19,181	20.3	−31.4	20,098	21.3	−28.1
	Warm transition			17,269	18.3	−38.2	17,277	18.3	−38.1
	Warm			44,236	46.9	273.9	41,226	43.7	248.5
	Very warm			8,535	9.1	726.2	9,906	10.5	859.0

Table 9. Predictions of stream temperature thermal class (Lyons and others, 2009) and projected change summarized by length and as a percentage of total length (94,341 kilometers) for current (1990–2008) and future (2046–2065 and 2081–2100) climate conditions for 10 General Circulation Models.—Continued

[GCM, General Circulation Model; km, kilometer]

GCM code	Thermal class (subclass)	Current time period (1990–2008)		Future (2046–2065)			Future (2081–2100)		
		Length (km)	Length (percent of total)	Length (km)	Length (percent of total)	Length (percent change from current)	Length (km)	Length (percent of total)	Length (percent change from current)
GISS	Cold			17,442	18.5	−31.9	11,041	11.7	−56.9
	Cold transition			23,099	24.5	−17.4	20,781	22.0	−25.7
	Warm transition			20,430	21.6	−26.8	19,268	20.4	−31.0
	Warm			30,709	32.6	159.6	39,144	41.5	230.9
	Very warm			2,661	2.8	157.6	4,108	4.4	297.7
INGV	Cold			16,928	17.9	−33.9	9,787	10.4	−61.8
	Cold transition			22,761	24.1	−18.6	20,450	21.7	−26.9
	Warm transition			23,591	25.1	−15.5	17,343	18.4	−37.9
	Warm			28,582	30.3	141.6	40,258	42.6	240.3
	Very warm			2,479	2.6	140.0	6,504	6.9	529.6
IPSL	Cold			15,042	15.9	−41.2	12,077	12.8	−52.8
	Cold transition			21,842	23.2	−21.9	21,109	22.4	−24.5
	Warm transition			18,983	20.1	−32.0	17,204	18.2	−38.4
	Warm			35,416	37.6	199.4	38,971	41.3	229.4
	Very warm			3,058	3.2	196.0	4,978	5.3	381.9
MIROC	Cold			8,102	8.6	−68.3	3,940	4.2	−84.6
	Cold transition			20,569	21.8	−26.4	18,235	19.3	−34.8
	Warm transition			17,819	18.9	−36.2	16,070	17.0	−42.5
	Warm			41,262	43.7	248.8	37,993	40.3	221.2
	Very warm			6,589	7.0	537.9	18,103	19.2	1,652.5

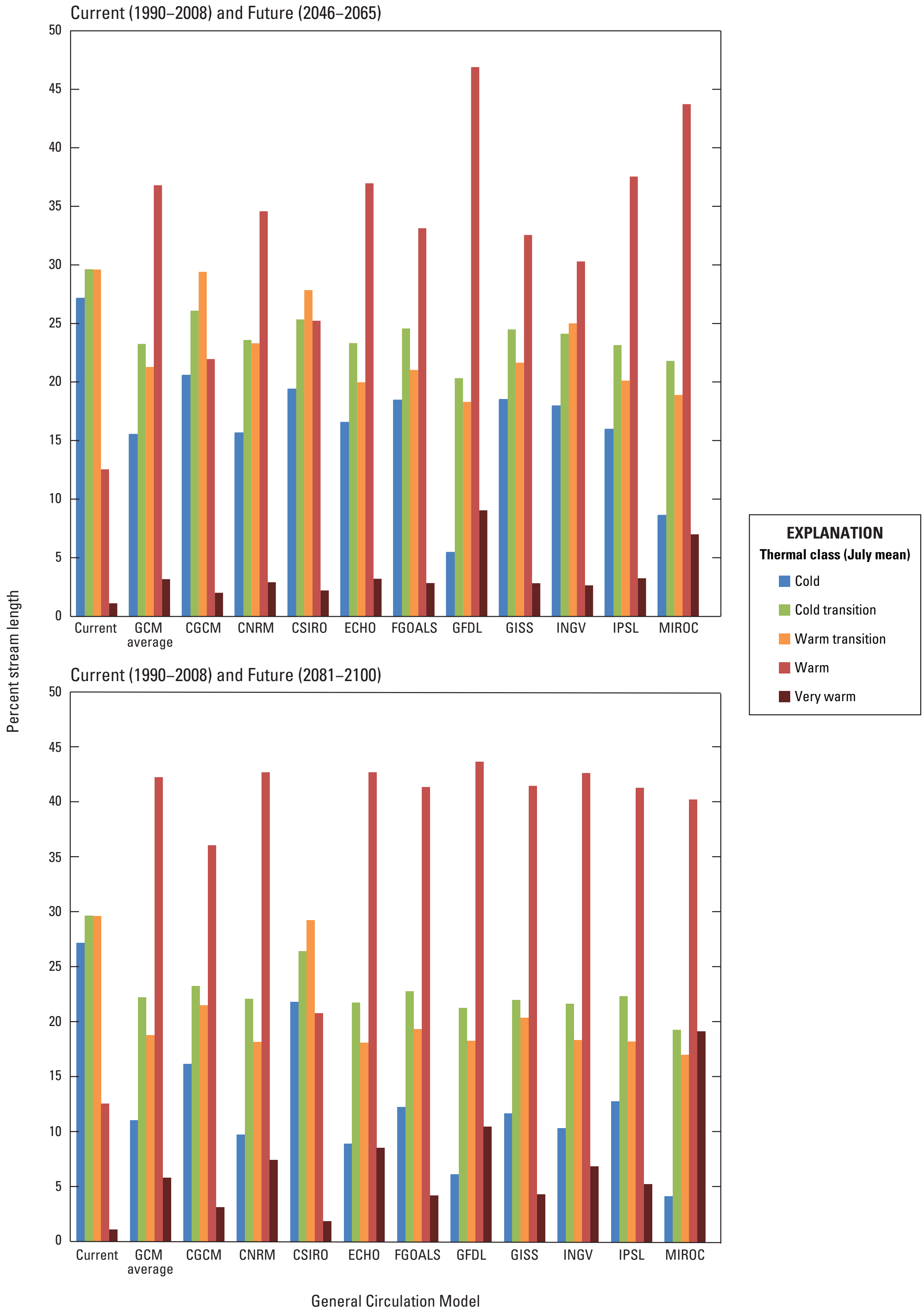

Figure 13. Percent stream length for stream temperature thermal classes under current (1990–2008) and future (2046–2065 and 2081–2100) climate conditions for 10 General Circulation Models (GCMs).

warm streams, there were about 2.9 times as many projected by mid-century and about 5.3 times as many projected by late-century for the GCM average. These directional shifts occurred and varied in magnitude by as much as 15 percent in SWB-ANNv1 models using climate data from each of the 10 GCMs (table 9; fig. 13).

Change in the Amount of Stream Habitat Summarized by Thermal Class

The change in the amount of stream habitat was evaluated by comparing the percent of stream kilometers lost or gained by thermal class from current to future time periods. Losses occurred for cold-water, cold-transition, and warm-transition streams and gains occurred for the warm-water and very warm streams for both mid- and late-century. The greatest and comparable losses occurred for cold streams for both mid- and late-century and the greatest gains occurred for warm streams by mid-century, and for very warm streams by late-century based on the GCM average (table 9; fig. 13).

Cold-Water Streams

The GCM average projected a mid-century loss of 42.9 percent and late-century loss of 59.3 percent of the 25,597 stream kilometers predicted to be cold under current climate conditions. Mid-century projected losses ranged from a low of 24.3 percent (model CGCM climate data) to a high of 80 percent (model GFDL climate data). Late-century projected losses ranged from a low of 19.7 percent (model CSIRO climate data) to a high of 84.6 percent (model MIROC climate data). This worst-case scenario using model MIROC climate data projected only 4.2 percent (3,940 km) of all stream kilometers remaining as cold at late-century compared to 27.1 percent under current climate conditions.

Cold-Transition Streams

For cold-transition streams, the SWB-ANNv1 model GCM averages projected a mid-century loss of 21.6 percent and late-century loss of 25.1 percent of the 27,958 stream kilometers predicted to be cold transition under current climate conditions (table 9; fig. 13). Mid-century projected losses ranged from a low of 12.0 percent (model CGCM climate data) to a high of 31.4 percent (model GFDL climate data). Late-century projected losses ranged from a low of 10.9 percent (model CSIRO climate data) to a high of 34.8 percent (model MIROC climate data).

Warm-Transition Streams

The SWB-ANNv1 model GCM averages projected a mid-century loss of 28.1 percent and late-century loss of 36.6 percent of the 27,924 stream kilometers predicted to be warm transition under current climate conditions. Mid-century projected losses ranged from a low of 0.7 percent (model CGCM climate data) to a high of 38.2 percent (model GFDL climate data). Late-century projected losses ranged from a low of 1.3 percent (model CSIRO climate data) to a high of 42.5 percent (model MIROC climate data).

Warm-Water Streams

The SWB-ANNv1 model GCM averages projected the greatest gain at mid-century of 194 percent and late-century gain of 237 percent of the 11,830 stream kilometers predicted to be warm under current climate conditions (table 9; fig. 13). Mid-century projected gains ranged from a low of 75.1 percent (model CGCM climate data) to a high of 274 percent (model GFDL climate data). Late-century projected gains ranged from a low of 65.6 percent (model CSIRO climate data) to a high of 248 percent (model GFDL climate data).

Very Warm Streams

The SWB-ANNv1 model GCM averages projected a mid-century gain of 189 percent and late-century gain of 429 percent of the 1,033 stream kilometers predicted to be very warm under current climate conditions (table 9; fig. 13). Mid-century projected gains ranged from a low of 82.3 percent (model CGCM climate data) to a high of 726 percent (model GFDL climate data). Late-century projected gains ranged from as little as 68.2 percent (model CSIRO climate data) to as high as 1,653 percent (model MIROC climate data).

Change in the Distribution of Stream Habitat Summarized by Thermal Class

Maps of the spatial distribution of streams by thermal class showed how the distribution of thermal classes were projected to change for SWB-ANNv1 GCM averages and each individual GCM at mid-century (fig. 14) and late-century (fig. 15). Under current climate conditions, cold and cold-transition streams are predominantly located across western and southern Wisconsin, including the Driftless Area (fig. 1), and in the north along Lake Superior. Warm and warm-transition streams are predominantly located in the eastern half of Wisconsin, with warm-transition streams also located across northern Wisconsin adjacent to the Upper Peninsula of Michigan. At mid- and late-century, based on GCM averages, mapped projections showed a contraction of cold streams in the Driftless Area and an expansion of warm streams across northern Wisconsin as compared to current climate conditions (figs. 14 and 15). When considering individual GCMs, the range of projected cold-water contraction versus warm-water expansion varied among models for both mid- and late-century (figs. 14 and 15).

At mid-century, the map of projections based on model CGCM climate data showed the lowest loss of cold, cold transition, and warm transition stream kilometers and the lowest gain of warm and very warm stream kilometers (fig. 14). Conversely, the map of projections based on model GFDL showed the highest loss of cold, cold transition, and warm transition stream kilometers and the highest gain of warm and very

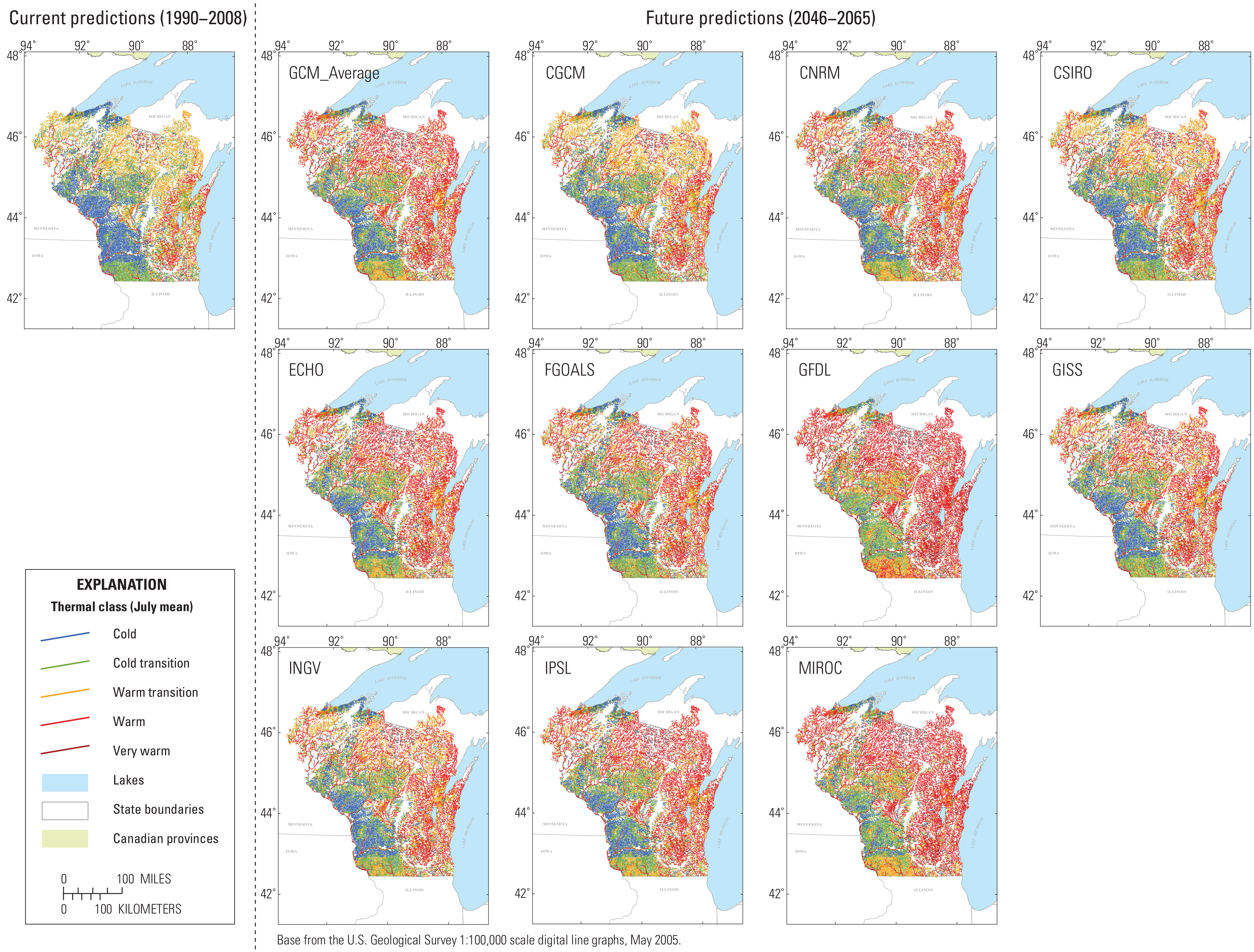

Figure 14. Distribution of stream temperature thermal classes (July mean) by individual stream segment, predicted for current (1990–2008) climate conditions and projected for future (2046–2065) mid-21st century climate conditions for 10 General Circulation Models (GCMs).

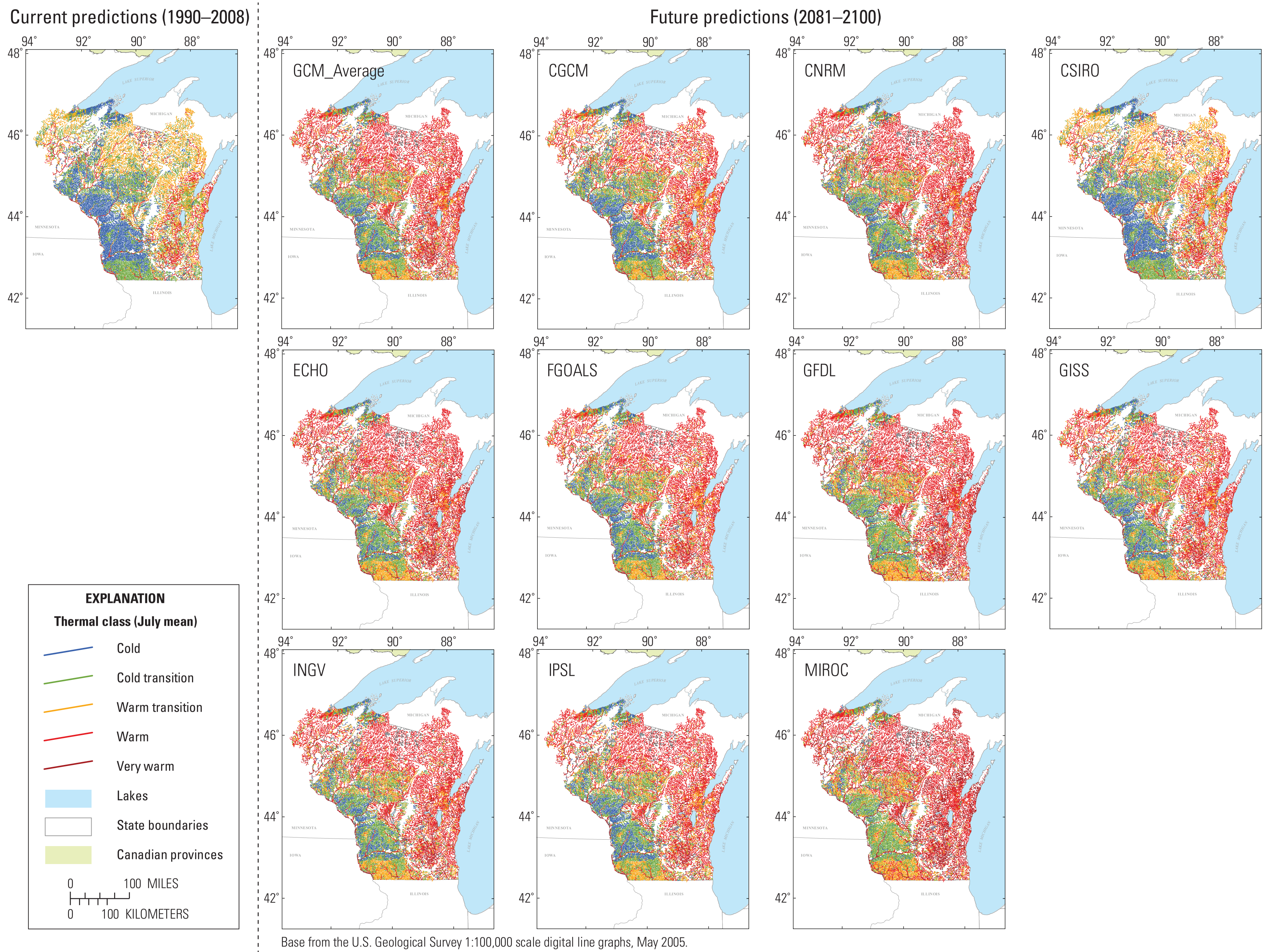

Figure 15. Distribution of stream temperature thermal classes (July mean) by individual stream segment, predicted for current (1990–2008) climate conditions and projected for future (2081–2100) late-21st century climate conditions for 10 General Circulation Models (GCMs).

warm stream kilometers (fig. 14). At late-century, the map of projections based on model CSIRO climate data showed the lowest loss of cold, cold transition, and warm transition stream kilometers and the lowest gain of warm and very warm stream kilometers (fig. 15). Conversely, the map of projections based on model MIROC climate data showed the highest loss of cold, cold transition, and warm transition stream kilometers and the highest gain of very warm stream kilometers (the gain for warm stream kilometers was slightly higher for projections based on model GFDL climate data, 249 percent) versus model MIROC climate data (221 percent) (fig. 15).

Change in Absolute Temperature

All stream segments were projected to become warmer, by mid- and late-century for all SWB-ANNv1 model results based on climate data from each of the GCMs (table 10; figs. 16 and 17). On average, about 80 percent of stream kilometers were projected to increase by 1 to 2 °C in July mean stream temperature by mid-century; the other 20 percent were projected to increase by less than 1 °C. By late-century, about 99 percent were projected to increase more than 1°C by late-century, with 31 percent of those increasing by more than 2 °C. Increases in stream temperature were projected to be greater at late-century than at mid-century for SWB-ANNv1 models based on climate data from 8 of the 10 GCMs. The projected change was about equal for future time periods using model CSIRO climate data; for model GFDL climate data, projected increases were slightly greater at mid-century as compared to late-century.

The maximum change in July mean stream temperature projected by SWB-ANNv1 models varied based on climate data from different GCMs. Projections based on climate data from two GCMs projected mid-century maximum changes in July mean stream temperatures less than 1 °C, from six GCMs projected maximum changes between 1 and 2 °C, and from two GCMs projected maximum changes between 2 and 3 °C (table 10). For the late-century time period, SWB-ANNv1

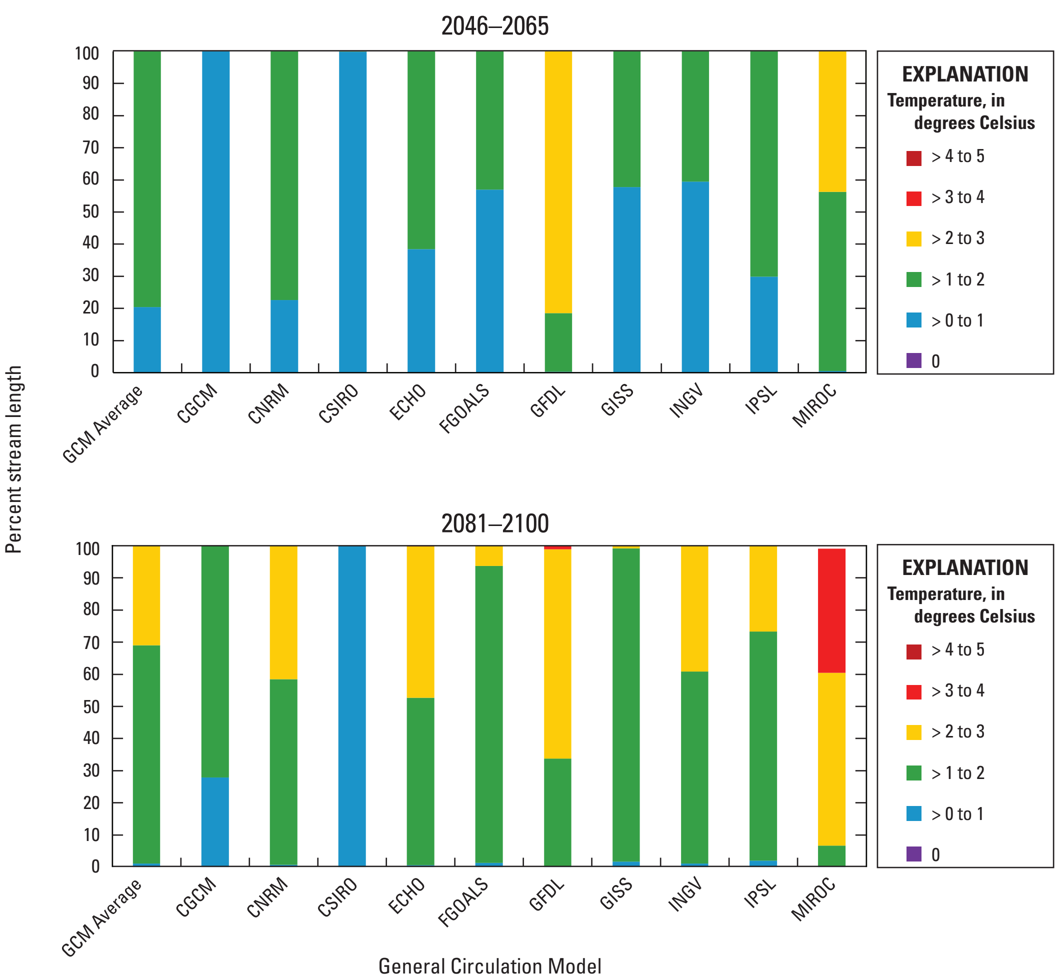

Figure 16. Absolute change in stream temperature summarized by percent stream length for future (2046–2065 and 2081–2100) climate conditions for 10 General Circulation Models (GCMs) relative to current (1990–2008) climate conditions.

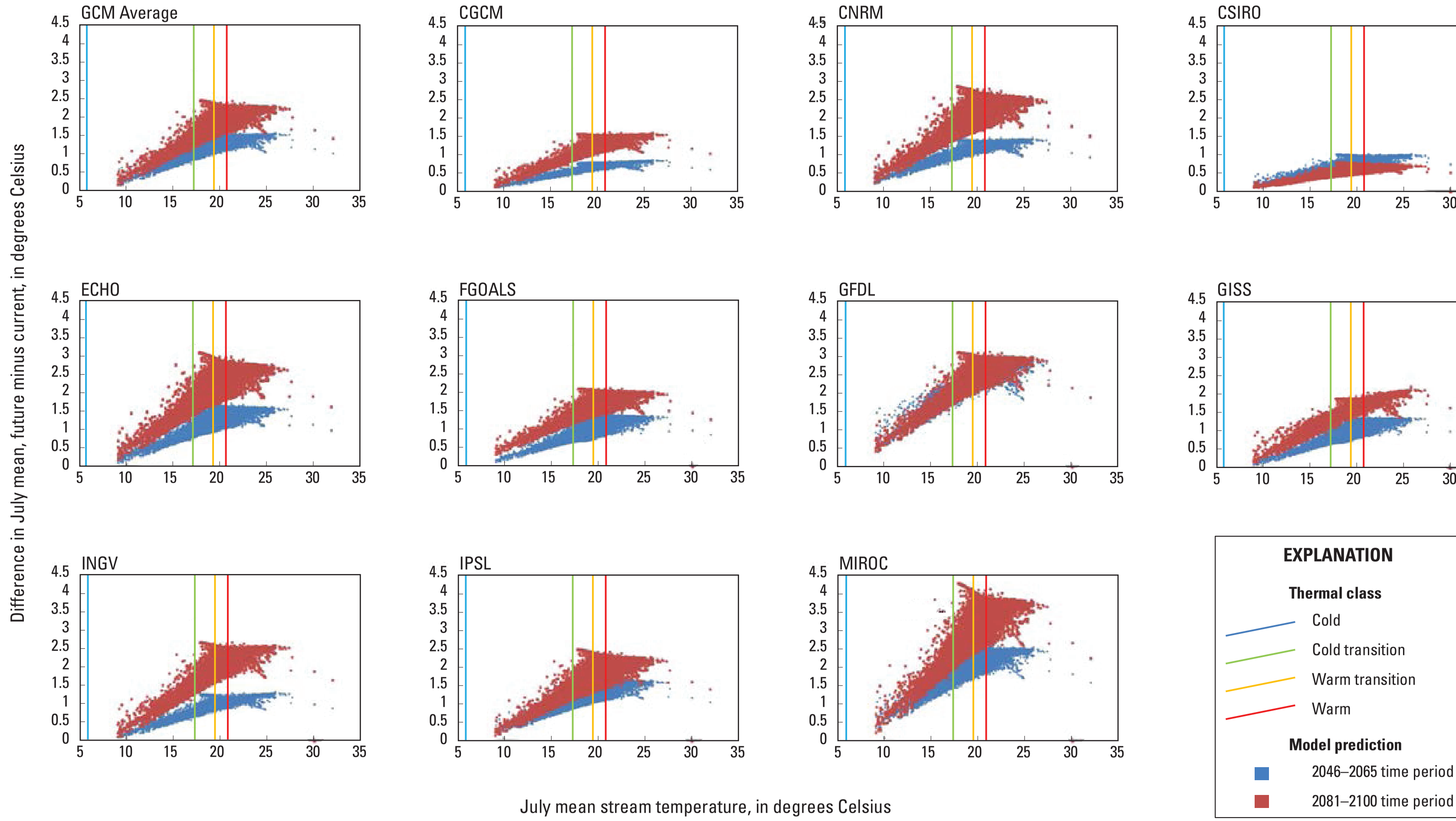

Figure 17. Projected absolute change in stream temperature for future (2046–2065 and 2081–2100) climate conditions for 10 General Circulation Models (GCMs) relative to current (1990–2008) climate conditions.

Table 10. Projections of absolute change in stream temperature summarized by length and as a percentage of total length (94,341 kilometers) for current (1990–2008) and future (2046–2065 and 2081–2100) climate conditions for 10 General Circulation Models.

[GCM, General Circulation Model; km, kilometer; >, greater than]

GCM code	Change (degrees Celsius)	Future (2046–2065)		Future (2081–2100)	
		Length (km)	Length (percent of total)	Length (km)	Length (percent of total)
GCM Average	0	0	0	0	0
	> 0 to 1	19,287	20.4	1,062	1.1
	> 1 to 2	75,054	79.6	64,069	67.9
	> 2 to 3	0	0	29,210	31.0
	> 3 to 4	0	0	0	0
	> 4 to 5	0	0	0	0
CGCM	0	0	0	0	0
	> 0 to 1	94,341	100	26,368	27.9
	> 1 to 2	0	0	67,973	72.1
	> 2 to 3	0	0	0	0
	> 3 to 4	0	0	0	0
	> 4 to 5	0	0	0	0
CNRM	0	0	0	0	0
	> 0 to 1	21,351	22.6	680	0.7
	> 1 to 2	72,990	77.4	54,548	57.8
	> 2 to 3	0	0	39,113	41.5
	> 3 to 4	0	0	0	0
	> 4 to 5	0	0	0	0
CSIRO	0	0	0	0	0
	> 0 to 1	94,284	99.9	94,341	100
	> 1 to 2	57	0.1	0	0
	> 2 to 3	0	0	0	0
	> 3 to 4	0	0	0	0
	> 4 to 5	0	0	0	0
ECHO	0	0	0	0	0
	> 0 to 1	36,352	38.5	610	0.6
	> 1 to 2	57,989	61.5	49,123	52.1
	> 2 to 3	0	0	44,397	47.1
	> 3 to 4	0	0	211	0.2
	> 4 to 5	0	0	0	0
FGOALS	0	0	0	0	0
	> 0 to 1	53,790	57	1,244	1.3
	> 1 to 2	40,551	43	87,125	92.4
	> 2 to 3	0	0	5,972	6.3
	> 3 to 4	0	0	0	0
	> 4 to 5	0	0	0	0

Table 10. Projections of absolute change in stream temperature summarized by length and as a percentage of total length (94,341 kilometers) for current (1990–2008) and future (2046–2065 and 2081–2100) climate conditions for 10 General Circulation Models.—Continued

[GCM, General Circulation Model; km, kilometer; >, greater than]

GCM code	Change (degrees Celsius)	Future (2046–2065)		Future (2081–2100)	
		Length (km)	Length (percent of total)	Length (km)	Length (percent of total)
GFDL	0	0	0	0	0
	> 0 to 1	278	0.3	290	0.3
	> 1 to 2	17,241	18.3	31,647	33.5
	> 2 to 3	76,822	81.4	61,406	65.1
	> 3 to 4	0	0	998	1.1
	> 4 to 5	0	0	0	0
GISS	0	0	0	0	0
	> 0 to 1	54,565	57.8	1,612	1.7
	> 1 to 2	39,775	42.2	92,017	97.5
	> 2 to 3	0	0	712	0.8
	> 3 to 4	0	0	0	0
	> 4 to 5	0	0	0	0
INGV	0	0	0	0	0
	> 0 to 1	56,135	59.5	1,039	1.1
	> 1 to 2	38,206	40.5	56,342	59.7
	> 2 to 3	0	0	36,960	39.2
	> 3 to 4	0	0	0	0
	> 4 to 5	0	0	0	0
IPSL	0	0	0	0	0
	> 0 to 1	28,232	29.9	1,863	2.0
	> 1 to 2	66,109	70.1	67,280	71.3
	> 2 to 3	0	0	25,198	26.7
	> 3 to 4	0	0	0	0
	> 4 to 5	0	0	0	0
MIROC	0	0	0	0	0
	> 0 to 1	493	0.5	266	0.3
	> 1 to 2	52,657	55.8	6,033	6.4
	> 2 to 3	41,191	43.7	50,661	53.7
	> 3 to 4	0	0	36,524	38.7
	> 4 to 5	0	0	857	0.9

models projected a maximum change in July mean stream temperature less than 1 °C using climate data from one GCM, a maximum change between 1 and 2 °C for climate data from one GCM, maximum changes between 2 and 3 °C for climate data from five GCMs, maximum changes between 3 and 4 °C for climate data from two GCMs, and a maximum change between 4 and 5 °C for climate data from one GCM (table 10).

The average change in July mean stream temperature between the current time period and mid-century, across all stream segments and for all GCM climate data, ranged from 0.63 °C (model CGCM climate data) to 2.25 °C (model GFDL climate data); the minimum change ranged from 0.07 °C (model GISS climate data) to 0.41 °C (model GFDL climate data); and the maximum change ranged from 0.87 °C (model CGCM climate data) to 2.95 °C (model GFDL climate data) (fig. 17). Between the current time period and late-century, the average change in July mean stream temperature, across all stream segments and for all GCM climate data, ranged from 0.53 °C (model CSIRO climate data) to 2.77 °C (model MIROC climate data); the minimum change ranged from 0.09 °C (model CSIRO climate data) to 0.41 °C (model GFDL climate data); and the maximum change ranged from 0.77 °C (model CSIRO climate data) to 4.28 °C (model MIROC climate data).

Stream segments in the cold thermal class showed the greatest amount of variation in warming (fig. 17). In comparisons of July mean stream temperatures between the current time period and mid-century or late-century, the “coldest” streams within the cold thermal class warmed the least and the “warmest” streams within the cold thermal class warmed the most. For those stream segments classified as cold for the current time period, as the July mean stream temperature approached the 17.5 °C thermal threshold between cold and cold transition (table 1), the projected difference in July mean stream temperature became greater. As stream segment temperature predictions increased past 17.5 °C the projected difference became less and began to plateau, as can be seen by the flattening of the graphed points in figure 17. Maps of the spatial distribution of temperature change from the current time period to the mid-21st century showed that for projections based on GCM averages, in general there are smaller changes in the southwestern portion of the State and along Lake Superior (i.e., changes between 0 and 1 °C) and larger changes in the eastern and northern portions of the State (i.e., changes between 1 and 2 °C) (fig. 18). The spatial distribution of temperature change for SWB-ANNv1 model projections based on climate data from individual GCMs ranged from changes only between 0 and 1 °C statewide (model CGCM climate data) to about 81 percent of streams changing between 2 and 3 °C (model GFDL climate data), with the remainder changing less and largely confined to the Driftless Area and Lake Superior shoreline (table 10; fig. 18).

Maps of the spatial distribution of temperature change from the current time period to the late-21st century (fig. 19) showed largely the same pattern as projected for mid-century (fig. 18) but with a wider range of temperature change among SWB-ANNv1 models based on climate data from individual GCMs and a larger change when based on GCM averages. For the SWB-ANNv1 model GCM averages, the greatest change of 2 to 3 °C was projected to occur predominantly across the north and to a lesser extent across the eastern half of the State. Projections based on model CSIRO climate data showed the least amount of change, with all streams projected to change between 0 and 1 °C. Projections based on model MIROC climate data showed the most change, with about 54 percent of stream segments across the State changing between 2 and 3 °C and about 39 percent of stream segments predominantly across the north and to a lesser extent the east projected to change between 3 and 4 °C (table 10; fig. 19).

Change in Thermal Class

The effect of temperature change on fish distribution may be understood by evaluating changes in thermal classes of streams. Projected changes in stream temperature for both the mid- and late-21st century time periods indicated that streams either remained in the same thermal class or changed to a warmer thermal class, either one or two classes warmer, but never changed to a colder thermal class (table 11). On average, and for all individual GCMs, there were fewer streams projected in cold, cold-transition, and warm-transition thermal classes in future time periods and more projected in warm and very-warm thermal classes. Such changes in thermal classes would shift the composition of fish communities across Wisconsin (Lyons and others, 2010).

Stream segments classified as cold for the current time period either remained cold or changed to cold transition by mid-century and late-century for GCM averages (table 11). The loss of 43 percent of cold stream segments by mid-century and 59 percent by late-century for projections based on GCM averages (table 9) translated solely to gains for the cold-transition thermal class (table 11). The spatial distribution of these cold transition gains, while necessarily confined to the original predicted distribution of cold thermal class streams, occurred largely on the periphery of the Driftless Area (figs. 1, 20, and 21). However, for SWB-ANNv1 models based on climate data from individual GCMs, two (models GFDL and MIROC climate data) projected a small percentage of stream segments changing from cold to warm transition by mid-century and late-century (table 11).

Stream segments classified as cold transition for the current time period either remained cold transition or changed to warm transition or warm by mid- and late-century for SWB-ANNv1 models based on GCM averages (table 11). Those stream segments that changed thermal class, however, predominantly changed to warm transition. At mid-century, the loss of cold-transition streams as projected by models using climate data based on GCM averages resulted in about 60 percent of cold-transition stream kilometers changing to warm transition and 0.7 percent changing to warm. At late-century, the loss of cold-transition streams resulted in about

Table 11. Projections of change in stream temperature thermal class (Lyons and others, 2009) summarized by length and as a percentage of total length (94,341 kilometers) for 10 General Circulation Models for the mid-21st century (2046–2065) and late-21st century (2081–2100).

[GCM, General Circulation Model; km, kilometer]

GCM code	Change in thermal class	Future (2046–2065)		Future (2081–2100)	
		Length (km)	Length (percent of total)	Length (km)	Length (percent of total)
GCM average	Cold (no change)	14,628	15.5	10,417	11.0
	Cold to cold transition	10,969	11.6	15,180	16.1
	Cold to warm transition	0	0	0	0
	Cold to warm	0	0	0	0
	Cold to very warm	0	0	0	0
	Cold transition to cold	0	0	0	0
	Cold transition (no change)	10,961	11.6	5,758	6.1
	Cold transition to warm transition	16,790	17.8	17,701	18.8
	Cold transition to warm	207	0.2	4,499	4.8
	Cold transition to very warm	0	0	0	0
	Warm transition to cold	0	0	0	0
	Warm transition to cold transition	0	0	0	0
	Warm transition (no change)	3,286	3.5	0	0
	Warm transition to warm	24,638	26.1	27,924	29.6
	Warm transition to very warm	0	0	0	0
	Warm to cold	0	0	0	0
	Warm to cold transition	0	0	0	0
	Warm to warm transition	0	0	0	0
	Warm (no change)	9,874	10.5	7,398	7.8
	Warm to very warm	1,955	2.1	4,431	4.7
	Very warm (no change)	1,033	1.1	1,033	1.1
CGCM	Cold (no change)	19,389	20.6	15,238	16.2
	Cold to cold transition	6,208	6.6	10,358	11.0
	Cold to warm transition	0	0	0	0
	Cold to warm	0	0	0	0
	Cold to very warm	0	0	0	0
	Cold transition to cold	0	0	0	0
	Cold transition (no change)	18,402	19.5	11,551	12.2
	Cold transition to warm transition	9,555	10.1	16,327	17.3
	Cold transition to warm	0	0	80	0.1
	Cold transition to very warm	0	0	0	0
	Warm transition to cold	0	0	0	0
	Warm transition to cold transition	0	0	0	0
	Warm transition (no change)	18,186	19.3	3,934	4.2
	Warm transition to warm	9,738	10.3	23,990	25.4
	Warm transition to very warm	0	0	0	0

Table 11. Projections of change in stream temperature thermal class (Lyons and others, 2009) summarized by length and as a percentage of total length (94,341 kilometers) for 10 General Circulation Models for the mid-21st century (2046–2065) and late-21st century (2081–2100).—Continued

[GCM, General Circulation Model; km, kilometer]

GCM code	Change in thermal class	Future (2046–2065)		Future (2081–2100)	
		Length (km)	Length (percent of total)	Length (km)	Length (percent of total)
CGCM, continued	Warm to cold	0	0	0	0
	Warm to cold transition	0	0	0	0
	Warm to warm transition	0	0	0	0
	Warm (no change)	10,979	11.6	9,922	10.5
	Warm to very warm	851	0.9	1,907	2.0
	Very warm (no change)	1,033	1.1	1,033	1.1
CNRM	Cold (no change)	14,748	15.6	9,157	9.7
	Cold to cold transition	10,849	11.5	16,421	17.4
	Cold to warm transition	0	0	19	0.02
	Cold to warm	0	0	0	0
	Cold to very warm	0	0	0	0
	Cold transition to cold	0	0	0	0
	Cold transition (no change)	11,400	12.1	4,405	4.7
	Cold transition to warm transition	16,557	17.6	17,088	18.1
	Cold transition to warm	0	0	6,465	6.9
	Cold transition to very warm	0	0	0	0
	Warm transition to cold	0	0	0	0
	Warm transition to cold transition	0	0	0	0
	Warm transition (no change)	5,433	5.8	0	0
	Warm transition to warm	22,491	23.8	27,924	29.6
	Warm transition to very warm	0	0	0	0
	Warm to cold	0	0	0	0
	Warm to cold transition	0	0	0	0
	Warm to warm transition	0	0	0	0
	Warm (no change)	10,134	10.7	5,874	6.2
	Warm to very warm	1,695	1.8	5,955	6.3
	Very warm (no change)	1,033	1.1	1,033	1.1
CSIRO	Cold (no change)	18,271	19.4	20,543	21.8
	Cold to cold transition	7,326	7.8	5,054	5.4
	Cold to warm transition	0	0	0	0
	Cold to warm	0	0	0	0
	Cold to very warm	0	0	0	0
	Cold transition to cold	0	0	0	0
	Cold transition (no change)	16,585	17.6	19,864	21.1
	Cold transition to warm transition	11,372	12.1	8,094	8.6
	Cold transition to warm	0	0	0	0
	Cold transition to very warm	0	0	0	0

Table 11. Projections of change in stream temperature thermal class (Lyons and others, 2009) summarized by length and as a percentage of total length (94,341 kilometers) for 10 General Circulation Models for the mid-21st century (2046–2065) and late-21st century (2081–2100).—Continued

[GCM, General Circulation Model; km, kilometer]

GCM code	Change in thermal class	Future (2046–2065)		Future (2081–2100)	
		Length (km)	Length (percent of total)	Length (km)	Length (percent of total)
CSIRO, continued	Warm transition to cold	0	0	0	0
	Warm transition to cold transition	0	0	0	0
	Warm transition (no change)	14,902	15.8	19,459	20.6
	Warm transition to warm	13,022	13.8	8,465	9.0
	Warm transition to very warm	0	0	0	0
	Warm to cold	0	0	0	0
	Warm to cold transition	0	0	0	0
	Warm to warm transition	0	0	0	0
	Warm (no change)	10,786	11.4	11,125	11.8
	Warm to very warm	1,043	1.1	705	0.7
	Very warm (no change)	1,033	1.1	1,033	1.1
ECHO	Cold (no change)	15,597	16.5	8,419	8.9
	Cold to cold transition	10,000	10.6	17,128	18.2
	Cold to warm transition	0	0	50	0.1
	Cold to warm	0	0	0	0
	Cold to very warm	0	0	0	0
	Cold transition to cold	0	0	0	0
	Cold transition (no change)	12,003	12.7	3,394	3.6
	Cold transition to warm transition	15,524	16.5	17,021	18.0
	Cold transition to warm	431	0.5	7,543	8.0
	Cold transition to very warm	0	0	0	0
	Warm transition to cold	0	0	0	0
	Warm transition to cold transition	0	0	0	0
	Warm transition (no change)	3,324	3.5	0	0
	Warm transition to warm	24,600	26.1	27,924	29.6
	Warm transition to very warm	0	0	0	0
	Warm to cold	0	0	0	0
	Warm to cold transition	0	0	0	0
	Warm to warm transition	0	0	0	0
	Warm (no change)	9,846	10.4	4,815	5.1
	Warm to very warm	1,983	2.1	7,015	7.4
	Very warm (no change)	1,033	1.1	1,033	1.1

Table 11. Projections of change in stream temperature thermal class (Lyons and others, 2009) summarized by length and as a percentage of total length (94,341 kilometers) for 10 General Circulation Models for the mid-21st century (2046–2065) and late-21st century (2081–2100).—Continued

[GCM, General Circulation Model; km, kilometer]

GCM code	Change in thermal class	Future (2046–2065)		Future (2081–2100)	
		Length (km)	Length (percent of total)	Length (km)	Length (percent of total)
FGOALS	Cold (no change)	17,390	18.4	11,582	12.3
	Cold to cold transition	8,207	8.7	14,015	14.9
	Cold to warm transition	0	0	0	0
	Cold to warm	0	0	0	0
	Cold to very warm	0	0	0	0
	Cold transition to cold	0	0	0	0
	Cold transition (no change)	14,975	15.9	7,486	7.9
	Cold transition to warm transition	12,983	13.8	18,042	19.1
	Cold transition to warm	0	0	2,430	2.6
	Cold transition to very warm	0	0	0	0
	Warm transition to cold	0	0	0	0
	Warm transition to cold transition	0	0	0	0
	Warm transition (no change)	6,859	7.3	202	0.2
	Warm transition to warm	21,065	22.3	27,722	29.4
	Warm transition to very warm	0	0	0	0
	Warm to cold	0	0	0	0
	Warm to cold transition	0	0	0	0
	Warm to warm transition	0	0	0	0
	Warm (no change)	10,193	10.8	8,875	9.4
	Warm to very warm	1,637	1.7	2,954	3.1
	Very warm (no change)	1,033	1.1	1,033	1.1
GFDL	Cold (no change)	5,120	5.4	5,834	6.2
	Cold to cold transition	19,025	20.2	19,528	20.7
	Cold to warm transition	1,452	1.5	235	0.2
	Cold to warm	0	0	0	0
	Cold to very warm	0	0	0	0
	Cold transition to cold	0	0	0	0
	Cold transition (no change)	156	0.2	570	0.6
	Cold transition to warm transition	15,817	16.8	17,042	18.1
	Cold transition to warm	11,984	12.7	10,345	11.0
	Cold transition to very warm	0	0	0	0

Table 11. Projections of change in stream temperature thermal class (Lyons and others, 2009) summarized by length and as a percentage of total length (94,341 kilometers) for 10 General Circulation Models for the mid-21st century (2046–2065) and late-21st century (2081–2100).—Continued

[GCM, General Circulation Model; km, kilometer]

GCM code	Change in thermal class	Future (2046–2065)		Future (2081–2100)	
		Length (km)	Length (percent of total)	Length (km)	Length (percent of total)
GFDL, continued	Warm transition to cold	0	0	0	0
	Warm transition to cold transition	0	0	0	0
	Warm transition (no change)	0	0	0	0
	Warm transition to warm	27,924	29.6	27,924	29.6
	Warm transition to very warm	0	0	0	0
	Warm to cold	0	0	0	0
	Warm to cold transition	0	0	0	0
	Warm to warm transition	0	0	0	0
	Warm (no change)	4,328	4.6	2,957	3.1
	Warm to very warm	7,502	8.0	8,873	9.4
	Very warm (no change)	1,033	1.1	1,033	1.1
GISS	Cold (no change)	17,442	18.5	11,041	11.7
	Cold to cold transition	8,155	8.6	14,556	15.4
	Cold to warm transition	0	0	0	0
	Cold to warm	0	0	0	0
	Cold to very warm	0	0	0	0
	Cold transition to cold	0	0	0	0
	Cold transition (no change)	14,944	15.8	6,225	6.6
	Cold transition to warm transition	13,014	13.8	19,259	20.4
	Cold transition to warm	0	0	2,474	2.6
	Cold transition to very warm	0	0	0	0
	Warm transition to cold	0	0	0	0
	Warm transition to cold transition	0	0	0	0
	Warm transition (no change)	7,416	7.9	9	0.01
	Warm transition to warm	20,508	21.7	27,915	29.6
	Warm transition to very warm	0	0	0	0
	Warm to cold	0	0	0	0
	Warm to cold transition	0	0	0	0
	Warm to warm transition	0	0	0	0
	Warm (no change)	10,201	10.8	8,755	9.3
	Warm to very warm	1,628	1.7	3,075	3.3
	Very warm (no change)	1,033	1.1	1,033	1.1

Table 11. Projections of change in stream temperature thermal class (Lyons and others, 2009) summarized by length and as a percentage of total length (94,341 kilometers) for 10 General Circulation Models for the mid-21st century (2046–2065) and late-21st century (2081–2100).—Continued

[GCM, General Circulation Model; km, kilometer]

GCM code	Change in thermal class	Future (2046-2065)		Future (2081-2100)	
		Length (km)	Length (percent of total)	Length (km)	Length (percent of total)
INGV	Cold (no change)	16,928	17.9	9,787	10.4
	Cold to cold transition	8,668	9.2	15,805	16.8
	Cold to warm transition	0	0	6	0.01
	Cold to warm	0	0	0	0
	Cold to very warm	0	0	0	0
	Cold transition to cold	0	0	0	0
	Cold transition (no change)	14,092	14.9	4,645	4.9
	Cold transition to warm transition	13,865	14.7	17,337	18.4
	Cold transition to warm	0	0	5,975	6.3
	Cold transition to very warm	0	0	0	0
	Warm transition to cold	0	0	0	0
	Warm transition to cold transition	0	0	0	0
	Warm transition (no change)	9,726	10.3	0	0
	Warm transition to warm	18,198	19.3	27,924	29.6
	Warm transition to very warm	0	0	0	0
	Warm to cold	0	0	0	0
	Warm to cold transition	0	0	0	0
	Warm to warm transition	0	0	0	0
	Warm (no change)	10,384	11.0	6,359	6.7
	Warm to very warm	1,446	1.5	5,471	5.8
	Very warm (no change)	1,033	1.1	1,033	1.1
IPSL	Cold (no change)	15,042	15.9	12,077	12.8
	Cold to cold transition	10,555	11.2	13,520	14.3
	Cold to warm transition	0	0	0	0
	Cold to warm	0	0	0	0
	Cold to very warm	0	0	0	0
	Cold transition to cold	0	0	0	0
	Cold transition (no change)	11,287	12.0	7,590	8.0
	Cold transition to warm transition	16,152	17.1	16,930	17.9
	Cold transition to warm	519	0.5	3,437	3.6
	Cold transition to very warm	0	0	0	0

Table 11. Projections of change in stream temperature thermal class (Lyons and others, 2009) summarized by length and as a percentage of total length (94,341 kilometers) for 10 General Circulation Models for the mid-21st century (2046–2065) and late-21st century (2081–2100).—Continued

[GCM, General Circulation Model; km, kilometer]

GCM code	Change in thermal class	Future (2046-2065)		Future (2081-2100)	
		Length (km)	Length (percent of total)	Length (km)	Length (percent of total)
IPSL, continued	Warm transition to cold	0	0	0	0
	Warm transition to cold transition	0	0	0	0
	Warm transition (no change)	2,831	3.0	274	0.3
	Warm transition to warm	25,093	26.6	27,650	29.3
	Warm transition to very warm	0	0	0	0
	Warm to cold	0	0	0	0
	Warm to cold transition	0	0	0	0
	Warm to warm transition	0	0	0	0
	Warm (no change)	9,804	10.4	7,884	8.4
	Warm to very warm	2,025	2.1	3,946	4.2
	Very warm (no change)	1,033	1.1	1,033	1.1
MIROC	Cold (no change)	8,101	8.6	8,419	8.9
	Cold to cold transition	17,489	18.5	17,128	18.2
	Cold to warm transition	6	0.006	50	0.1
	Cold to warm	0	0	0	0
	Cold to very warm	0	0	0	0
	Cold transition to cold	0	0	0	0
	Cold transition (no change)	3,080	3.3	3,394	3.6
	Cold transition to warm transition	17,813	18.9	17,021	18.0
	Cold transition to warm	7,064	7.5	7,543	8.0
	Cold transition to very warm	0	0	0	0
	Warm transition to cold	0	0	0	0
	Warm transition to cold transition	0	0	0	0
	Warm transition (no change)	0	0	0	0
	Warm transition to warm	27,924	29.6	27,924	29.6
	Warm transition to very warm	0	0	0	0
	Warm to cold	0	0	0	0
	Warm to cold transition	0	0	0	0
	Warm to warm transition	0	0	0	0
	Warm (no change)	6,274	6.6	4,815	5.1
	Warm to very warm	5,556	5.9	7,015	7.4
	Very warm (no change)	1,033	1.1	1,033	1.1

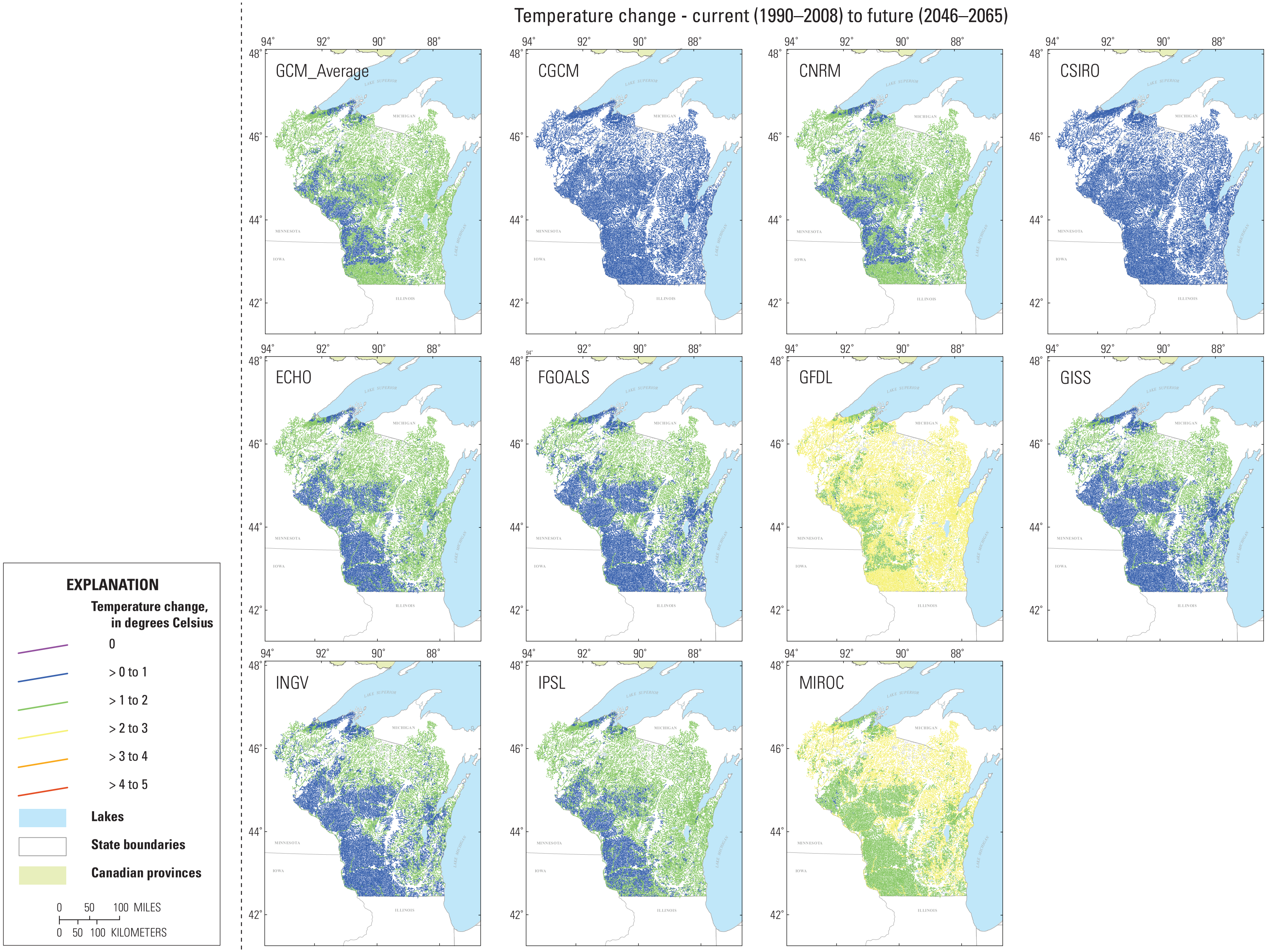

Base from the U.S. Geological Survey 1:100,000 scale digital line graphs, May 2005.

Figure 18. Projected absolute change in stream temperature for future (2046–2065) climate conditions for 10 General Circulation Models (GCMs) relative to current (1990–2008) climate conditions.

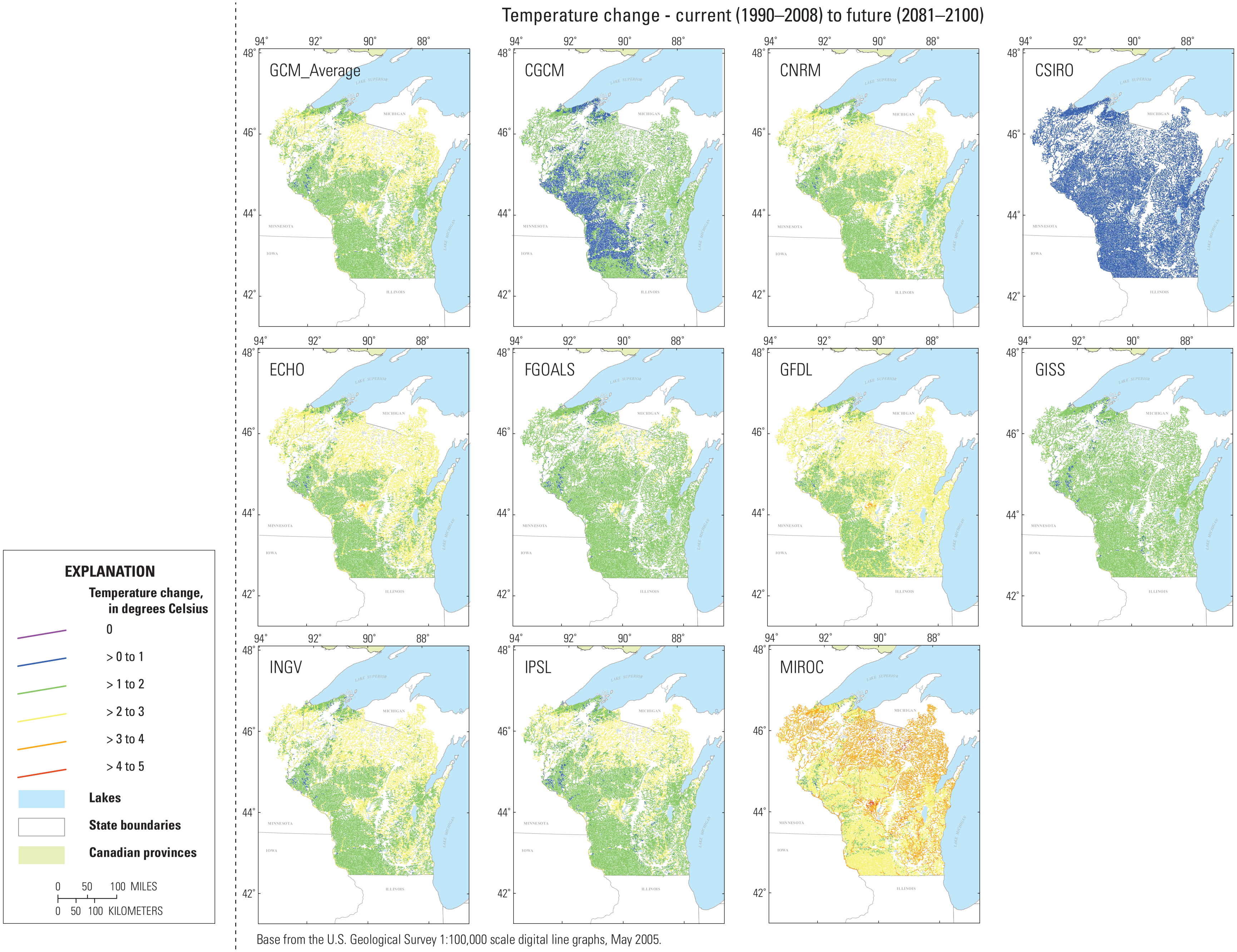

Base from the U.S. Geological Survey 1:100,000 scale digital line graphs, May 2005.

Figure 19. Projected absolute change in stream temperature for future climate conditions (2081–2100) for 10 General Circulation Models (GCMs) relative to current (1990–2008) climate conditions.

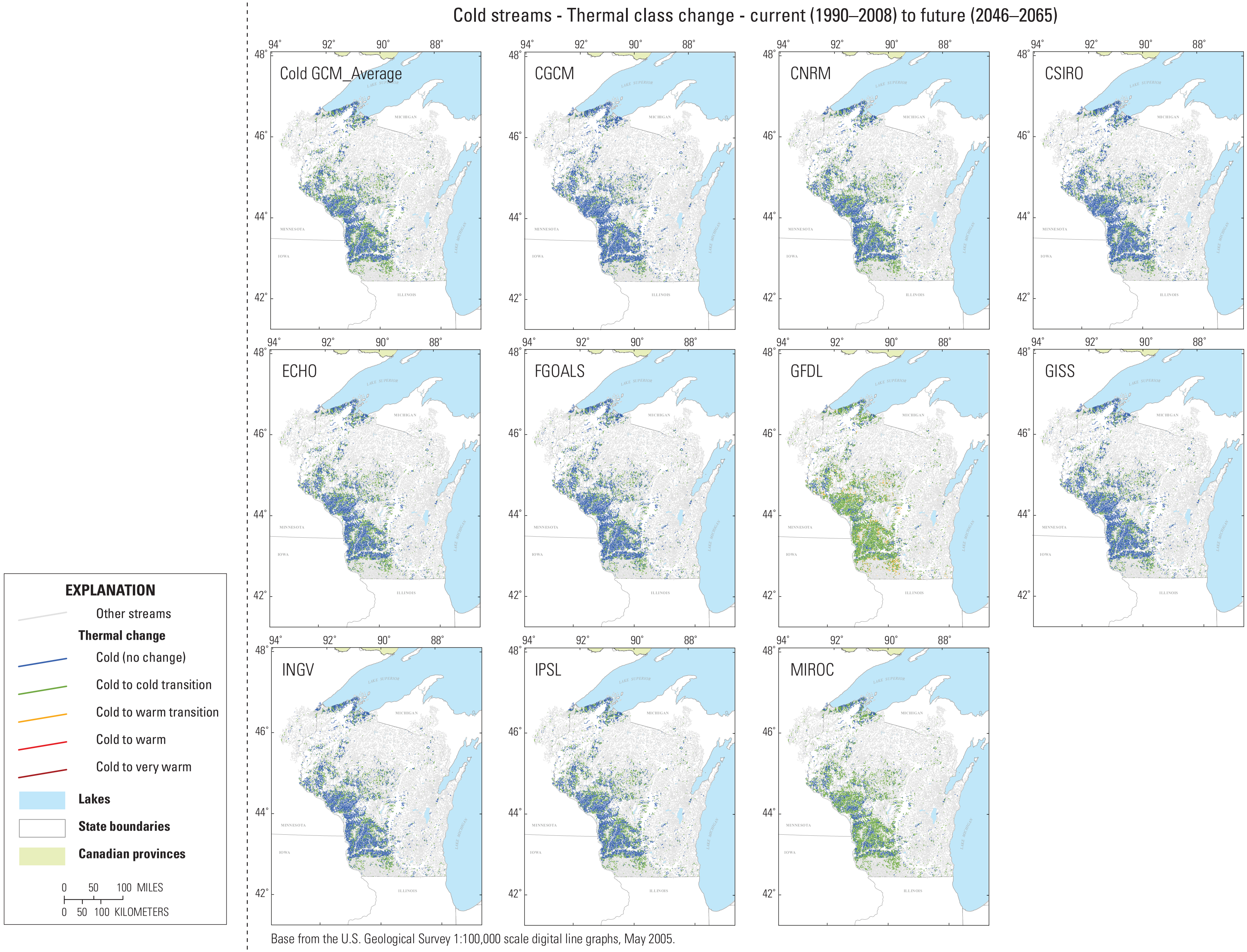

Base from the U.S. Geological Survey 1:100,000 scale digital line graphs, May 2005.

Figure 20. Projected change in stream temperature thermal class for cold-water streams from current (1990–2008) to future (2046–2065) climate conditions for 10 General Circulation Models (GCMs).

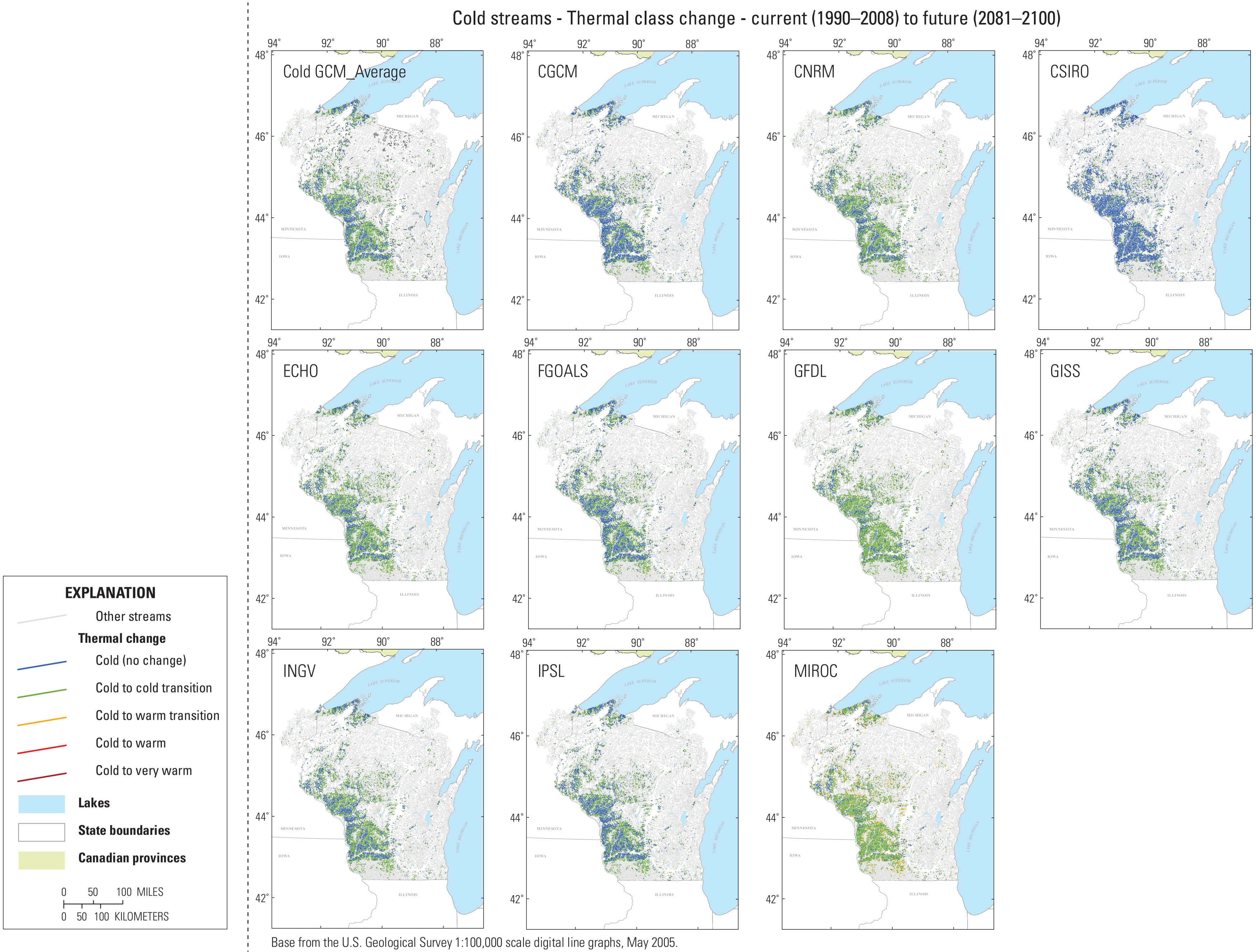

Figure 21. Projected change in stream temperature thermal class for cold-water streams from current (1990–2008) to future (2081–2100) climate conditions for 10 General Circulation Models (GCMs).

63 percent of stream kilometers changing to warm transition and 16 percent changing to warm (table 11). The spatial distribution of the change in stream segments at mid-century from cold transition to warm transition occurred across the State but with a heavier concentration of changed stream segments along the southern border of the State (fig. 22). At late-century, additional stream segments changed to warm transition across the southern part of the State, and changes to warm stream segments occurred across the northern part of the State (fig. 23). Among models based on climate data from the 10 individual GCMs, at mid-century 6 projected only changes from cold transition to warm transition and the other 4 projected additional changes to warm (table 11; fig. 22). At late-century only one model, using model CSIRO climate data, projected changes solely to warm transition, and nine projected changes to both warm transition and warm (table 11; fig. 23).

The greatest projected change in thermal class was for warm-transition stream segments, of which 88 percent of stream kilometers were projected to change to warm by mid-century and 100 percent were projected to change to warm by late-century for the GCM average (table 11). The SWB-ANNv1 model using climate data from 8 of the 10 individual GCMs projected some warm-transition stream segments to remain as such at mid-century, ranging from about 10 percent of stream kilometers (model IPSL climate data) to about 65 percent (model CGCM climate data). Despite SWB-ANNv1 model projecting a 100 percent change from warm transition to warm at late-century for the GCM average, projections based on climate data for five individual GCMs showed some stream segments remaining as warm transition at late-century (table 11). The SWB-ANNv1 model using climate data from model CSIRO projected about 70 percent of stream kilometers remaining as warm transition; however, the use of climate data from model CGCM projected about 14 percent remaining and the use of climate data from three other GCMs projected less than 1 percent remaining (table 11). Maps of the spatial distribution of thermal class change, or lack thereof, among warm-transition stream segments showed changes occurring throughout the State at both mid- and late-century (figs. 24 and 25).

Stream segments classified as warm using current climate data mostly remained warm at mid-century (83 percent of stream kilometers) and late-century (63 percent of stream kilometers) with the remainder changing to very warm, as projected by the SWB-ANNv1 model GCM average (table 11). The SWB-ANNv1 model using climate data from each of the 10 GCMs projected some change in thermal classes among stream segments, from warm to very warm. At mid-century, SWB-ANNv1 models projected from about 7 percent (model CGCM climate data) to about 63 percent (model GFDL climate data) of stream kilometers changing from warm to very warm (table 11). At late-century, SWB-ANNv1 models projected from about 6 percent (model CSIRO climate data) to about 75 percent (model GFDL climate data) of stream kilometers changing from warm to very warm (table 11). Maps of the spatial distribution of stream segments remaining warm and changing to very warm showed these changes occurring throughout the State at both mid- and late-century (figs. 26 and 27).

Data and Model Limitations

Model output of stream temperatures for mid- and late-21st century time periods were considered projections of what could happen rather than predictions of what will happen. Projections are probabilistic statements about the future concerning what is possible under certain conditions as described in the model should those conditions be realized in the future. For example, our models assumed the A1B emissions scenario for the remainder of the 21st century. The A1B emissions scenario is a “middle-of-the-road” scenario, developed by the Intergovernmental Panel on Climate Change (IPCC, 2007), which assumes a balanced approach to energy production between fossil and non-fossil fuels. Should carbon emissions increase at a slower rate (B2 emissions scenario) or a faster rate (A1 emissions scenario), then the climate input data used in our model would not accurately represent future conditions. Predictions of what changes in climate will occur are inherently difficult to make because predictions of realized future emissions of greenhouse gases are uncertain.

Model projections were further constrained by the use of statistical downscaling to project future climate conditions at a scale appropriate for the study area of Wisconsin. The UWCCR used statistical downscaling to relate climate trends at the global scale to climate conditions at the State level in Wisconsin (Notaro and others, 2011). In this application of downscaling, large-scale air temperature and precipitation variables from GCMs were statistically related to local climate conditions in Wisconsin. The UWCCR validated this technique using historical climate data for Wisconsin (WICCI, 2011). Researchers at the UWCCR are continuing work on downscaling additional climatological parameters, which may be of relevance to our understanding of climate change impacts on stream temperature. Such parameters include evapotranspiration, humidity, and solar radiation. Future advances in our understanding of climate change at local versus global scales may lead to improvements in our ability to relate changes in climate to changes in stream temperature.

Additional model assumptions critical to understanding climate impacts on stream temperature include changes in land use and streamflow. Land use was assumed to remain constant at current conditions. Although land use is expected to change over time, the extent to which land use will change is difficult to predict. For example, land use may change in response to economic conditions. In recent years, increases in commodity prices and demand for ethanol have led to the rotation of protected land out of the Conservation Reserve Program (CRP) and into agricultural production (Streitfeld, 2008; Allen and Vandever, 2012). If environmentally sensitive CRP land is returned to corn production, there is the potential for increased surface-water runoff and less infiltration into groundwater, which may affect stream temperatures (Panuska and others, 2007; Marshall and others, 2008).

Future changes in urbanization also may affect how changes in climate impact stream temperature. Urbanization is expected to increase over time, but predictions of such change are inherently uncertain. Wang and others (2003) measured urbanization as the percent of connected impervious area in a watershed. Urbanization may impact stream temperature in a number of ways. Impervious surfaces may limit groundwater recharge and reduce stream base flow and may increase surface-water input to streams, including warmer thermal inputs following precipitation events during summertime. Wang and others (2003) found that streams in watersheds with levels of connected imperviousness in the threshold region of 6–11 percent can experience major changes in thermal conditions as a result of minor changes in urbanization. Any changes in urbanization, as well as other forms of land use, may affect how changes in climate impact stream temperatures.

Streamflow also may change over time as a result of climate change, and changes in streamflow may impact stream temperature. UWCCR projections of climatic change in precipitation for Wisconsin are uncertain; projections from individual climate models indicate changes both positive and negative to streamflow may occur in the future, depending on the time of year. Increases in precipitation may positively impact groundwater recharge and help maintain lower summertime stream temperatures, particularly in cold-water streams. However, increases in precipitation during warmer summertime months may lead to increases in warm surface runoff that may increase stream temperatures. The interaction of precipitation and land use will be important in determining how these factors impact stream temperature as climate changes occur. Unpublished data for cold-water streams in the Driftless Area of Wisconsin shows how stream temperature relates to precipitation events. Streams heavily influenced by groundwater remained consistently cold during the absence of precipitation events in summer 2012, whereas spikes in stream temperature closely tracked the many precipitation events that occurred in summer 2010 (Matthew Mitro, Wisconsin Department of Natural Resources, oral commun., [2013]).

Applications of the Integrated Soil-Water-Balance and Artificial Neural Network version 1 Stream Temperature Model

The SWB-ANNv1 stream temperature model described in this report represents an important advance over ANNv1 described by Stewart and others (2006). The development and integration of the SWB model with the ANN model allowed for the parameterization of the connection between precipitation, groundwater, and stream temperature. This approach also provided a way to link projections of future changes in climate to groundwater recharge and ultimately to stream temperature. The thermal predictions for streams from the SWB-ANNv1 model under current climate conditions and projections under future climate scenarios will enhance the ability of fisheries managers to make appropriate recommendations and decisions pertaining to stream management.

The SWB-ANNv1 stream temperature model will serve as an important tool for fisheries management because of the importance of water temperature to fish and the ability of the model to make inferences about temperature and fish assemblages in all stream segments across Wisconsin. Fish assemblages in streams vary in relation to differences in thermal conditions in streams (Lyons and others, 2009). However, the thermal characteristics of many Wisconsin streams are unknown. The stream temperature model will serve as an important tool in mapping and quantifying streams by thermal class, guiding stream surveys, mapping distributions of stream fishes, and making management decisions pertaining to stream-habitat protection and restoration to support important fisheries.

Wisconsin is recognized as an important cold-water State from the perspective of both trout fisheries and fish biodiversity. Brook trout are the only native salmonid found in cold-water streams in Wisconsin. However, Wisconsin is at the southern edge of the brook trout's distributional range, where the species is at increased risk to changes in climate. The SWB-ANNv1 stream temperature model estimates can be used in fish species occurrence models to project those streams that may have suitable habitat for brook trout under future climate scenarios (Lyons and others, 2010; Mitro and others, 2010a; WICCI, 2011).

In addition to cold-water streams, Wisconsin hosts a diversity of streams across a continuous thermal gradient, which can be categorized into discrete thermal classes, each represented by fish assemblages adapted to particular thermal conditions and potentially threatened by changes in climate. Warm-water and warm-transition streams have almost a completely different fish fauna compared to cold-water and cold-transition streams (Lyons and others, 2010). Lyons and others (2009) identified the thermal guild for 99 fish species found in Wisconsin and Michigan streams. There were 65 species classified as warm water, 26 as transitional (i.e., cold transition or warm transition), and 8 as cold water. Warm-water streams, while being small in number, support a significantly higher number of fish species than cold-water and transitional streams combined. SWB-ANNv1 model predictions may be helpful in identifying the small percentage of streams that may be critical to preserving warm-water fish species diversity in Wisconsin streams and in identifying potential impacts of climate change on these streams.

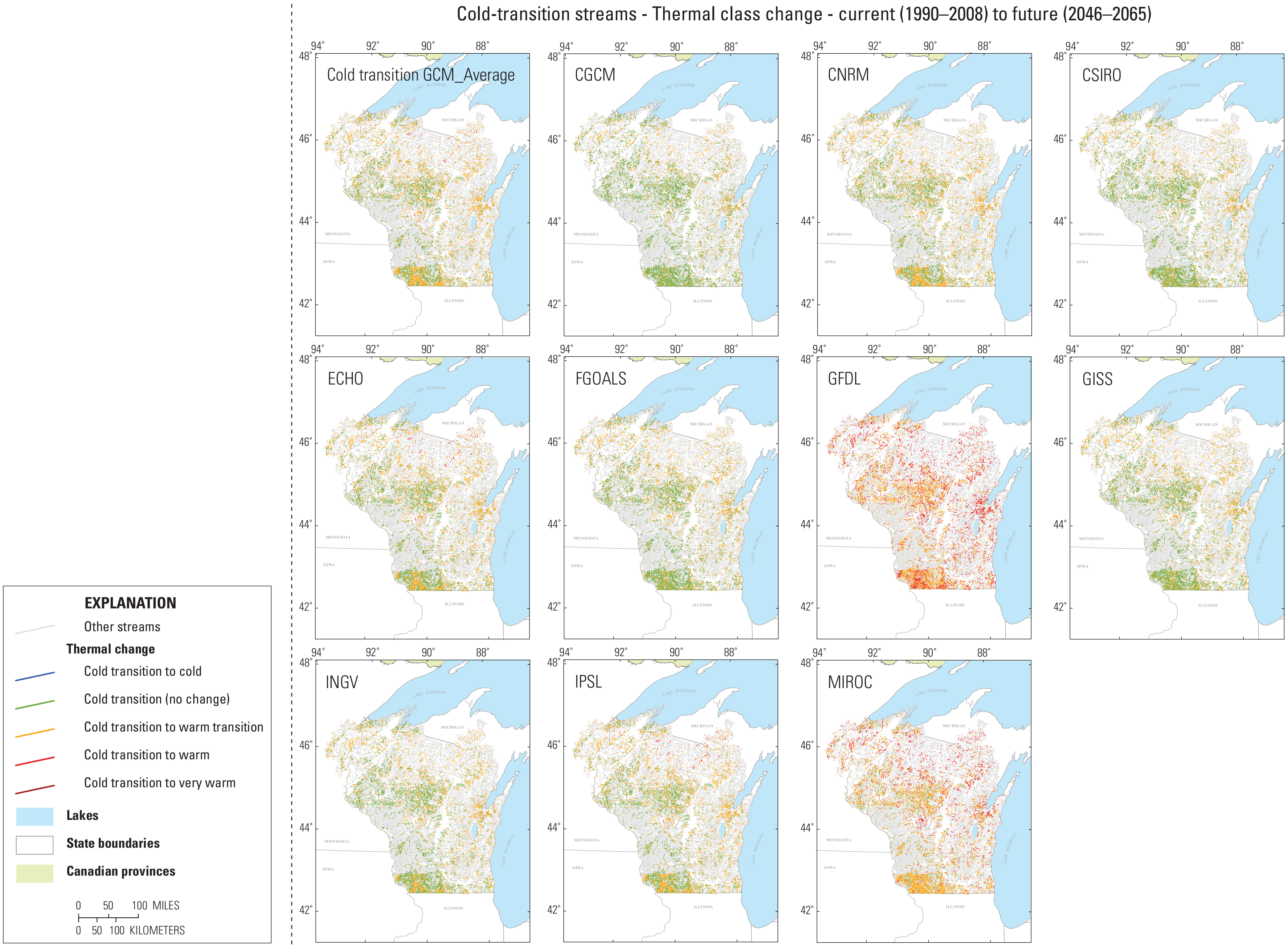

Base from the U.S. Geological Survey 1:100,000 scale digital line graphs, May 2005.

Figure 22. Projected change in stream temperature thermal class for cold-transition streams from current (1990–2008) to future (2046–2065) climate conditions for 10 General Circulation Models (GCMs).

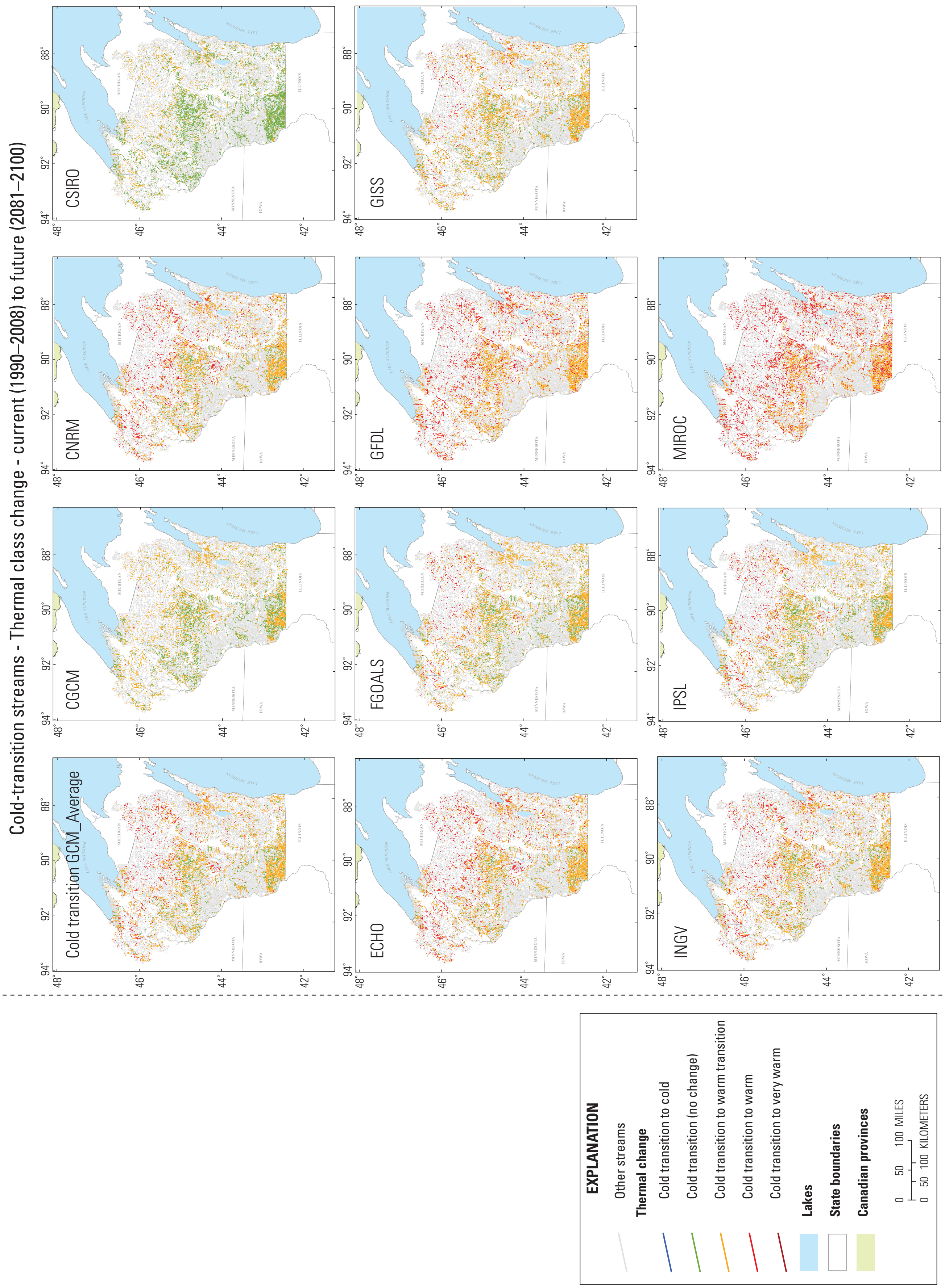

Base from the U.S. Geological Survey 1:100,000 scale digital line graphs, May 2005.

Figure 23. Projected change in stream temperature thermal class for cold-transition streams from current (1990–2008) to future (2081–2100) climate conditions for 10 General Circulation Models (GCMs).

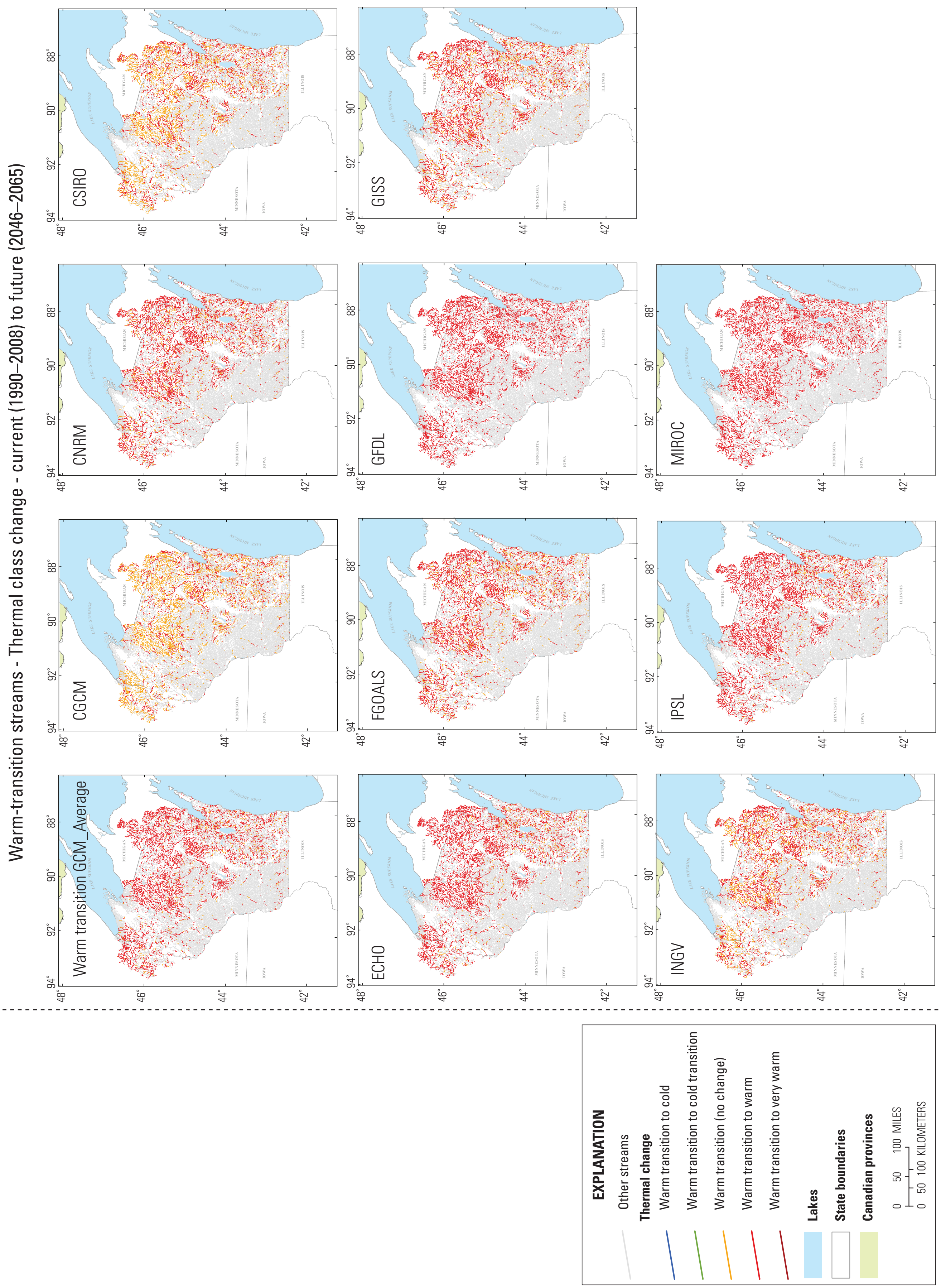

Base from the U.S. Geological Survey 1:100,000 scale digital line graphs, May 2005.

Figure 24. Projected change in stream temperature thermal class for warm-transition streams from current (1990–2008) to future (2046–2065) climate conditions for 10 General Circulation Models (GCMs).

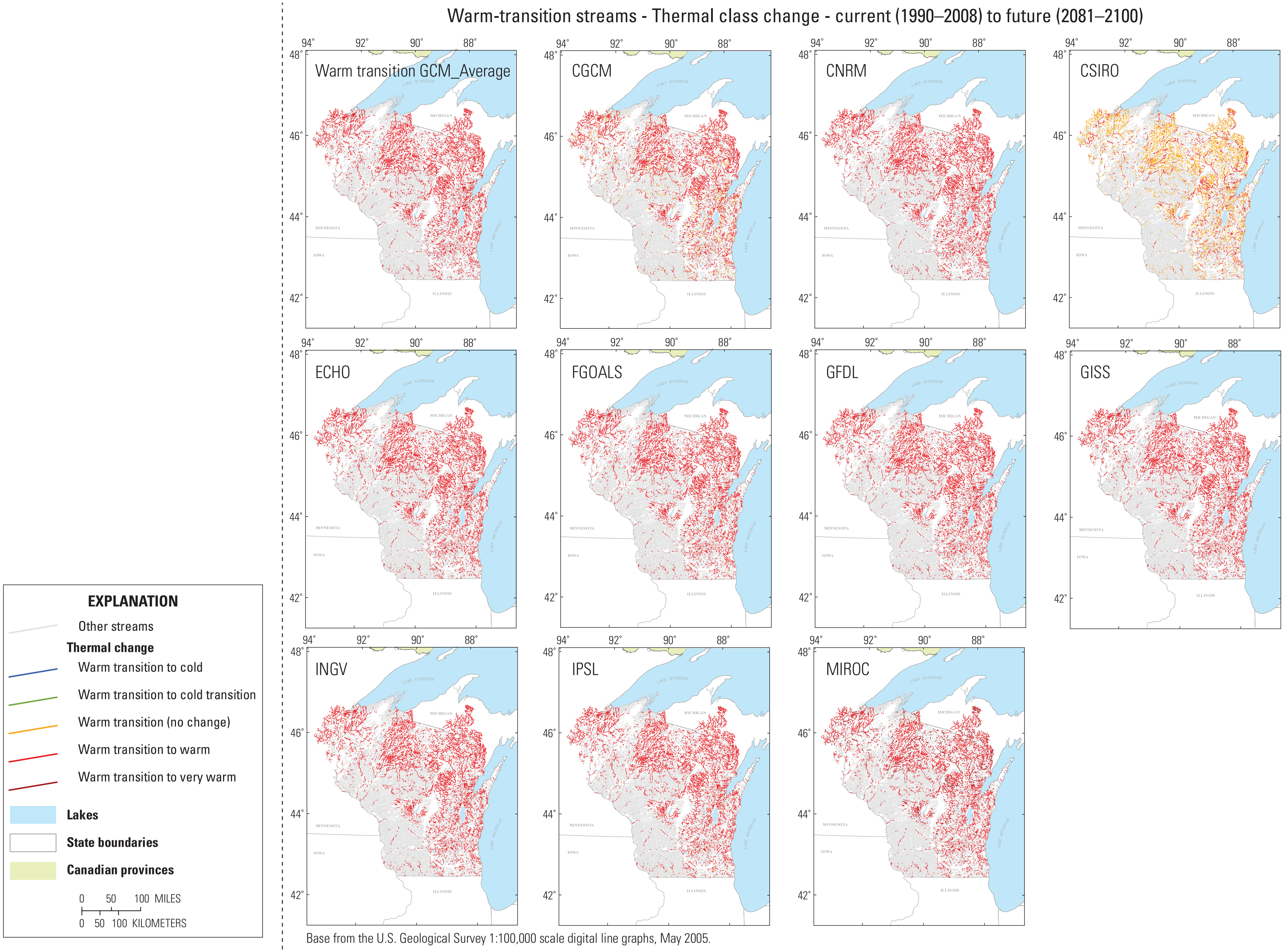

Figure 25. Projected change in stream temperature thermal class for warm-transition streams from current (1990–2008) to future (2081–2100) climate conditions for 10 General Circulation Models (GCMs).

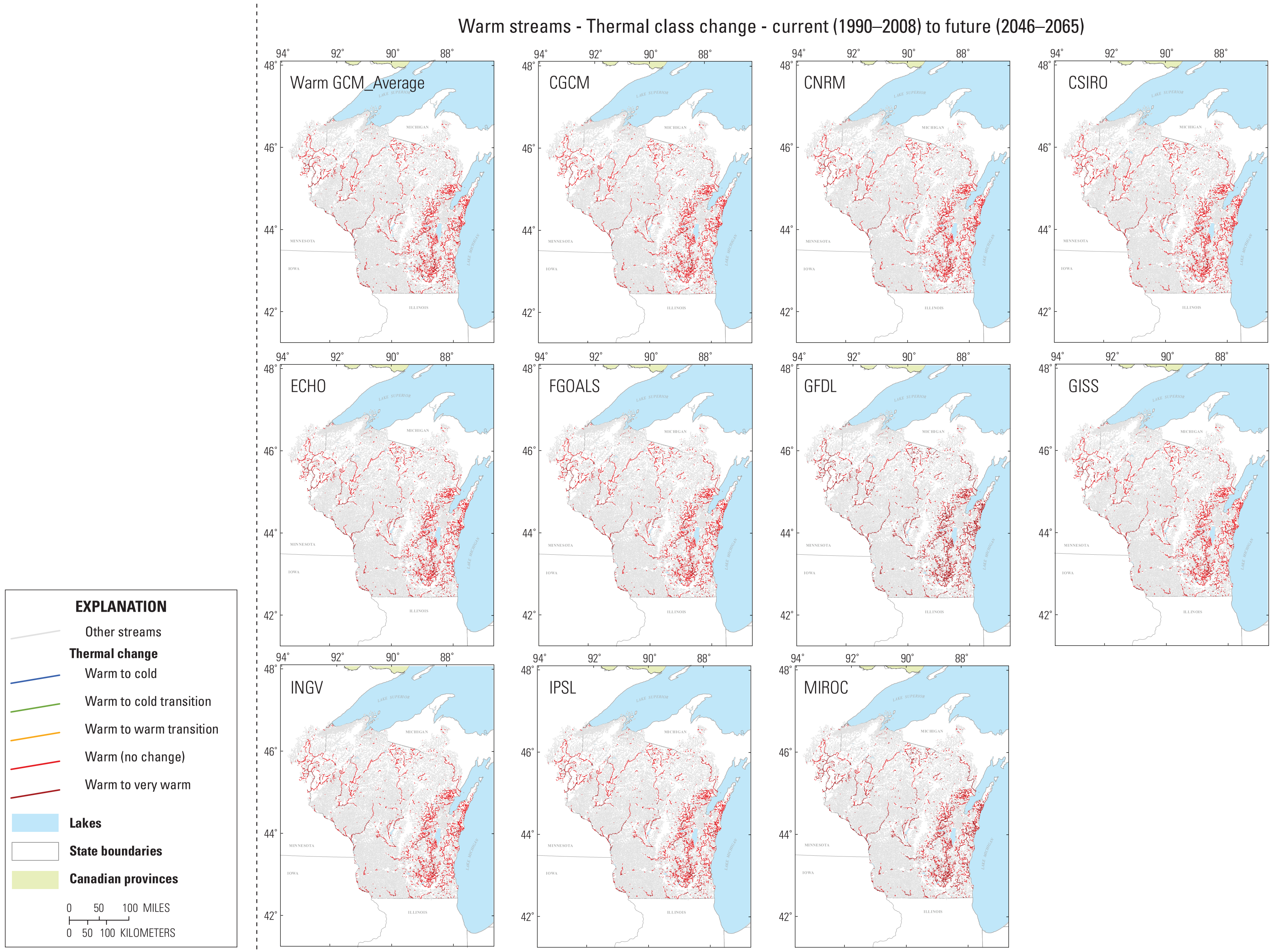

Base from the U.S. Geological Survey 1:100,000 scale digital line graphs, May 2005.

Figure 26. Projected change in stream temperature thermal class for warm-water streams from current (1990–2008) to future (2046–2065) climate conditions for 10 General Circulation Models (GCMs).

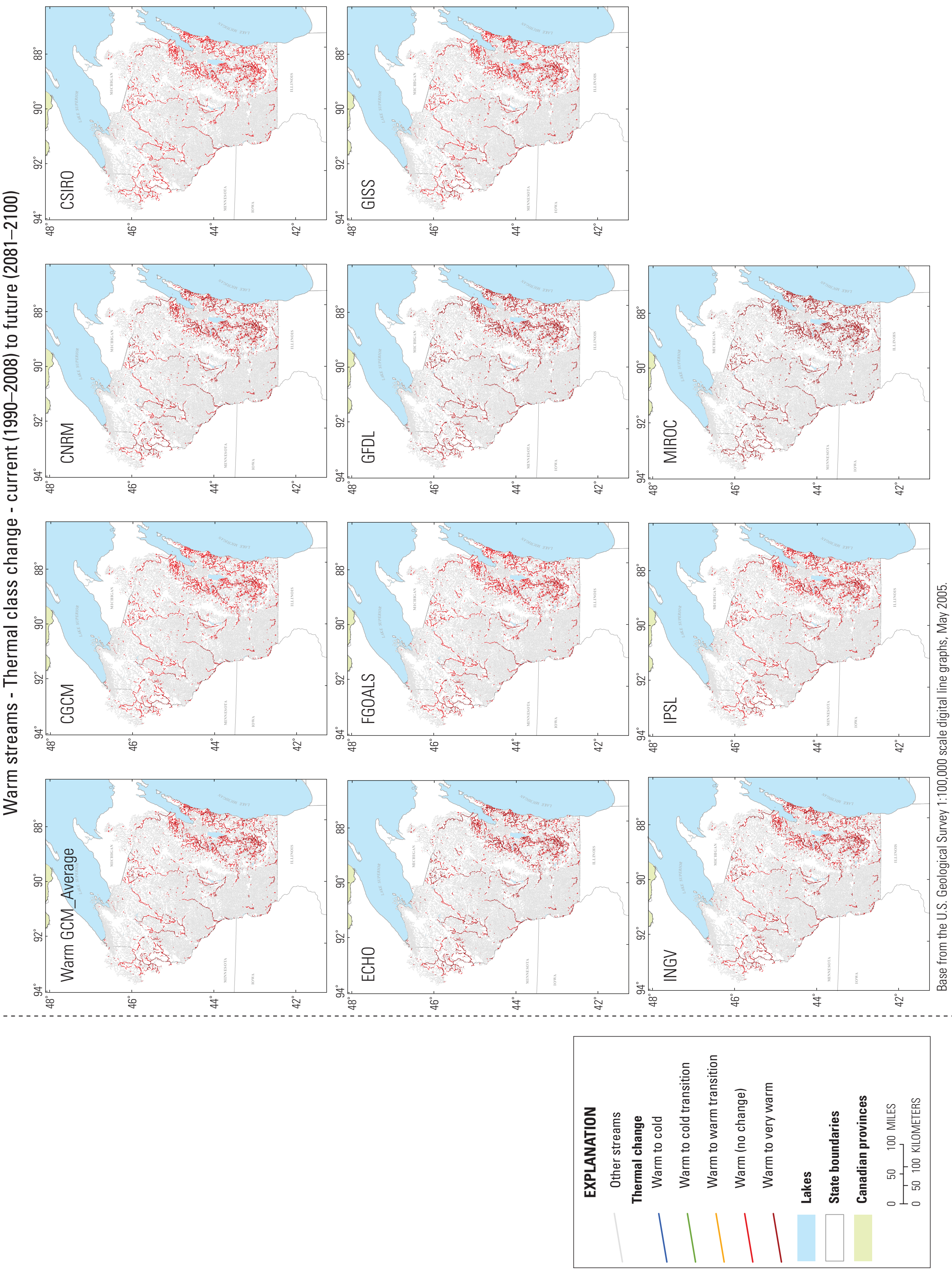

Figure 27. Projected change in stream temperature thermal class for warm-water streams from current (1990–2008) to future (2081–2100) climate conditions for 10 General Circulation Models (GCMs).

The Wisconsin Initiative on Climate Change Impacts (WICCI) (WICCI, 2011) produced the first adaptive assessment for Wisconsin to address the vulnerabilities and sensitivities of natural resources to climate change impacts and to propose adaptation strategies to build resiliency and lessen the impacts. The ANNv1 stream temperature model (Stewart and others, 2006; Westenbroek and others, 2010b) played an integral role in identifying the vulnerabilities and sensitivities of Wisconsin streams and stream fishes to potential warming scenarios associated with changes in climate (Lyons and others, 2010; Mitro and others, 2010a; WICCI, 2011). The SWB-ANNv1 model will further advance our understanding of climate impacts on Wisconsin streams and aid in the development of adaptation strategies managers can use to protect fisheries.

An important initial use of the SWB-ANNv1 model has been as a tool to understand current and future distributions of trout and smallmouth bass as part of the development of a master plan for managing WDNR land holdings and easements along streams in the Driftless Area of Wisconsin (WDNR, 2013). The Driftless Master Plan is a forward-looking document, and the use of SWB-ANNv1 model predictions (current time period) and projections (mid-21st century time period) represents the first time a WDNR master plan explicitly addresses climate change impacts on streams as an important factor in making decisions on agency land management (WDNR, 2013). The plan includes the identification of where trout and smallmouth bass are currently found in streams and where they are likely to be in the future given changing climate conditions. The plan ultimately will guide land-protection goals, objectives, and strategies to ensure public access to desired fisheries recognizing the threat posed by climate change to the existence of such fisheries in some streams.

Thermal predictions (current climate conditions) and projections (future climate scenarios) for streams will enhance the ability of resource managers to make appropriate recommendations and decisions pertaining to stream and fisheries management. One example is the WDNR's classification of streams as "trout waters." Streams shown by fish surveys to support trout are classified as trout streams. Such classification is important from a resource-management perspective in that trout water classification affords a stream a higher level of protection from activities that may lead to the degradation of cold-water thermal habitat. SWB-ANNv1 model predictions that more than one-half of Wisconsin's stream kilometers are thermally suitable for trout (as compared to the 24 percent currently classified as trout waters) will be instrumental in supporting efforts to survey and classify additional trout waters. Cold stream temperatures are necessary, but not sufficient, to support trout. Thermal class predictions can be used to help guide stream survey efforts to focus on those streams most likely to contain trout and thus warrant trout-classification status.

Another use of SWB-ANNv1 model predictions and projections of stream temperatures is to guide the expenditure of financial resources on stream habitat projects. Anglers fishing Wisconsin streams are required to purchase a trout stamp, in addition to a fishing license, and the trout stamp funds are dedicated to trout stream habitat projects (WDNR, 2011). Similar to the use of the SWB-ANNv1 model in the Driftless master planning process, modeling the impacts of future climate scenarios on stream thermal class will be used to guide trout stream habitat projects (Mitro and others, 2010a). Mitro and others (2010a) describe a triage approach to prioritizing fund expenditures on stream habitat projects. Fisheries managers may forgo spending limited funds on streams projected to change thermal classes such that trout losses may be inevitable. Streams projected to be resilient to climate change impacts on thermal class such that they are likely to remain cold-water streams may be best suited to protection efforts. Rather, funds may be dedicated to streams in which the persistence of trout may be contingent upon management actions likely to build resiliency to climate change impacts on stream temperature. Stream-restoration efforts to build resiliency to climate impacts may include in-stream habitat work used to narrow and deepen the stream channel and reduce bank erosion to help maintain cold groundwater temperatures over the course of the stream (Mitro and others, 2010a and b). Riparian management to provide shade cover also may help maintain cold thermal temperatures in streams (Cross and others, 2013).

Summary and Conclusions

This study simulated daily summertime water temperatures under current (1990–2008) climate conditions and projected water temperature under future climate conditions for 94,341 kilometers (km) of streams across Wisconsin (1:100,000 scale U.S. National Hydrography Dataset). Water temperature is a critical factor in identifying the suitability of streams for different species of fish across this geographic area. As ongoing changes in climate progress, stream thermal conditions and fish distributions are expected to change and models may help quantify such change.

A stream temperature model (SWB-ANNv1) to predict stream temperatures in all stream segments during the summertime (June–August) period was developed by building upon an Artificial Neural Network (ANN) version 1 model (ANNv1) by Stewart and others (2006). The ANN model is an empirical model that captures the dynamics of spatially expansive and behaviorally heterogeneous hydrologic systems using static landscape data and dynamic climate time-series data. ANNv1 methodology was further expanded upon by integrating a Soil-Water-Balance (SWB) model with the ANN model to parameterize potential groundwater recharge, thereby linking precipitation, groundwater, and stream temperature. The resulting integrated SWB and ANN version 1 (SWB-ANNv1) Model was used to predict daily summertime stream temperatures using current climate data and to project daily stream temperatures at mid- and late-21st century time periods

(2046–65 and 2081–2100). Mid- and late-century climate projections were based on the A1B emissions scenario and the downscaled projections of air temperature and precipitation amounts from 10 Global Circulation Models (GCMs) (Notaro and others, 2011). The July mean stream temperature was derived from mean daily stream temperatures and was used to identify the thermal classification of each stream segment: cold (<17.5 degrees Celsius (°C), cold transition (17.5–19.5 °C), warm transition (19.5–21 °C), warm (21–24 °C), and very warm (>24 °C) (Lyons and others, 2009).

The SWB-ANNv1 model captured the overall trend in daily summertime stream temperature data with a percent model error (PME) of 8.8 percent. The SWB-ANNv1 model explained 76 percent of the variation in stream temperature, as compared to 67 percent for the ANNv1 model, a nine percentage point improvement (Stewart and others, 2006). The approach for integrating SWB with the ANN model also provided a means to evaluate the effect of changing air temperature and precipitation on groundwater recharge and soil moisture and in turn provided a mechanism by which downscaled global or regional climate model results could be used to estimate the potential effects of climate change on stream temperature.

The SWB-ANNv1 model was based on eight static landscape variables (six describing the total upstream watershed, one the total upstream 60-meter riparian buffer, and one the local channel), six dynamic climate variables describing air temperature groups, and three dynamic variables describing groundwater recharge. The SWB-ANNv1 model was developed using a training dataset and tested using an independent validation dataset. About 47 percent of the July mean stream temperature predictions were within 1 °C of observed values, about 77 percent were within 2 °C, and about 93 percent were within 3 °C. More than one-half of the stream kilometers were predicted suitable for cold-water fishes such as trout or sculpins for the current time period (27.1 percent cold and 29.6 percent cold transition). The remaining stream kilometers were predicted suitable for warm-water fishes such as minnows and sunfishes (29.6 percent warm transition, 12.5 percent warm-water, and 1.1 percent very warm). Cold and cold-transition streams were predicted to primarily occur in the Driftless Area of western and southern Wisconsin and along Lake Superior to the north. Warm-transition and warm streams were primarily in the eastern half of Wisconsin, with warm-transition streams also prominent across the north. Overall, the SWB-ANNv1 model predicted an additional 5.7 percent of stream kilometers as suitable for cold-water fishes in Wisconsin, as compared to the ANNv1 model, with about equal proportions of cold and cold transition stream kilometers.

Projections of stream temperatures at mid- and late-century based on climate data from 10 GCMs showed warming for all stream segments. The GCM average projected about 80 percent of stream kilometers increasing by 1 to 2 °C by mid-century and about 99 percent increasing by 1 to 3 °C by late-century, with 31 percent of those increasing by more than 2 °C in the late-century. Stream segments in the cold thermal class showed the greatest amount of variation in warming with the “coldest” streams warming the least and those approaching the upper end of the cold thermal class warming the most, based on July mean stream temperature. This may suggest that cold-water streams dominated by groundwater contributions may have a higher capacity for maintaining cold temperatures than cold-water streams with a lower proportion of groundwater input even under future climate warming scenarios.

The effect of temperature change on fish distribution may be understood by evaluating changes in thermal classes of streams. Projected changes in stream temperature for both the mid- and late-21st century time periods indicated that streams either remained in the same thermal class or changed to a warmer thermal class, but never changed to a colder thermal class. On average, and for all individual GCMs, there were fewer stream kilometers projected in cold, cold-transition, and warm-transition thermal classes in future time periods and more projected in warm and very-warm thermal classes. Such changes in thermal classes would shift the composition of fish communities across Wisconsin, with a loss in the distribution of cold-water fishes and increase in the distribution of warm-water fishes. Less than two-fifths of stream kilometers at mid-century and one-third at late-century would be thermally suitable for cold-water fishes resulting in an 18 to 23 percent loss of suitable habitat at mid- and late-21st century, respectively, based on the GCM averages. These directional shifts occurred and varied in magnitude by as much as 15 percent in SWB-ANNv1 models using climate data from each of the 10 GCMs. The range of cold and cold-transition streams is projected to contract within the Driftless Area and along Lake Superior, and the range of warm streams is projected to expand in the east and particularly across the north in Wisconsin.

Projected losses of cold-water stream habitat may result in losses of cold-water stream fisheries for species such as brook trout and brown trout. Concomitant increases in warm-water stream habitat may benefit many warm-water fishes, but warm-water sport fishes like smallmouth bass may not replace fisheries for trout because of other habitat limitations. Many headwater streams that currently support trout, for example, are physically too small to support smallmouth bass. Therefore, projected changes in thermal habitat attributable to climate change may result in net losses of fisheries, posing a challenge to fisheries and resource managers. The SWB-ANNv1 model developed in this study provides a tool to resource managers to assist in identifying vulnerabilities in streams to climate change impacts; to guide stream surveys and classification, land-protection strategies, and expenditures of financial resources for habitat restoration; and to aid in making strategic decisions concerning approaches to climate change adaptation to best protect and enhance resiliency in stream thermal habitat.

References Cited

ADMi, 2011, iQuestTM data-mining software: Greenville, South Carolina, accessed April 2011 at *http://www.advdmi.com*.

Allen, A.W., and Vandever, M.W., 2012, Conservation Reserve Program (CRP) contributions to wildlife habitat, management issues, challenges and policy choices—An annotated bibliography: U.S. Geological Survey Scientific Investigations Report 2012–5066, 185 p.

Allen, D.M., 2008, Development and application of a process-based, basin-scale stream temperature model: Berkeley, University of California, Ph.D. dissertation, 183 p.

Baker, M.E., Wiley, M.J, and Seelbach, P.W., 2003a, GIS-based models of potential groundwater loading in glaciated landscapes—Considerations and development in Lower Michigan: Ann Arbor, Mich., Michigan Department of Natural Resources, Fisheries Division, Fisheries Research Report 2064, 22 p.

Baker, M.E., Wiley, M.J., Seelbach, P.W., and Carlson, M.L., 2003b, A GIS model of subsurface water potential for aquatic resource inventory, assessment, and environmental management: Environmental Management, v. 32, no. 6, p.706–719.

Benyahya, Loubna; Caissie, Daniel; St-Hilaire, Andre; Ouarda, Taha; and Bobee, Bernard, 2007, A review of statistical water temperature models: Canadian Water Resources Journal, v. 32, no. 3, p. 179–192.

Brenden, T.O., Clark, R.D., Jr., Cooper, A.R., Seelbach, P.W., Wang, Lizhu, Aichele, S.S., Bissell, E.G., and Stewart, J.S., 2006, A GIS framework for collecting, managing, and analyzing multiscale landscape variables across large regions for river conservation and management, *in* Landscape Influences on Stream Habitats and Biological Assemblages, Hughes, R.M., Wang, L., and Seelbach, P.W., eds.: Bethesda, Md., American Fisheries Society, v. 48, p. 49–74.

Burkett, V.R., Kirtland, D.A., Taylor, I.L., Belnap, Jayne, Cronin, T.M., Dettinger, M.D., Frazier, E.L., Haines, J.W., Loveland, T.R., Milly, P.C.D., O'Malley, Robin, Thompson, R.S., Maule, A.G., McMahon, Gerard, and Striegl, R.G., 2013, U.S. Geological Survey climate and land use change science strategy—A framework for understanding and responding to global change: U.S. Geological Circular 1383–A, 43 p.

Chenard, J.F., and Caissie, Daniel, 2008, Stream temperature modelling using artificial neural networks—Application on Catamaran Brook, New Brunswick, Canada: Hydrologic Processes, v. 22, no. 17, p. 3361–3372.

Chu, Cindy, Jones, N.E., Mandrak, N.E., Piggott, A.R., and Minns, C.K., 2008, The influence of air temperature, groundwater discharge, and climate change on the thermal diversity of stream fishes in southern Ontario watersheds: Canadian Journal of Fisheries and Aquatic Sciences, v. 65, no. 2, p. 297–308.

Conrads, P.A., Roehl, E.A., Jr., Daamen, R.C., and Cook, J.B., 2013, Simulation of salinity intrusion along the Georgia and South Carolina coasts using climate-change scenarios: U.S. Geological Survey Scientific Investigations Report 2013–5036, 92 p., and 5 apps, at *http://pubs.usgs.gov/sir/2013/5036/*.

Cox, M.M., and Bolte, J.P., 2007, A spatially explicit network-based model for estimating stream temperature distribution: Environmental Modelling & Software, v. 22, no. 4, p. 502–514.

Cronshey, R., McCuen, R., Miller, N., Rawls, W., Robbins, S., and Woodward, D., 1986, Urban hydrology for small watersheds—TR-55 (2d ed.): Washington, D.C., U.S. Department of Agriculture, Soil Conservation Service, Engineering Division, Technical Release 55, 164 p.

Cross, B.K., Bozek, M.A., and Mitro, M.G., 2013, Influences of riparian vegetation on trout stream temperatures in central Wisconsin: North American Journal of Fisheries Management, v. 33, no. 4, p. 682–692.

Doherty, John, 2009, PEST—Model-independent parameter estimation user manual (5th ed.): Brisbane, Australia, Watermark Numerical Computing, 336 p.

Dripps, W.R., and Bradbury, K.R., 2007, A simple daily soil–water balance model for estimating the spatial and temporal distribution of groundwater recharge in temperate humid areas: Hydrogeology Journal, v. 15, no. 3, p. 433–444.

Fields Development Team, 2006, Fields—Tools for spatial data: Boulder, Colo., National Center for Atmospheric Research, accessed January 2008 at *http://www.image.ucar.edu/Software/Fields*.

Forgy, E.W., 1965, Cluster analysis of multivariate data—Efficiency versus interpretability of classification: Biometrics, v. 21, no. 3, p. 768–769.

Fullerton, D.S., Bush, C.A., and Pennell, J.N., 2003, Map of surficial deposits and materials in the eastern and central United States (east of 102° west longitude) (ver. 1.0): U.S. Geological Survey Geologic Investigations Series I-2789.

Gaffield, S.J., Potter, K.W., and Wang, Lizhu, 2005, Predicting the summer temperature of small streams in Southwestern Wisconsin: Journal of the American Water Resources Association, v. 41, no. 1, p. 25–36.

Gebert, W.A., Radloff, M.J., Considine, E.J., and Kennedy, J.L., 2007, Use of streamflow data to estimate base flow/ground-water recharge for Wisconsin: Journal of the American Water Resources Association, v. 43, no. 1, p. 220–236.

Haerter, J.O., Hagemann, S., Moseley, C., and Piani, C., 2011, Climate model bias correction and the role of timescales: Hydrology and Earth System Sciences, v. 15, no. 3, p. 1065–1079.

Hart, David; Schoephoester, Peter; and Bradbury, Kenneth, 2009, Groundwater recharge in Dane County, Wisconsin, estimated by a GIS-based water-balance model: Wisconsin Geological and Natural History Survey Open File Report 2009–01, 16 p.

Hartigan, J.A., and Wong, M.A., 1979, Algorithm AS 136—A k-means clustering algorithm, in Applied Statistics, v. 28, no.1, p. 100–108.

Hinton, G.E., 1992, How neural networks learn from experience: Scientific American, v. 267, no. 3, p. 144–151.

Intergovernmental Panel on Climate Change (IPCC), 2007, Climate change 2007—Impacts, adaptation and vulnerability—Contribution of Working Group II to the Fourth Assessment Report of the Intergovernmental Panel on Climate Change: Cambridge, U.K., Cambridge University Press, 976 p.

Lyons, John; Stewart, Jana; and Mitro, Matthew, 2010, Predicted effects of climate warming on the distribution of 50 stream fishes in Wisconsin, USA: Journal of Fish Biology, v. 77, no. 8, p. 1867–1898.

Lyons, John; Zorn, Troy; Stewart, Jana; Seelbach, Paul; Wehrly, Kevin; and Wang, Lizhu, 2009, Defining and characterizing coolwater streams and their fish assemblages in Michigan and Wisconsin, USA: North American Journal of Fisheries Management, v. 29, no. 4, p. 1130–1151.

Magnuson, J.J., Crowder, L.B., and Medvick, P.A., 1979, Temperature as an ecological Resource: American Zoologist, v. 19, p. 331–343.

Magnuson, J.J., Webster, K.E., Assel, R.A., Bowser, C.J., Dillon, P.J., Eaton, J.G., Evans, H.E., Fee, E.J., Hall, R.I., Mortsch, L.R., Schindler, D.W., and Quinn, F.H., 1997, Potential effects of climate changes on aquatic systems—Laurentian Great Lakes and Precambrian Shield Region: Hydrological Processes, v. 11, no. 8, p. 825–871.

Marshall, D.W., Fayram, A.H., Panuska, J.C., Baumann, James, and Hennessy, Joseph, 2008, Positive effects of agricultural land use changes on coldwater fish communities in southwest Wisconsin streams: North American Journal of Fisheries Management, v. 28, no. 3, p. 944–953.

McKenna, J.E., Jr., Butryn, R.S., and McDonald, R.P, 2010, Summer stream water temperature models for Great Lakes streams—New York: Transactions of the American Fisheries Society, v. 139, no. 5, p. 1399–1414.

Mitro, Matthew; Lyons, John; and Sharma, Sapna, 2010a, Wisconsin initiative on climate change impacts—Coldwater fish and fisheries working group report: Madison, Wis., University of Wisconsin-Madison and the Wisconsin Department of Natural Resources, Nelson Institute for Environmental Studies, 31 p., *http://www.wicci.wisc.edu/publications.php*.

Mitro, M.G., Lyons, J.D., and Stewart, J.S., 2010b, Predicted effects of climate change on the distribution of wild brook trout and brown trout in Wisconsin streams, in Conserving wild trout, Carline, R.F., and LoSapio, C., eds.: Bozeman, Mont., Proceedings of the Wild Trout X symposium, p. 69–76.

Mohseni, Omid, Erickson, T.R., and Stefan, H.G., 1999, Sensitivity of stream temperatures in the United States to air temperatures projected under a global warming scenario: Water Resources Research, v. 35, no. 12, p. 3723–3733.

Mohseni, Omid, Stefan, H.G., and Eaton, J.G., 2003, Global warming and potential changes in fish habitat in U.S. streams: Climatic Change, v. 59, no. 3, p. 389–409.

National Oceanic and Atmospheric Administration, 2011, NCDC—Online climate data directory, accessed September 2012 at *http://www.ncdc.noaa.gov/oa/climate/climatedata.html#daily*.

Notaro, Michael; Lorenz, D.J.; Vimont, Daniel; Vavrus, Stephen; Kucharik, Christopher; and Franz, Kristie, 2011, 21st century Wisconsin snow projections based on an operational snow model driven by statistically downscaled climate data: International Journal of Climatology, v. 31, no. 11, p. 1615–1633.

Panuska, John, Good, L.W., and Wolkowski, Richard, 2007, Converting CRP land to corn—Minimizing soil loss: University of Wisconsin Extension, A3830, 4 p., accessed June 2014 at *http://learningstore.uwex.edu/*.

Pilgrim, J.M., Fang, Xing, and Stefan, H.G., 1998, Stream temperature correlations with air temperatures in Minnesota—Implications for climate warming: Journal of the American Water Resources Association, v. 34, no. 5, p. 1109–1121.

R Development Core Team, 2011, A language and environment for statistical computing: Vienna, Austria, R Foundation for Statistical Computing, accessed April 2011 at *http://www.R-project.org/*.

Risley, J.C., Roehl, E.A., Jr., and Conrads, P.A., 2003, Estimating water temperatures in small streams in Western Oregon using neural network models: U.S. Geological Survey Water-Resources Investigations Report 02–4218, 59 p.

Roehl, Edwin; Risley, John; Stewart, Jana; and Mitro, Matthew, 2006, Numerically optimized empirical modeling of highly dynamic, spatially expansive, and behaviorally heterogeneous hydrologic systems—Part 1, *in* Voinov, A., Jakeman, A.J., Rizzoli, and A.E., eds., Proceedings of the International Environmental Modeling and Software Society (iEMSs) Third Biennial Meeting—Summit on Environmental Modelling and Software: Burlington , Vt., International Environmental Modelling and Software Society, accessed June 2013 at *http://www.iemss.org/iemss2006/sessions/all.html*.

Rubin, Jerrold, 1967, Optimal classification into groups—An approach for solving the taxonomy problem: Journal of Theoretical Biology, v. 15, no. 1, p. 103–144.

Rumelhart, D.E., Hinton, G.E., and Williams, R.J., 1986, Learning internal representation by error propagation, in Rumelhart, D.E. and others, eds., Parallel distributed processing: Cambridge, Mass., Massachusetts Institute of Technology Press, p. 318–362.

Serbin, S.P., and Kucharik, C.J., 2009, Spatiotemporal mapping of temperature and precipitation for the development of a multidecadal climatic dataset for Wisconsin: Journal of Applied Meteorology and Climatology, v. 48, no. 4, p. 742–757.

Shreve, R.L, 1967, Infinite topologically random channel networks: Journal of Geology, v. 75, no. 2, p. 178–186.

Steen, P.J., Zorn, T.G., Seelbach, P.W., and Schaeffer, J.S., 2008, Classification tree models for predicting distributions of Michigan stream fish from landscape variables: Transactions of the American Fisheries Society, v. 137, no. 4, p. 976–996.

Stewart, Jana, Mitro, Matthew, Roehl, E.A., Jr., and Risley, John, 2006, Numerically optimized empirical modeling of highly dynamic, spatially expansive, and behaviorally heterogeneous hydrologic systems—Part 2, *in* Proceedings of the 7th International Conference on Hydroinformatics: Nice, France, 8 p.

Streitfeld, David, 2008, As prices rise, farmers spurn conservation program: New York Times, 9 April 2008, accessed June 30, 2014, at *http://www.nytimes.com/2008/04/09/business/09conserve.html?_r=0*.

Thornthwaite, C.W., Mather, J.R., and Carter, D.B., 1957, Instructions and tables for computing potential evapotranspiration and the water balance: Centerton, N.J., Drexel Institute of Technology, Laboratory of Climatology, Publications in Climatology, v. 10, no. 3, p. 185–311.

Trout Unlimited, 2005, The driftless area—A landscape of opportunities—Trout Unlimited Driftless Area Restoration Effort (TUDARE), accessed [2014], at *http://namekagon.org/wp-content/uploads/2013/07/Driftless-A-Landscape-of-Opportunities.pdf*.

U.S. Department of Agriculture, 2009, Soil Survey Geographic (SSURGO) Database for Wisconsin, accessed [2013], at *http://websoilsurvey.sc.egov.usda.gov/App/HomePage.htm*.

U.S. Geological Survey, 2003, National land cover database 2001 (NLCD 2001), accessed June 30, 2014, at *http://www.mrlc.gov/mrlc2k_nlcd.asp*.

U.S. Geological Survey, 2004a, National elevation dataset, accessed August 2004 at *http:ned.usgs.gov/*.

U.S. Geological Survey, 2004b, National hydrography dataset, accessed August 2004 at *http:nhd.usgs.gov/*.

Wagner, R.W., Stacey, Mark, Brown, L.R., and Dettinger, Michael, 2011, Statistical models of temperature in the Sacramento-San Joaquin Delta under climate-change scenarios and ecological implications: Estuaries and Coasts, v. 34, no. 3, p. 544–556.

Wang, Lizhu; Lyons, John; and Kanehl, Paul, 2003, Impacts of urban land cover on trout streams in Wisconsin and Minnesota: Transactions of the American Fisheries Society, v. 132, no. 5, p. 825–839.

Wehrly, K.E., Wiley, M.J., and Seelbach, P.W., 1998, Landscape-based models that predict July thermal characteristics of Lower Michigan rivers: Ann Arbor, Mich., Michigan Department of Natural Resources, Fisheries Research Report 2037, 22 p.

Wehrly, K.E., Wiley, M.J., and Seelbach, P. W., 2003, Classifying regional variation in thermal regime based on stream fish community patterns: Transactions of the American Fisheries Society, v. 132, no. 1, p. 18–38.

Wehrly, K.E., Wiley, M.J., and Seelbach, P.W., 2006, Influence of landscape features on summer water temperatures in Lower Michigan streams, *in* Landscape influences on stream habitats and biological assemblages, Hughes, R.M., Wang, L., and Seelbach, P.W., eds.: Bethesda, Md., American Fisheries Society, Symposium 48, p. 113–127.

Weiss, S.M., and Indurkhya, Nitin, 1997, Predictive Data Mining, Morgan Kaufmann, accessed [2013], at *http://www.data-miner.com*.

Westenbroek, S.M., Kelson, V.A., Dripps, W.R., Hunt, R.J., and Bradbury, K.R., 2010a, SWB—A modified Thornthwaite-Mather Soil-Water-Balance code for estimating groundwater recharge: U.S. Geological Survey Techniques and Methods, 6-A31, p. 60.

Westenbroek, S.M., Stewart, J.S, Buchwald, C.A., Mitro, M., Lyons, J.D., and Greb, S., 2010b, A model for evaluating stream temperature response to climate change scenarios in Wisconsin, in Proceedings of Watershed Management 2010: Madison, Wis., p. 1–12.

Wisconsin Department of Natural Resources (WDNR), 2011, Expenditures of inland water trout stamp revenues—Fiscal years 2008–2010: Madison, Wis., Administrative Report No. 67, 41 p.

Wisconsin Department of Natural Resources (WDNR), 2013, Regional and property analysis for the development of a master plan for Department of Natural Resources' properties along trout and smallmouth bass streams in the Driftless Area, DNR PUB-LF-071 2013, *http://dnr.wi.gov/topic/Lands/MasterPlanning/DriftlessStreams/*.

Wisconsin Initiative on Climate Change Impacts (WICCI), 2011, Wisconsin's changing climate—Impacts and adaptation: Madison, Wis., Nelson Institute for Environmental Studies, University of Wisconsin-Madison and Wisconsin Department of Natural Resources, 217 p., accessed June 30, 2014, at *http://www.wicci.wisc.edu/publications.php*.

Zorn, T.G., Seelbach, P.W., and Wiley, M.J., 2002, Distributions of stream fishes and their relationship to stream size and hydrology in Michigan's Lower Peninsula: Transactions of the American Fisheries Society, v. 131, no. 1, p. 70–85.

Appendix 1. Stream identification information, location information, agency collecting stream temperature data, number of summers with stream temperature data collection, years of stream temperature data collection, July mean stream temperature, stream temperature thermal class, and model partition for 371 stream temperature modeling sites.

Available as a seperate download.

Appendix 2. Climate station identification and location information for 160 air temperature stations.

Available as a seperate download.

Publishing support provided by:
U.S. Geological Survey Science Publishing Network,
Columbus and Raleigh Publishing Service Centers

For more information concerning this publication, please contact:
Center Director,
USGS Wisconsin Water Science Center
U.S. Geological Survey
8505 Research Way
Middleton, Wisconsin 53562
(608) 821-3810

Or visit the USGS Wisconsin Water Science Center Web site at:
http://wi.water.usgs.gov/

J.S. Stewart and others—**A Model for Evaluating Stream Temperature Response to Climate Change in Wisconsin**—Scientific Investigations Report 2014–5186

ISSN 2328-0328 (online)
http://dx.doi.org/10.3133/sir20145186